Université de Montréal

Systematic construction of models for the exchange hole of density functional theory

par
Rodrigo Wang

Département de chimie
Faculté des arts et des sciences

Mémoire présenté à la Faculté des études supérieures et postdoctorales
en vue de l'obtention du grade de Maître ès sciences (M.Sc.)
en chimie

08, 2015

RÉSUMÉ

Dans ce travail, nous étendons le nombre de conditions physiques actuellement connues du trou d'échange exact avec la dérivation de l'expansion de quatrième ordre du trou d'échange sphérique moyenne exacte. Nous comparons les expansions de deuxième et de quatrième ordre avec le trou d'échange exact pour des systèmes atomiques et moléculaires. Nous avons constaté que, en général, l'expansion du quatrième ordre reproduit plus fidèlement le trou d'échange exact pour les petites valeurs de la distance interélectronique. Nous démontrons que les ensembles de base de type gaussiennes ont une influence significative sur les termes de cette nouvelle condition, en étudiant comment les oscillations causées par ces ensembles de bases affectent son premier terme. Aussi, nous proposons quatre modèles de trous d'échange analytiques auxquels nous imposons toutes les conditions actuellement connues du trou d'échange exact et la nouvelle présentée dans ce travail. Nous évaluons la performance des modèles en calculant des énergies d'échange et ses contributions à des énergies d'atomisation. On constate que les oscillations causeés par les bases de type gaussiennes peuvent compromettre la précision et la solution des modèles.

Mots clés DFT, Fonctionnelle d'énergie d'échange

ABSTRACT

In this work, we extend the number of currently known physical conditions of the exact exchange hole with the derivation of the fourth-order expansion of the exact spherically averaged exchange hole. We compare the second- and fourth-order expansions with the exact exchange hole for atomic and molecular systems. We found that, in general, the fourth-order expansion reproduces more accurately the exact exchange hole for small values of the interelectronic distance. We demonstrate that Gaussian-type basis sets have a significant influence on the terms of this new condition, by studying how oscillations originated in these basis sets affects its leading term. Also, we propose four analytical exchange hole models to which we impose all currently known conditions of the exact exchange hole and the new one presented in this work. We assess the performance of the models by computing exchange energies and its contributions to atomization energies. It is found that oscillations originated in Gaussian-type basis sets can compromise the accuracy and solution of the models.

Keywords: DFT, Exchange energy functional

CONTENTS

LIST OF TABLES

LIST OF FIGURES

LIST OF APPENDICES

LIST OF ABBREVIATIONS

B3	Version 03 of the exchange density functional of Becke
BLYP	Density functional of Becke, Lee, Yang and Parr
BO	Approximation of Born and Oppenheimer
BR	Exchange hole model of Becke and Roussel
DFT	Density functional theory
HF	Hartree and Fock
HGGA	Hyper generalized gradient approximation
HK	Hohenberg and Kohn
GGA	Generalized gradient approximation
KS	Kohn and Sham
LCAO	Linear combination of atomic orbitals
LDA	Local density approximation
LSDA	Local spin-density approximation
MGGA	Meta generalized gradient approximation
PBE	Density functional of Perdew, Burke and Ernzerhof
PBE0	Hybrid density functional of Perdew, Burke and Ernzerhof
PW86	Version 86 of the density functional of Perdew and Wang
PW91	Version 91 of the density functional of Perdew and Wang
TPSS	Density functional of Tao, Perdew, Staroverov and Scuseria
TPSSh	Hybrid density functional of Tao, Perdew, Staroverov and Scuseria
UEG	Uniform electron gas
VM	Variational method
VP	Variational principle
PT	Pertubation theory

To my family and friends.

ACKNOWLEDGMENTS

I would like to express my deepest gratitude to my supervisor Matthias Ernzerhof for giving me the oportunity to work in his group.

I would also like to thank my great friend João Rodolfo for uncountable discussions about this work and many other subjects ranging from theoretical chemistry to power-lifting.

I would like to thank my friend and colleague Yongxi Zhou for all your support in aiding me to realize this work.

I would like to thank professor Radu Iftimie for giving me the chance to be his teacher assistant.

I would like to thank professor José Politi and Kleber Mundim at Universidade de Brasília for showing me the beauty of theoretical chemistry.

I would like to thank my friends Pedro Lima, Lucas Guimarães, Adriano Utsch, Tiago Borges, Conrado Brunacci, Lucas Lima and David Oliveira, for all these years of friendship, soccer and death metal.

I would like to thank my parents and my brother for their love, patience and support throughout my life.

Finally, I would like to dedicate and send my warmest heartily thanks to my beloved Patricia Ciraulo for always being there and for giving me the most precious gifts of life, Erik and our unborn baby who will soon join us in this journey.

CHAPTER 1

INTRODUCTION

Electronic structure theory (EST) addresses a wide range of phenomena in areas such as chemistry, physics, materials science, and biology. Since the beginning of the 20^{th} century, after the discovery of the electron, EST has provided the language of chemistry and many of its models and tools. An early cornerstone of EST is provided by the Lewis theory [1] of atomic and molecular structure. Lewis formulas play an important role in chemistry to this day even though they have numerous limitations. Many molecular properties, such as electronic excitations, cannot be described by them and they do not provide any quantitative predictions. Quantum mechanics, developed in the 1920s provides an exact formal description of electrons through Schrödinger's equation. However, the development of quantitative models for chemistry was hampered by the enormous complexity of Schrödinger's equation for many-electron systems. Since the 1980s improvements of theories and computational techniques, as well as the increase in computer power, moved computational modeling to the forefront in chemistry. In particular the development of density functional theory (DFT) initiated an ongoing transformation of many areas of science. The key quantity which has to be approximated in DFT is the exchange-correlation energy functional. We focus on approximations to the exchange energy functional where the latter can be expressed in terms of the exchange hole. Building on the work of Becke and collaborators [2, 3], that the exact exchange hole in inhomogeneous systems can be approximated by an analytic model, where it depends on the Taylor series expansion of the exact spherically averaged exchange hole up to the second order in the interelectronic distance. With respect to the related work mentioned, I extend the Taylor series expansion of the exact spherically averaged exchange hole up to the fourth order in the interelectronic distance and construct new analytic exchange hole models that depend on the new extended Taylor series expansion. The purpose is to obtain exchange hole approximations that are more accurate than the existing ones.

1.1 The Schrödinger equation

In the electronic structure of matter, the time dependent Schrödinger equation

$$\hat{H}\Psi = i\frac{\partial \Psi}{\partial t}, \tag{1.1}$$

is the most fundamental equation which describes how quantum states of a physical system develop in time. The time-dependent Schrödinger equation has applications to scattering and spectral theory, charge transport, etc. For those cases in which one is mainly concerned with systems without interactions evolving in time, the time-independent variant of the Schrödinger equation is used. The non-relativistic Schrödinger equation plays in quantum mechanics the same role of non-relativistic Hamilton's laws of motion in classical mechanics.

All properties of any atom or molecule in any of their possible stationary states may be obtained in principle by the solution of the time-independent Schrödinger equation. The representation of the problem of a many-electron system is

$$\hat{H}\Psi(\boldsymbol{R}_1,...,\boldsymbol{R}_M,\boldsymbol{r}_1,..,\boldsymbol{r}_N) = E\Psi(\boldsymbol{R}_1,...,\boldsymbol{R}_M,\boldsymbol{r}_1,..,\boldsymbol{r}_N) \tag{1.2}$$

where $\hat{H}$ is the Hamiltonian operator in atomic units

$$\hat{H} = \sum_{i=1}^{N}\left(-\frac{1}{2}\nabla_i^2\right) + \sum_{A=1}^{M}\left(-\frac{1}{2M_A}\nabla_A^2\right) - \sum_{i=1}^{N}\sum_{A=1}^{M}\frac{Z_A}{r_{iA}} + \sum_{i=1}^{N}\sum_{j>i}^{N}\frac{1}{r_{ij}} + \sum_{A=1}^{M}\sum_{B>A}^{M}\frac{Z_A Z_B}{R_{AB}}, \tag{1.3}$$

where the first two terms represent the kinetic energy operator of the electrons and nuclei in which the indexes i and j indicates the i-th and j-th electrons and the indexes A and B the A-th and B-th nuclei. The last three terms describe potential energies due to electron-nucleus, electron-electron and nucleus-nucleus interactions, respectively. Moreover, the quantities r_{ij}, r_{iA} and r_{AB} are distances between electrons, electron and nucleus and nuclei. Also, note that $j > i$ in the electron-electron interaction operator and $B > A$ in the nucleus-nucleus interaction operator are used to avoid double counting of electrons and nuclei. The wavefunction $\Psi(\boldsymbol{R}_1,...,\boldsymbol{R}_M,\boldsymbol{r}_1,..,\boldsymbol{r}_N)$ depends on all M nuclei and N

electrons variables and E is the total energy for this wavefunction, respectively.

The wavefunction Ψ, also called the probability amplitude, contains all the information concerning the system but has no physical interpretation. At the other hand, when Ψ is normalized the square of its absolute value $|\Psi|^2$ has the physical interpretation that $|\Psi|^2 d^3r_1 \dots d^3r_N$ is the probability to find electron $1, \dots, N$ in volume elements $d^3r_1 \dots d^3r_N$.

The Schrödinger's equation presented in equation 1.2 is a eigenvalue equation that has exact solutions for very simple systems. The wavefunctions that solve the eigenvalue equation are called eigenstates of the Hamiltonian operator $\hat{H}$ while the energies associated with this solution are called eigenvalues. The eigenstates Ψ of $\hat{H}$ are stationary states that have well-defined energies E where the state of lowest energy is called the ground state of the system and it is denoted by Ψ_0 .

We observe that the problem at hand is a partial differential equation of a large number of variables. For instance consider the benzene molecule composed of 12 nuclei and 42 electrons. In this system one needs to solve a problem with 162 variables where only spatial-coordinates are taken into consideration. Hence, solutions for many-electron systems need to be approximated. Furthermore, a direct solution of the eigenvalue problem of equation 1.2 cannot have a closed form due to the electron-electron interaction operator $1/r_{ij}$. If one wishes to deal with electronic structure and properties of atoms and molecules, which is the subject of the present work, a possible separation of variables should be envisioned. Then mathematical methods can be employed to provide approximate solutions to the electronic Schrödinger equation. In the following section we present a short introduction to an approximation proposed by Max Born and Julius Robert Oppenheimer[4] that allows a separation of variables of the wavefunction. In this work we use atomic units where the length unit is the Bohr radius a_0, the charge unit is the charge of the electron e, and the mass unit is the mass of the electron m.

1.2 The Born-Oppenheimer approximation

The first step to reduce the complexity of the problem was made in the early days of quantum mechanics by Max Born and Julius Robert Oppenheimer. In the Born-Oppenheimer (BO) approximation[4] the nuclei are taken as fixed because of their much larger mass, while electrons respond almost instantaneously to changes in the nuclei configurations. Under this assumption, the wavefunction can be factorized into two parts: one part entails information about the electrons and is called the electronic wavefunction while the other part contains essentially nuclei information and is called the nuclear wavefunction,

$$\Psi(\boldsymbol{R}_1,...,\boldsymbol{R}_M,\boldsymbol{r}_1,..,\boldsymbol{r}_N) = \Psi_{nuc}(\boldsymbol{R}_1,...,\boldsymbol{R}_M)\Psi_{elec}(\boldsymbol{R}_1,...,\boldsymbol{R}_M,\boldsymbol{r}_1,..,\boldsymbol{r}_N) \tag{1.4}$$

where the subscripts *nuc* and *elec* indicate nucleus and electron parts of the wavefunction, respectively. Born and Oppenheimer and Born and Huang[5] expanded the total molecular wavefunction and showed that a single product of electronic and nuclear wavefunctions is a good approximation. Under this approximation, the electronic wavefunction defined by

$$\Psi_{elec}(\boldsymbol{R}_1,...,\boldsymbol{R}_M,\boldsymbol{r}_1,..,\boldsymbol{r}_N), \tag{1.5}$$

is then a valid solution to equation 1.2 . Note that the electronic wavefunction depends directly on electrons coordinates and parametrically on nuclei coordinates. Thus, we have a different electronic wavefunction and energy for each different arrangement of the nuclei. The electronic Schrödinger equation takes the following form

$$\hat{H}_{elec}\Psi_{elec}(\boldsymbol{R}_1,...,\boldsymbol{R}_M,\boldsymbol{r}_1,..,\boldsymbol{r}_N) = E_{elec}\Psi_{elec}(\boldsymbol{R}_1,...,\boldsymbol{R}_M,\boldsymbol{r}_1,..,\boldsymbol{r}_N), \tag{1.6}$$

where $\hat{H}_{elec}$ is the electronic Hamiltonian operator defined as,

$$\begin{aligned}\hat{H}_{elec} &= \sum_{i=1}^{N} -\frac{1}{2}\nabla_i^2 - \sum_{i=1}^{N}\sum_{A=1}^{M}\frac{Z_A}{r_{iA}} + \sum_{i=1}\sum_{j>i}^{N}\frac{1}{r_{ij}} \\ &= \sum_{i=1}^{N}\left(-\frac{1}{2}\nabla_i^2\right) + \sum_{i=1}^{N} v(\boldsymbol{r}_i) + \sum_{i=1}\sum_{j>i}^{N}\frac{1}{r_{ij}} \\ &= \hat{T} + \hat{V}_{ne} + \hat{V}_{ee}.\end{aligned} \tag{1.7}$$

All possible solutions of equation 1.6 are stationary states and each of of them have an associated electronic energy

$$E_{elec} \equiv E_{elec}(\boldsymbol{R}_1, ..., \boldsymbol{R}_M), \tag{1.8}$$

which also depends parametrically on the nuclei coordinates. Furthermore, the total energy

$$E_{tot} = E_{elec} + \sum_{A=1}^{M}\sum_{B>A}^{M}\frac{Z_A Z_B}{R_{AB}}. \tag{1.9}$$

is obtained by adding the nucleus-nucleus repulsion energy term to the electronic energy.

Indeed, the BO approximation is critical to the study of electronic structure and properties of chemical systems. Because of the large difference between the masses of nuclei and electrons, the approximation is valid and permits one to focus on electronic properties only.

1.3 Wavefunction theory

The idea proposed in 1925 by Uhlenbeck and Goudsmit[6] to explain the fine structure of atomic spectra is that electrons have an intrinsic angular momentum which is called spin angular momentum or for short spin. So far we have not included electron spin into our equations because the Hamiltonian operator $\hat{H}$ does not depend on spin-coordinates thus leaving the non-relativistic Schrödinger equation unchanged. In order to describe quantum mechanical systems properly we introduce two functions $\alpha(\sigma)$ and $\beta(\sigma)$ which represent spin up and down, respectively. Note that $\alpha(\sigma)$ and $\beta(\sigma)$ are only

symbols to represent the spin functions. The mathematical definition of these functions is not in the scope of this work. Nevertheless, these two functions are complete and orthonormal

$$\sum_{\sigma} \alpha^*(\sigma)\alpha(\sigma) = \sum_{\sigma} \beta^*(\sigma)\beta(\sigma) = 1, \tag{1.10}$$

$$\sum_{\sigma} \alpha^*(\sigma)\beta(\sigma) = \sum_{\sigma} \beta^*(\sigma)\alpha(\sigma) = 0. \tag{1.11}$$

With a space coordinate $\boldsymbol{r}$ and a spin coordinate σ we can define a new variable

$$\boldsymbol{x} = \{(\boldsymbol{r}, \sigma)\} \tag{1.12}$$

which represents the four coordinates; three spatial-coordinates $\boldsymbol{r}$ and one spin-coordinate σ. The composite spatial plus spin coordinate of the electrons $\boldsymbol{x}$ is then used to construct spin-orbitals

$$\chi \equiv \chi(\boldsymbol{x}), \tag{1.13}$$

where the product between each spatial orbital and one of the two spin functions forms two spin orbitals,

$$\chi(\boldsymbol{x}) = \begin{cases} \phi(\boldsymbol{r})\alpha(\sigma) \\ \text{or} \\ \phi(\boldsymbol{r})\beta(\sigma). \end{cases} \tag{1.14}$$

With the inclusion of spin-coordinates we complete the description of electrons. Because electrons are Fermi-Dirac particles of half integral, an additional condition are imposed on many-electrons wavefunction. By the symmetry principle[7, 8], many-electrons wavefunctions must be antisymmetric under particle coordinate exchange,

$$\Psi(\boldsymbol{x}_1, \ldots, \boldsymbol{x}_i, \ldots, \boldsymbol{x}_j, \ldots, \boldsymbol{x}_N) = -\Psi(\boldsymbol{x}_1, \ldots, \boldsymbol{x}_j, \ldots, \boldsymbol{x}_i, \ldots, \boldsymbol{x}_N). \tag{1.15}$$

These two configurations are physically indistinguishable and should occur with the same probability $|\Psi|^2$. From equation 1.15 we have that,

$$|\Psi(\boldsymbol{x}_1, \ldots, \boldsymbol{x}_i, \ldots, \boldsymbol{x}_j, \ldots, \boldsymbol{x}_N)|^2 = |\Psi(\boldsymbol{x}_1, \ldots, \boldsymbol{x}_j, \ldots, \boldsymbol{x}_i, \ldots, \boldsymbol{x}_N)|^2 \tag{1.16}$$

holds for all $N!$ distinct permutations of labels $1 \ldots N$ in equation 1.14 . Consider as a solution to equation 1.6 the product of N distinct orbitals each one containing one electron

$$\Psi(\boldsymbol{x}_1, \boldsymbol{x}_2, \ldots, \boldsymbol{x}_N) = \chi(\boldsymbol{x}_1)\chi(\boldsymbol{x}_2)\ldots\chi(\boldsymbol{x}_N). \tag{1.17}$$

From the symmetry principle we should have that equation 1.15 and consequently equation 1.16 hold true but this is not the case because we have,

$$|\Psi(\boldsymbol{x}_1, \boldsymbol{x}_2, \ldots, \boldsymbol{x}_N)|^2 dx_1 dx_2 \ldots dx_N = |\chi(\boldsymbol{x}_1)|^2 dx_1 |\chi(\boldsymbol{x}_2)|^2 dx_2 \ldots |\chi(\boldsymbol{x}_N)|^2 dx_N. \tag{1.18}$$

The last result says that the simultaneous probability of finding electron-one in volume element dx_1 and electron-two in volume element dx_2 and etc is equal to the product of probabilities of each individual event. In other words, the events are uncorrelated. Hence, the probabilities to find one electron at a given position is independent of the position of the other electrons. This uncorrelated wavefunction neglects completely Coulombic interactions for the case of opposite spin electrons and clearly does not satisfy the symmetry principle for indistinguishable particles.

Although wavefunctions as equation 1.17 are not antisymmetric under coordinate exchange, they are approximate solutions to systems of non-interacting electrons. These solutions are obtained without great effort since the method of separation of variables can be employed. Such systems are also linear eigenvalue equations as in equation 1.16 and proper linear combinations of equation 1.17 can be used produce wavefunctions that satisfy the exchange principle and are approximate solutions to equation 1.6.

1.3.1 Slater Determinants

In 1929 John Slater proposed a determinantal many-electron wavefunction which is constructed with an appropriate linear combination of symmetry wavefunctions as equation 1.17 . Such antisymmetric wavefunctions are called Slater determinants. The

Slater determinant[8, 9] for a system with N electrons is defined as

$$\Psi(\boldsymbol{x}_1,\ldots,\boldsymbol{x}_N) = \frac{1}{\sqrt{N}}\begin{vmatrix} \chi_i(\boldsymbol{x}_1) & \chi_j(\boldsymbol{x}_1) & \ldots & \chi_N(\boldsymbol{x}_1) \\ \chi_i(\boldsymbol{x}_2) & \chi_j(\boldsymbol{x}_2) & \ldots & \chi_N(\boldsymbol{x}_2) \\ \vdots & \vdots & & \vdots \\ \chi_i(\boldsymbol{x}_N) & \chi_j(\boldsymbol{x}_N) & \ldots & \chi_N(\boldsymbol{x}_N) \end{vmatrix}, \tag{1.19}$$

where $1/\sqrt{N!}$ is the normalization factor and the N electrons occupies χ_N orthogonal spin-orbitals. Moreover, each row in equation 1.19 is labeled by an electron and each column is labeled by a spin-orbital. We observe that the Slater determinant does not relate an electron with a specified orbital.

Some important aspects of chemical structures may be unveiled by a study of the exchange symmetry. For instance, if the labels of equation 1.19 are the same $i = j$ the wavefunction vanishes. Thus, two electrons cannot be in the same quantum state. This result gives the Pauli exclusion principle[7–9] which postulates that only the first three quantum numbers can be the same for any two electrons.

Solutions to the Schödinger equation need to be approximated with mathematical methods. These methods are able to determine the best form of the orbitals involved in the many-electron wavefunctions. Therefore, one can use approximate methods to minimize the energy of a given system. In the next section the Variational Method will be discussed.

1.4 The Variational Method

The Variational Method (VM) together with the Pertubation Theory (PT) are the most important methods[7–9] employed to find approximate solutions to the Schrödinger equation. The VM works by guessing a trial wavefunction for the eigenvalue equation. The trial wavefunction contains additional parameters introduced to aid in the determination of the best form of the orbitals. By varying these parameters one may find the minimum energy of the system. This procedure can also be applied to excited states.

For a many-electron system one has to find approximate solutions to the eigenvalue

equation for electrons

$$\hat{H}\widetilde{\Psi} = E\widetilde{\Psi}, \tag{1.20}$$

where $\widetilde{\Psi}$ and E are the trial wavefunction of a given nuclei configuration and the electronic energy, respectively. Moreover, $\hat{H}$ is the Hamiltonian operator for electrons defined in equation 1.6 . Note that the present eigenvalue equation was already defined in equation 1.6 but here we omit the subscript *elec*. The average of the electronic energy is,

$$E = \frac{\int d\tau \widetilde{\Psi}^* \hat{H} \widetilde{\Psi}}{\int d\tau \widetilde{\Psi}^* \widetilde{\Psi}} = \frac{\left\langle \widetilde{\Psi} | \hat{H} | \widetilde{\Psi} \right\rangle}{\left\langle \widetilde{\Psi} | \widetilde{\Psi} \right\rangle}. \tag{1.21}$$

At the end of the procedure the final wavefunction and its associated energy are approximations to the exact wavefunction and energy. The result given by the VM is supported by an important theorem called the Variational Principle (VP). The VP states that any energy calculated from a trial wavefunction is an upper bound to the lowest energy state ε_0 of the Hamiltonian $\hat{H}$,

$$\frac{\left\langle \widetilde{\Psi} | \hat{H} | \widetilde{\Psi} \right\rangle}{\left\langle \widetilde{\Psi} | \widetilde{\Psi} \right\rangle} \geqslant \varepsilon_0. \tag{1.22}$$

When normalized wavefunctions are used the denominator in equation 1.21 is equal to unity and we have that $E = \left\langle \widetilde{\Psi} | \hat{H} | \widetilde{\Psi} \right\rangle$.

We begin the proof of the VM expanding the trial wavefunction $\widetilde{\Psi}$ in terms of the eigenvectors of $\hat{H}$. This is possible since the Hamiltonian operator is a hermitian operator which implies that its eigenvectors are real and they form a complete orthogonal set,

$$\widetilde{\Psi} = \sum_{i=1}^{\infty} c_i \phi_i. \tag{1.23}$$

The omission of the orbital coordinates does not lead to loss of mathematical rigour in our equations and its use make the following equations shorter. Substituting equation

1.23 into equation 1.21 we obtain,

$$\begin{aligned} E[\widetilde{\Psi}] &= \frac{\sum_{i,j} c_i^* c_j \int d\tau \phi_i^* \hat{H} \phi_j}{\sum_{i,j} c_i^* c_j \int d\tau \phi_i^* \phi_j} \\ &= \frac{\sum_{i,j} c_i^* c_j \varepsilon_j \int d\tau \phi_i^* \phi_j}{\sum_{i,j} c_i^* c_j \int d\tau \phi_i^* \phi_j} \\ &= \frac{\sum_i c_i^* c_i \varepsilon_i}{\sum_i c_i^* c_i} \\ &= \frac{\sum_i |c_i|^2 \varepsilon_i}{\sum_i |c_i|^2}. \end{aligned} \tag{1.24}$$

At this point, we apply the VP theorem to the VM. Subtracting the exact ground-state energy ε_0 from both sides in equation 1.28 we have that,

$$E[\widetilde{\Psi}] - \varepsilon_0 = \frac{\sum_i |c_i|^2 (\varepsilon_i - \varepsilon_0)}{\sum_i |c_i|^2}. \tag{1.25}$$

In the right-hand side, every term of the summation is equal to or greater than zero, the left-hand side must also satisfy the same inequality which results in,

$$E[\widetilde{\Psi}] \geqslant \varepsilon_0. \tag{1.26}$$

We see from the last equation that the energy of any approximate wavefunction is always equal to or greater than the exact ground-state energy. The equality is attained only when the trial wavefunction is equal to the exact wavefunction.

The energy in equation 1.24 depends on the form of the trial wavefunction $\widetilde{\Psi}$ and is called a functional. Functionals are often present in the calculus of variations whence the VM belongs to. In functional analysis a functional is a mapping between vector spaces that can range from the real line to complex planes[10]. Thus, from equation 1.24 it is possible to define the mapping as,

$$E : \{c_k\} \mapsto \{\varepsilon_k\}. \tag{1.27}$$

Whence, we say that the energy is a functional that establishes a rule for going from a

function $\widetilde{\Psi}$ to a number ε_k. Thus, it is the functional form of $\widetilde{\Psi}$ that gives the values of $E[\widetilde{\Psi}]$, rather than any set of independent variables.

We seek now to minimize equation 1.28 that in mathematical language is translated to,

$$\delta E[\widetilde{\Psi}] = 0. \tag{1.28}$$

This consequently imposes the condition that $E[\widetilde{\Psi}]$ be stationary while one varies $\widetilde{\Psi}$. The task is to properly vary the form of the trial wavefunction by a small amount $\widetilde{\Psi} = \widetilde{\Psi} + \delta\widetilde{\Psi}$ in order to minimize the energy. By properly changing the parameters of the trial wavefunction, one can in principle obtain the optimal form of $\widetilde{\Psi}$ that minimizes the energy. The procedure is outlined as

$$\begin{aligned} E[\widetilde{\Psi} + \delta\widetilde{\Psi}] &= \langle \widetilde{\Psi} + \delta\widetilde{\Psi} | \hat{H} | \widetilde{\Psi} + \delta\widetilde{\Psi} \rangle \\ &= \langle \widetilde{\Psi} | \hat{H} | \widetilde{\Psi} \rangle + \langle \delta\widetilde{\Psi} | \hat{H} | \widetilde{\Psi} \rangle + \langle \widetilde{\Psi} | \hat{H} | \delta\widetilde{\Psi} \rangle + \dots \\ &= E[\widetilde{\Psi}] + \delta E[\widetilde{\Psi}] + \dots, \end{aligned} \tag{1.29}$$

where the second term contains all linear terms of the variation expansion of the energy functional. The infinite number of parameters necessary to calculate the energy turns out to be a challenging problem for molecular systems. Nonetheless, we can construct an approximation by linearly combining atomic orbitals to form molecular orbitals.

1.4.1 Linear Combination of Atomic Orbitals

In practical calculations the set of eigenvectors is not complete and we use instead a finite set of N basis functions that can only span a certain portion of space,

$$\widetilde{\Psi} = \sum_{i=1}^{N} c_i \phi_i(\boldsymbol{r}). \tag{1.30}$$

This is approximation is known as Linear Combination of Atomic Orbitals (LCAO)[7–9]. Thus, the function ϕ_i in equation 1.30 correspond to atomic orbitals of a polyatomic molecule. Notice that we have written the coordinate of the atomic orbitals ϕ_i. Here, these coordinates do not refer to a center of mass of the molecule but they can use

another reference i.e. the centers of of atoms as origins.

This approximation affects directly the accuracy of our calculations. However, the great advantage of the LCAO is the possibility to reduce the eigenvalue equation for electrons into a matrix diagonalization problem when only linear variations are taken into consideration in our calculations.

1.4.1.1 Matrix Eigenvalue Problem

In the matrix eigenvalue problem[9], the eigenvalue equation 1.20 is then recast into its matrix form. The representation of the Hamiltonian operator in the space spanned by equation 1.30 is **H** and the overlap matrix **S**. The elements of these matrices were already present in equation 1.24 . We now define them formally

$$H_{ij} = \int d\tau \phi_i^* \hat{H} \phi_j = \langle \phi_i^* | \hat{H} | \phi_j \rangle, \tag{1.31}$$

as the element ij of the Hamiltonian matrix **H** and

$$S_{ij} = \int d\tau \phi_i^* \phi_j = \langle \phi_i^* | \phi_j \rangle, \tag{1.32}$$

as the element ij of the overlap matrix **S**. Hence, we begin rewriting the eigenvalue equation into its matrix form using H_{ij} and S_{ij} ,

$$E[\widetilde{\Psi}] = \frac{\sum_{i,j} c_i^* c_j H_{ij}}{\sum_{i,j} c_i^* c_j S_{ij}}. \tag{1.33}$$

We impose on the VM that $\widetilde{\Psi}$ remains normalized during the minimization,

$$\langle \widetilde{\Psi} | \widetilde{\Psi} \rangle = 1. \tag{1.34}$$

This constraint ensures that the final $\widetilde{\Psi}$ will be normalized. Direct minimization of the N linear coefficients

$$\frac{\partial \langle \widetilde{\Psi} | \hat{H} | \widetilde{\Psi} \rangle}{\partial c_k} = 0 \qquad k = 0, \ldots N, \tag{1.35}$$

is not possible anymore because the N parameters are now coupled to each other by the normalization constraint of equation 1.34 . Minimization of a function with constraints can be dealt with by means of the Lagrange's method of undetermined multipliers. In this method the constraints are multiplied by auxiliary variables called Lagrange's multipliers. Then a new functional that contains the orthonormality condition is defined as

$$\begin{aligned} L(c_1,\ldots,c_N,E) &= \langle\widetilde{\Psi}|\hat{H}|\widetilde{\Psi}\rangle - E(\langle\widetilde{\Psi}|\widetilde{\Psi}\rangle - 1) \\ &= \sum_{i,j} c_i^* c_j \langle\phi_i|\hat{H}|\phi_j\rangle - \sum_{i,j}\varepsilon_{ij}\left(\sum_{i,j} c_i^* c_j\langle\phi_i|\phi_j\rangle - 1\right), \end{aligned} \tag{1.36}$$

where E denotes the Lagrange's multipliers. The next step of the VM is to apply arbitrary variations to the N parameters of L in order to to find a global minimum of this functional,

$$\begin{aligned} \delta L(c_1,\ldots,c_N,E) &= 0 \\ \delta\left[\langle\widetilde{\Psi}|\hat{H}|\widetilde{\Psi}\rangle - E\langle\widetilde{\Psi}|\widetilde{\Psi}\rangle\right] &= 0. \end{aligned} \tag{1.37}$$

Taking only the linear terms of δL the VM gives,

$$\begin{aligned} \delta L(c_1,\ldots,c_N,E) &= \sum_{i,j}\langle\phi_i|\hat{H}|\phi_j\rangle\delta c_i^* c_j - \sum_{i,j}\varepsilon_{ij}\left(\langle\phi_i|\phi_j\rangle\delta c_i^* c_j\right) \\ &+ \sum_{i,j}\langle\phi_i|\hat{H}|\phi_j\rangle c_i^*\delta c_j - \sum_{i,j}\varepsilon_{ij}\left(\langle\phi_i|\phi_j\rangle c_i^*\delta c_j\right) \\ &= \sum_i \delta c_i^*\left(\sum_j H_{ij}c_j - \sum_j \varepsilon_{ij}S_{ij}c_j\right) \\ &+ \sum_j \delta c_j\left(\sum_i H_{ij}c_i^* - \sum_i \varepsilon_{ij}S_{ij}c_i^*\right). \end{aligned} \tag{1.38}$$

The Lagrange multipliers ε_{ij} are eigenvalues of $\hat{H}$. They are real numbers and form a hermitian matrix E. This fact makes the two set of equations in 1.38 equivalent. We now

have to solve the homogeneous system of N linear equations

$$\sum_j H_{ij}c_j - \sum_j \varepsilon_{ij}S_{ij}c_j = 0, \tag{1.39}$$

for the coefficients c_j . The latter result has the following matrix form

$$\mathbf{HC} = \mathbf{ESC}, \tag{1.40}$$

where **H**, **S** and **E** are the matrix representation of the Hamiltonian operator, overlap integrals and the Lagrange's multipliers, respectively. The column vector **C** contains the coefficients or eigenvectors of $\hat{H}$ to be determined. The optimal c_j that minimize the energy are obtained by diagonalization of the matrix **H**.

1.5 Conclusion

The theories and methods introduced in this chapter lead us to a practical way to calculate the ground-state energy of atoms and molecules by the wavefunction method. In general, approximations to the wavefunction are necessary in order to accomplish this objective. Yet, the VM together with the LCAO had to be applied to ease the burden and make the calculation feasible.

We have seen that the procedure begins with the construction of the $\hat{H}$ operator. Once we have the external potential, $v(\boldsymbol{r}) = \sum_{i=1} v(\boldsymbol{r}_i)$, which is the potential due to nuclei charges action on the electrons and the number of electrons N we fix $\hat{H}$. Next, the ground state wavefunction is given, in principle, by equation 1.36. Finally, we obtain the ground state energy with equation 1.21 . The approach is represented schematically as,

$$\{v(\boldsymbol{r}), N\} \rightarrow \hat{H} \rightarrow \Psi \rightarrow E. \tag{1.41}$$

The VM allied with the method of Lagrange's multiplier is a powerful tool to tackle the eigenvalue problem for electrons. However, an attempt to apply the procedure described above to the problem of many-electron systems is extremely hard. The main cause is the

difficulty, to evaluate the electron-electron interaction energy term,

$$\sum_{i=1}\sum_{j>i}^{N}\frac{1}{r_{ij}}. \tag{1.42}$$

Many wave function-based methods avoids calculation of equation 1.42. The basic idea of these methods is to construct a Hamiltonian for a single electron in a *effective* field due to the nuclei and the remaining electrons. With respect to the electrons, this effective field can be the average potential acting on the $i-th$ electron due to the other electrons present in the system. In its very basic form, this approximation is called the Hartree-Fock method. This method was extensively reviewed [9] and it is known to provide only a qualitative guide for molecular calculations.

Therefore, the problem with respect to the correct description of electron-electron interactions leads to the development of new theories that could, in principle, account accurately for the correlated motion of electrons. This is the main motivation that took Pierre Hohenberg and Walter Kohn to develop the Density Functional Theory presented in the next chapter.

CHAPTER 2

DENSITY FUNCTIONAL THEORY

We open this chapter with the definition of its most important quantity: the electron density

$$\rho(\boldsymbol{r}) = N \int d\sigma_1 d\boldsymbol{x}_1 \ldots \boldsymbol{x}_N |\Psi(\boldsymbol{x}_1, \ldots, \boldsymbol{x}_N)|^2. \tag{2.1}$$

Note that Ψ is the wavefunction of a system composed of N electrons. The integration or average of $\rho(\boldsymbol{r})$ over all spin-coordinates and over all spatial variables not including the one of the first electron determines the probability of finding any of the N electrons in volume element $d\boldsymbol{r}_1$ with any spin configuration[8, 10].

The use of the electron density in the early development of this theory, as a basic quantity to obtain properties of atoms and molecules is not new in quantum mechanics. In the early development of this theory, important contributions were made by scientists like Thomas and Fermi[11]. The first attempts to circumvent the use of many-electron wavefunction failed to produce accurate approximations and to converge into a theory with rigorous basis. In 1964, Hohenberg and Kohn (HK) provided two fundamental theorems[12] that marked the birth of new theory called the Density Functional Theory (DFT).

2.1 The first theorem of Hohenberg and Kohn

We know that all properties of a chemical system are determined by its external potential $\upsilon(\boldsymbol{r})$ and by its number of electrons N. Both $\upsilon(\boldsymbol{r})$ and N determine completely and uniquely the ground state wavefunction Ψ_0 and the ground state energy E_0[10, 13]. The rigorous justification to use $\rho(\boldsymbol{r})$ to solve the many-electron problem is given by the first theorem of HK. Our approach to present the theorems is based on the original idea proposed by HK. The first theorem states that: *non-degenerate ground state density* $\rho_0(\boldsymbol{r})$ *determines uniquely the external potential* $\upsilon(\boldsymbol{r})$ *within a constant.* When potentials differ by a constant they are equivalent. Since the number of electrons N can be obtained from

$\rho(\boldsymbol{r})$ then, one is able to construct the Hamiltonian operator and consequently calculate the ground state of the system. Schematically, we have,

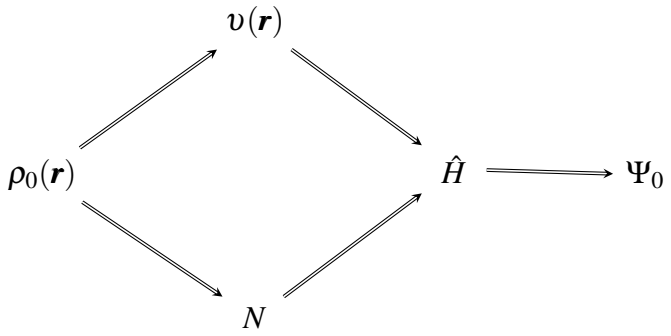

Figure 2.1: Schematically representation of the correspondence between density potential and wavefunction

We now present the mathematical development that leads to the first theorem. By solving the eigenvalue equation

$$\hat{H}\Psi_k = E\Psi_k, \tag{2.2}$$

we obtain the eigenstates Ψ_k of the Hamiltonian operator $\hat{H}$. In the set of eigenstates $|\Psi_k\rangle$ we have the ground-state $|\Psi_0\rangle$ of the system. Consider now the set of all operators $\hat{H}$ each one containing a $\upsilon(\boldsymbol{r})$ that when minimized by the (VM) gives a non-degenerate ground-state $|\Psi_0\rangle$. Thus, we define the set $\mathscr{V}$ of all external potentials that lead to a $|\Psi_0\rangle$. Furthermore, within $\mathscr{V}$ we have an infinite number of *equivalent* $\upsilon(\boldsymbol{r})$ where each one takes to the *same* ground-state $|\Psi_0\rangle$. We are now in a point where we can create a map between the external potentials and the ground-states,

$$P : \mathscr{V} \mapsto \{\Psi_0\}. \tag{2.3}$$

Because the ground state Ψ_0 determines the ground state density $\rho_0(\boldsymbol{r})$,

$$\rho_0(\boldsymbol{r}) = N \int d\sigma_1 d\boldsymbol{x}_2 \ldots \boldsymbol{x}_N |\Psi_0(\boldsymbol{x}_1, \ldots, \boldsymbol{x}_N)|^2. \tag{2.4}$$

We can define another map between the set of all ground states Ψ_0 and the set of all

ground state densities $\mathscr{D}$,

$$Q : \{\Psi_0\} \mapsto \mathscr{D}. \tag{2.5}$$

These two maps P and Q are originally surjectives: i.e. for any $v(\boldsymbol{r}) \in \mathscr{V}$ there exists an $|\Psi_0\rangle \in |\Psi_0\rangle$ for which the mapping is exists. Hohenberg and Kohn then proposed that both maps are bijectives. In other words, both maps can be inverted,

$$\begin{aligned} P^{-1} &: \{\Psi_0\} \mapsto \mathscr{V} \\ Q^{-1} &: \mathscr{D} \mapsto \{\Psi_0\}. \end{aligned} \tag{2.6}$$

These modifications of the mappings P and Q form the core of the first theorem and the resulting full inverse map can be defined as,

$$(PQ)^{-1} : \mathscr{D} \mapsto \mathscr{V}. \tag{2.7}$$

To prove the theorem we use the false assumption that two different[1] external potentials $v(\boldsymbol{r})$ and $v'(\boldsymbol{r})$, lead to the same eigenstate Ψ where we also have two different Hamiltonian operators $\hat{H} = \hat{T} + \hat{V}_{ne} + \hat{V}_{ee}$ and $\hat{H}' = \hat{T} + \hat{V}'_{ne} + \hat{V}_{ee}$ each one with its own ground-state Ψ_0 and Ψ'_0 , respectively. The representation of this assumption is schematically shown in figure 2.2

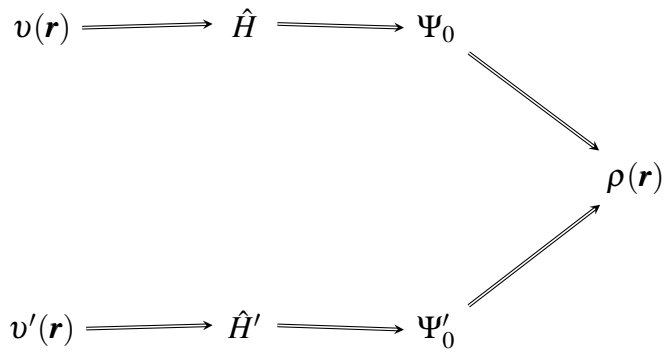

Figure 2.2: Schematically representation of the wrong correspondence between potential, wavefunction and density used to prove the first theorem.

[1] that differ by more than a constant

The two wavefunctions Ψ_0 and Ψ_0' are different and when the VP is applied we obtain,

$$E_0 = \langle \Psi_0 | \hat{H} | \Psi_0 \rangle < \langle \Psi_0' | \hat{H} | \Psi_0' \rangle. \tag{2.8}$$

where term in the right side of the inequality can be written as

$$\begin{aligned} \langle \Psi_0' | \hat{H} | \Psi_0' \rangle &= \langle \Psi_0' | \hat{H}' | \Psi_0' \rangle + \langle \Psi_0' | \hat{H} - H' | \Psi_0' \rangle \\ &= E_0' + \langle \Psi_0' | \hat{V}_{ne} - \hat{V}_n' | \Psi_0' \rangle \\ &= E_0' \int d\boldsymbol{r} \rho(\boldsymbol{r}) \left[\upsilon(\boldsymbol{r}) - \upsilon'(\boldsymbol{r}) \right]. \end{aligned} \tag{2.9}$$

Interchanging the primes of the inequality 2.8 we have by the VP that,

$$E_0' = \langle \Psi_0' | \hat{H}' | \Psi_0' \rangle < \langle \Psi_0 | \hat{H}' | \Psi_0 \rangle. \tag{2.10}$$

Following the same steps applied in 2.9 , we have that the right hand side of the latter inequality becomes,

$$\begin{aligned} \langle \Psi_0 | \hat{H}' | \Psi_0 \rangle &= E_0 - \langle \Psi_0' | \hat{V}_{ne}' - \hat{V}_n | \Psi_0' \rangle \\ &= E_0 - \int d\boldsymbol{r} \rho(\boldsymbol{r}) \left[\upsilon(\boldsymbol{r}) - \upsilon'(\boldsymbol{r}) \right]. \end{aligned} \tag{2.11}$$

We now add equations 2.9 and I.6 to obtain

$$E_0 + E_0' < E_0' + E_0, \tag{2.12}$$

which is clearly absurd.

This latter result proves the first theorem of HK where it shows that there cannot exist two different external potentials that lead to the same non-denegerate ground state density $\rho_0(\boldsymbol{r})$. From the viewpoint of the one-to-one mappings established by HK, the external potential $\upsilon(\boldsymbol{r})$ the ground state density $\rho_0(\boldsymbol{r})$ and the ground state Ψ_0 uniquely determines each other. Again schematically,

$$\upsilon(\boldsymbol{r}) \leftrightarrow \Psi_0 \leftrightarrow \rho_0(\boldsymbol{r}). \tag{2.13}$$

2.2 Second Theorem of Hohenberg and Kohn

The second theorem describes how we can obtain the ground state energy E_0 with the non-degenerate ground state density ρ_0 . To show this we first note that the inversed mapping Q^{-1} provides what is needed to establish that any expectation value of the ground state is a density functional. In the case of the ground state energy we obtain

$$\begin{aligned} E[\rho_0] &= \langle \Psi_0[\rho_0] | \hat{H} | \Psi_0[\rho_0] \rangle \\ &= F_{HK}[\rho_0] + \int d\boldsymbol{r} \rho_0(\boldsymbol{r}) \upsilon(\boldsymbol{r}), \end{aligned} \tag{2.14}$$

where Ψ_0 is the wavefunction of this particular ground-state density ρ_0 and $F_{HK}[\rho_0]$ is the Hohenberg-Kohn functional. $F_{HK}[\rho]$ is also known as the universal functional because it is independent of the external potential and it is defined by

$$\begin{aligned} F_{HK}[\rho_0] &= \langle \Psi_0[\rho_0] | \hat{T} + \hat{V}_{ee} | \Psi_0[\rho_0] \rangle \\ &= T[\rho] + V_{ee}[\rho] \\ &= T[\rho] + J[\rho] + E_{xc}[\rho], \end{aligned} \tag{2.15}$$

where $T[\rho]$ is the kinetic energy, $J[\rho]$ is the Coulomb repulsion energy and E_{xc} is the exchange-correlation energy, respectively. We delve into the exchange-correlation energy term in the next section.

The F_{HK} gives the minimum expectation value of $\langle \Psi_0 | \hat{T} + \hat{V}_{ee} | \Psi_0 \rangle$ when Ψ_0 is passed as input. Clearly, any density which is different from the ground-state density will have an energy higher than the ground-state energy,

$$E[\widetilde{\rho}] \geqslant \varepsilon_0. \tag{2.16}$$

This latter result is supported by the VP and the inversed mapping Q^{-1} proposed by HK.

At the beginning of this chapter we have emphasized that the two theorems were established for non-degenerate ground state. Another important consideration is the representability of the densities employed on the VP in the context of the second theorem.

We call υ-representable the density that is related to an antisymmetric wavefunction of a certain Hamiltonian operator with an external potential $\upsilon(\boldsymbol{r})$. Therewith we say that the set $\mathscr{D}$ is the set of υ-representable densities.

2.2.1 Constrained-Search

The restriction over degenerate states can be lifted with the use of the constrained-search proposed by Levy[14]. We feel that is beyond the scope of this work to prove the procedure and instead we present how it works.

We know that ρ_0 can be obtained by quadrature from a given wavefunction Ψ. But there is an infinite number of antisymmetric wavefunctions that are not necessarily from ground-states. It is possible to sift the space of trial wavefunctions to get that one that minimizes F_{HK} . We represent this procedure as,

$$F_{HK} = \min_{\Psi\to\rho_0} \langle\Psi_0|\hat{T}+\hat{V}_{ee}|\Psi_0\rangle. \tag{2.17}$$

The latter equation means that we search over all antisymmetric wavefunctions that can produce ρ_0 consequently minimizing $\langle\Psi_0|\hat{T}+\hat{V}_{ee}|\Psi_0\rangle$. Noting that the sifting modifies the space of trial wavefunctions to contain only those wavefunctions that can produce ρ_0 , we say that the variational search is constrained. Thus, the sifting of wavefunctions not only constrained the space of trial wavefunctions but also extended the domain $\mathscr{D}$ of F_{HK} from υ-representable to N-representable since the space of trial wavefunctions is the entire N-particle Hilbert space. Hence, we can define the universal functional

$$\begin{aligned} F[\rho] &= \min_{\Psi\to\rho} \langle\Psi|\hat{T}+\hat{V}_{ee}|\Psi\rangle \\ &= \langle\Psi_\rho^{min}|\hat{T}+\hat{V}_{ee}|\Psi_\rho^{min}\rangle \\ &= T[\rho]+J[\rho]+E_{xc}[\rho], \end{aligned} \tag{2.18}$$

that search the N-representable space of trial wavefunctions for ρ that gives the minimum expecation value of $\langle\Psi|\hat{T}+\hat{V}_{ee}|\Psi\rangle$. Equations 2.17 and 2.18 are the most important results of our description of the constrained-search procedure. Naturally,if equation 2.18

takes the υ-representable density as input it gives the same result as F_{HK} ,

$$F_{HK}[\rho_0] = F[\rho_0]. \tag{2.19}$$

Furthermore, energy minimization can be split into two parts for a better understanding of the procedure. Within the context of DFT this procedure can be recast as,

$$E_0 = \min_{\rho}\left\{ \min_{\Psi\to\rho} \left[\langle\Psi|\hat{T} + \hat{V}_{ee}|\Psi\rangle + \int d^3\rho(\boldsymbol{r})\upsilon(\boldsymbol{r}) \right] \right\}. \tag{2.20}$$

The inner minimization works by searching all wavefunctions that are associated with a given ρ. Then, the outer minimization searches the space of $\rho(\boldsymbol{r})$ only where this space is of N-representable densities. Conveniently, we can use the universal functional to rewrite equation 2.20 as

$$\begin{aligned} E_0 &= \min_{\rho}\left\{ F[\rho] + \int d^3\rho(\boldsymbol{r})\upsilon(\boldsymbol{r}) \right\} \\ &= \min_{\rho} E[\rho], \end{aligned} \tag{2.21}$$

where the energy as functional of the density is,

$$E[\rho] = F[\rho] + \int d^3\rho(\rho)\upsilon(\boldsymbol{r}). \tag{2.22}$$

Therefore, the constrained-search is essential to turn the theorems of HK into an applicable method by releasing the restrictions of υ-representable densities for the energy minimization procedure. Moreover, it also lifts the restrictions of non-degenerate states.

2.3 The Kohn-Sham Method

Although the HK theorems provide a powerful theory to address the many-electron problem in terms of the electron density, the theory as it is presents a high degree of difficulty due to the calculation of the kinetic energy term $T[\rho]$ present in $F[\rho]$. The kinetic energy of a non-degenerate closed-shell system which can be described by a single

Slater determinant needs to be expressed in terms of the density. But what is the exact form of $T[\rho]$? The first attempts to approximate $T[\rho]$ used the uniform electron gas density as a starting point. These approximations[11, 15] proposed initially by Thomas, Fermi, Weizsacker and Dirac and their extensions fail to give accurate results and are incapable to describe shell structure or chemical bonds. The method proposed by Kohn and Sham[16] (KS) solves the lack of accuracy of the theory by giving up the direct solution with the electron density. They introduced orbitals in order to find a way around the evaluation of the exact kinetic energy. We now present the KS method and its equations.

The KS method begin by defining a non-interacting reference system where the only terms in the Hamiltonian operator,

$$\hat{H}_s = \sum_i^N \left(-\frac{1}{2}\nabla_i^2 \right) + \sum_i^N \upsilon_s(\boldsymbol{r}_i) \tag{2.23}$$

of N electrons are the kinetic and potential operators, respectively. The Schrödinger equation of the non-interacting reference system is,

$$\hat{h}_s \chi_i = \varepsilon_i \chi_i \tag{2.24}$$

where the one-electron Hamiltonian operator is defined as,

$$\hat{h}_s = -\frac{1}{2}\nabla^2 + \upsilon_s(\boldsymbol{r}). \tag{2.25}$$

Solving 2.24 gives the N lowest eigenfunctions χ_i that form the exact ground-state wavefunction of the reference system,

$$\Psi_s(\boldsymbol{x}_1, \ldots, \boldsymbol{x}_N) = \frac{1}{\sqrt{N}} \det\left[\chi_1(\boldsymbol{x}_1) \ldots \chi_N(\boldsymbol{x}_N)\right]. \tag{2.26}$$

Consequently, the density can be written as,

$$\rho(\boldsymbol{r}) = \sum_i^N \sum_\sigma |\chi_i(\boldsymbol{r}, \sigma)|^2. \tag{2.27}$$

It is important to note that $\rho(\boldsymbol{r})$ obtained from Ψ_s is non-interacting v-representable since it is associated to a unique potential $v_s(\boldsymbol{r})$. We face again the issue of uniquely defining a functional for any N-representable density. Yet, we apply the constrained-search to remove the restrictions over $\rho(\boldsymbol{r})$ which yields

$$T_s[\rho] = \min_{\Psi\to\rho} \langle \Psi_s|\hat{T}|\Psi_s\rangle = \langle \Phi_\rho^{min}|\hat{T}|\Phi_\rho^{min}\rangle, \tag{2.28}$$

where Φ_ρ^{min} is the wavefunction that minimizes the kinetic energy of the non-interacting system. Hence, it is now possible to define the kinetic energy for any N-representable $\rho(\boldsymbol{r})$ that can be uniquely decomposed in terms of orbitals,

$$\begin{aligned} T_s[\rho] &= \langle \Psi_{s,\rho}|\sum_i^N \left(-\frac{1}{2}\nabla_i^2\right)|\Psi_{s,\rho}\rangle \\ &= \sum_i^N \langle \psi_i| -\frac{1}{2}\nabla_i^2|\psi_i\rangle. \end{aligned} \tag{2.29}$$

Consequently, the universal functional of the reference system is written as,

$$F_s[\rho] = T_s[\rho] + \int d\boldsymbol{r}\rho(\boldsymbol{r})v_s(\boldsymbol{r}). \tag{2.30}$$

With the reference system defined, KS assumed that ground-state density $\rho(\boldsymbol{r})$ is both interacting and non-interacting. In other words, they assumed that for any interacting system with the ground-state density there is a non-interacting system that has the same ground-state density.

Under the latter assumption KS proposed to write $F[\rho]$ with $T_s[\rho]$ being the principal part of the kinetic energy,

$$F[\rho] = T_s[\rho] + J[\rho] + E_{xc}[\rho]. \tag{2.31}$$

This decomposition of $F[\rho]$ leaves all terms whose forms are unknown to the exchange-correlation energy

$$E_{xc}[\rho] = T[\rho] - T_s[\rho] + V_{ee}[\rho] - J[\rho], \tag{2.32}$$

where we note the difference between kinetic energies of the real and the reference system and the difference between the electron-electron repulsion energy and the classical Coulomb repulsion energy. The first difference in $E_{xc}[\rho]$ is small because $T_s[\rho]$ gives the major contribution to the kinetic energy while in the second difference the result is the non-classical contribution of $V_{ee}[\rho]$ due to the Pauli principle.

The energy of the reference system is written as,

$$\begin{aligned} E_s[\rho] &= F_s[\rho] + \int d\boldsymbol{r}\rho(\boldsymbol{r})\upsilon_s(\boldsymbol{r}) \\ &= T_s[\rho] + \int d\boldsymbol{r}\rho(\boldsymbol{r})\upsilon(\boldsymbol{r}). \end{aligned} \tag{2.33}$$

At this point one can apply the (VM) to $E_s[\rho]$ restricting the search of the minimum to the space of orthonormal orbitals,

$$\langle \chi_i | \chi_j \rangle = \delta_{ij}. \tag{2.34}$$

Then, a new functional which corresponds to the new boundary problem is defined by

$$L[\{\chi_i\}] = E_s[\rho] - \sum_{ij}^{N} \varepsilon_{ij} \int d\tau \chi_i^* \chi_j, \tag{2.35}$$

where ε_{ij} are the Lagrange multipliers. Minimization implies that $\delta L[\{\chi_i\}] = 0$ which yields

$$\begin{aligned} \frac{\delta T_s[\rho]}{\delta\rho(\boldsymbol{r})} + \upsilon_s(\boldsymbol{r}) &= \frac{\delta}{\delta\rho(\boldsymbol{r})} \sum_{ij} \varepsilon_{ij} \int d\tau \chi_i^* \chi_j \\ \frac{\delta T_s[\rho]}{\delta\rho(\boldsymbol{r})} + \upsilon_s(\boldsymbol{r}) &= \mu_s, \end{aligned} \tag{2.36}$$

where μ_s is the chemical potential of the reference system. The energy of the interacting

system is written as,

$$\begin{aligned} E[\rho] &= F[\rho] + \int d\boldsymbol{r}\rho(\boldsymbol{r})\upsilon(\boldsymbol{r}) \\ &= T_s[\rho] + J[\rho] + E_{xc}[\rho] + \int d\boldsymbol{r}\rho(\boldsymbol{r})\upsilon(\boldsymbol{r}). \end{aligned} \tag{2.37}$$

Following the same steps previously used with $E_s[\rho]$ one can minimize $E[\rho]$ yielding

$$\frac{\delta T_s[\rho]}{\delta\rho(\boldsymbol{r})} + \frac{\delta J[\rho]}{\delta\rho(\boldsymbol{r})} + \frac{\delta E_{xc}[\rho]}{\delta\rho(\boldsymbol{r})} + \upsilon(\boldsymbol{r}) = \mu, \tag{2.38}$$

where μ is the chemical potential of the interacting system. Therefore, from the assumption that the ground-state density is both interacting and non-interacting we vary μ_s until we have that $\mu_s = \mu$. Once the chemical potential condition is attained it gives

$$\upsilon_s(\boldsymbol{r}) = \frac{\delta J[\rho]}{\delta\rho(\boldsymbol{r})} + \frac{\delta E_{xc}[\rho]}{\delta\rho(\boldsymbol{r})} + \upsilon(\boldsymbol{r}), \tag{2.39}$$

which completely defines the non-interacting potential also called the effective potential or KS potential. The process that takes one to satisfy the latter condition can be outlined as follows:

1. Initial guess of $\rho(\boldsymbol{r})$

2. Construction of $\upsilon_s(\boldsymbol{r})$ with $\rho(\boldsymbol{r})$:

$$\upsilon_s(\boldsymbol{r}) = \frac{\delta J[\rho]}{\delta\rho(\boldsymbol{r})} + \frac{\delta E_{xc}[\rho]}{\delta\rho(\boldsymbol{r})} + \upsilon(\boldsymbol{r}) \tag{2.40}$$

3. Solution of the N one-electron equations:

$$\left(-\frac{1}{2}\nabla^2 + \upsilon_s(\boldsymbol{r})\right)\chi_i = \varepsilon_i\chi_i \tag{2.41}$$

4. Form new:

$$\rho(\boldsymbol{r}) = \sum_i^N \sum_\sigma |\chi_i(\boldsymbol{r},\sigma)|^2 \tag{2.42}$$

Steps (2) to (4) are repeated until self consistency is obtained which means that the final density satisfies equation 2.42 . Conveniently, the total energy can be calculated with equation 2.37 [10, 13]. Hence, equations 2.40 , 2.41 and 2.42 are the KS equations[16].

The KS method provides a very interesting approximation to the problem of many-electron systems. By introducing orbitals into the HK theorems one obtains the KS equations which can be solved self-consistenly while the theory is, in principle exact. The advantage of calculating the non-interacting kinetic energy exactly while leaving the approximation to the exchange-correlation energy is appealing since the former contributes with a large part to the total energy while the exchange-correlation contribution is small. Therefore, approximations to the exchange-correlation energy are an ongoing field of research in chemistry and physics and are fundamental to the success of DFT.

2.3.1 The Exchange-Correlation Functional

Although the exchange-correlation energy has been defined in equation 2.32 , its expression is not appropriate to construct good approximations since it is formed from two different contributions, one from the difference between kinetic energies of the real system and the reference system and the other from the difference between the $V_{ee}[\rho]$ and $J[\rho]$. Nevertheless, we will see that it is possible to express $E_{xc}[\rho]$ in form more suitable to design new functionals.

Before we proceed, we want to write the exchange-correlation energy in terms of its exchange and correlation components

$$E_{xc}[\rho] = E_x[\rho] + E_c[\rho], \tag{2.43}$$

where the exchange part can be defined exactly for closed-shell systems by the following expression,

$$E_x[\rho] = \langle \Phi_\rho^{min} | \hat{V}_{ee} | \Phi_\rho^{min} \rangle - J[\rho]. \tag{2.44}$$

This is true when Φ_ρ^{min} is a single Slater determinant which is the case in practical calculations. When we have one electron in the system the electron-electron interaction

energy vanish[17] and the exchange energy is defined as,

$$E_x = -J[\rho]. \tag{2.45}$$

Recalling the universal functional of equation 2.18, we define the correlation energy as,

$$\begin{aligned} E_c[\rho] &= E_{xc}[\rho] - E_x[\rho] \\ &= F[\rho] - \{T_s[\rho] + J[\rho] + E_x[\rho]\} \\ &= \langle \Psi_\rho^{min} | \hat{T} + \hat{V}_{ee} | \Psi_\rho^{min} \rangle - \langle \Phi_\rho^{min} | \hat{T} + \hat{V}_{ee} | \Phi_\rho^{min} \rangle \end{aligned} \tag{2.46}$$

Unfortunately, these definitions of the exchange and correlation energies still need to be transformed into more useful expressions to construct approximations.

We now introduce two important functions that are very useful to statistically describe the behavior of a system of N electrons. They are called density matrices[8]: the one-particle density matrix is

$$\gamma_1(\boldsymbol{r}_1\sigma_1, \boldsymbol{r}_1'\sigma_1') = N \int d\boldsymbol{r}_2 \ldots d\boldsymbol{r}_N \Psi^*(\boldsymbol{r}_1\sigma_1, \ldots, \boldsymbol{r}_N\sigma_N)\Psi(\boldsymbol{r}_1'\sigma_1', \boldsymbol{r}_2\sigma_2, \ldots, \boldsymbol{r}_N\sigma_N), \tag{2.47}$$

and two-particle density matrix,

$$\begin{aligned} \gamma_2(\boldsymbol{r}_1\sigma_1, \boldsymbol{r}_2\sigma_2; \boldsymbol{r}_1'\sigma_1', \boldsymbol{r}_2'\sigma_2') = N(N-1) \int d\boldsymbol{r}_3 \ldots d\boldsymbol{r}_N \Psi^*(\boldsymbol{r}_1\sigma_1, \boldsymbol{r}_2\sigma_2, \boldsymbol{r}_3\sigma_3, \ldots, \boldsymbol{r}_N\sigma_N) \\ \times \Psi(\boldsymbol{r}_1'\sigma_1', \boldsymbol{r}_2'\sigma_2', \boldsymbol{r}_3\sigma_3, \ldots, \boldsymbol{r}_N\sigma_N). \end{aligned} \tag{2.48}$$

The first density function γ_1 gives the probability to find an electron in $d\boldsymbol{r}_1\sigma_1$ at point r_1 with spin σ_1 and the second density function γ_2 gives the joint probability to find one electron at $\boldsymbol{r}_1$ with spin σ_1 in volume element $d\boldsymbol{r}_1$ and an electron at $\boldsymbol{r}_2$ with spin σ_2 in volume element $d\boldsymbol{r}_2$. Moreover, the two factors N and $N(N-1)$ enforce the normalization of the equation 2.47 and 2.48, respectively.

Note that the use of primes in these density functions is merely a mathematical artifact to allow us to express expectation values in terms of density functions only. Any

given "real" operator (e.g. with differentiation or integration) will act on the term Ψ in its right side first before we had a chance to take Ψ^* round to the right of the operator to obtain the density[8].

It is straightfoward to verify that the γ_1 normalizes to the number of electrons

$$N = \int d\boldsymbol{r}_1 d\sigma_1 \gamma_1(\boldsymbol{r}_1\sigma_1, \boldsymbol{r}_1\sigma_1), \tag{2.49}$$

and that γ_2 normalizes to the number of electron pairs

$$N(N-1) = \int d\boldsymbol{r}_1 d\sigma_1 d\boldsymbol{r}_2 d\sigma_2 \gamma_2(\boldsymbol{r}_1\sigma_1, \boldsymbol{r}_2\sigma_2; \boldsymbol{r}_1\sigma_1, \boldsymbol{r}_2\sigma_2). \tag{2.50}$$

The spinless versions of γ_1 and γ_2 can be obtained summing over all spin configurations. Averaging the spins of the one-particle and two-particle density matrices yields respectively

$$\rho_1(\boldsymbol{r}_1; \boldsymbol{r}_1') = \int d\sigma_1 \gamma_1(\boldsymbol{r}_1\sigma_1, \boldsymbol{r}_1'\sigma_1), \tag{2.51}$$

and

$$\rho_2(\boldsymbol{r}_1, \boldsymbol{r}_2; \boldsymbol{r}_1', \boldsymbol{r}_2') = \int d\sigma_1 d\sigma_2 \gamma_2(\boldsymbol{r}_1\sigma_1, \boldsymbol{r}_2\sigma_2; \boldsymbol{r}_1'\sigma_1, \boldsymbol{r}_2'\sigma_2). \tag{2.52}$$

The ground-state energy of a general Hamiltonian is then written in terms of the two density functions[10]

$$\begin{aligned} E = &\int d\boldsymbol{r}_1 \left[-\frac{1}{2}\nabla^2_{\boldsymbol{r}_1'} \rho_1(\boldsymbol{r}_1; \boldsymbol{r}_1') \right]_{\boldsymbol{r}_1 = \boldsymbol{r}_1'} + \int d\boldsymbol{r}_1 \left[\rho_1(\boldsymbol{r}_1; \boldsymbol{r}_1') \upsilon(\boldsymbol{r}_1) \right]_{\boldsymbol{r}_1 = \boldsymbol{r}_1'} \\ &+ \frac{1}{2} \int d\boldsymbol{r}_1 d\boldsymbol{r}_2 \left[\frac{\rho_2(\boldsymbol{r}_1, \boldsymbol{r}_2; \boldsymbol{r}_1', \boldsymbol{r}_2')}{|\boldsymbol{r}_1 - \boldsymbol{r}_2|} \right]_{\boldsymbol{r}_1 = \boldsymbol{r}_1'; \boldsymbol{r}_2 = \boldsymbol{r}_2'}, \end{aligned} \tag{2.53}$$

where the subscript $\boldsymbol{r}_1'$ in the Laplacian operator indicates that it acts on this coordinate only and all terms have been defined in section 1. After the operators act on the density

functions, we set $\boldsymbol{r}_1 = \boldsymbol{r}'_1$ before we evaluate the integral to get,

$$\begin{aligned} E &= \int d\boldsymbol{r}_1 \left[-\frac{1}{2}\nabla^2 \rho_1(\boldsymbol{r}_1) \right] + \int d\boldsymbol{r}_1 \rho_1(\boldsymbol{r}_1) \upsilon(\boldsymbol{r}_1) + \frac{1}{2} \int d\boldsymbol{r}_1 d\boldsymbol{r}_2 \frac{\rho_2(\boldsymbol{r}_1, \boldsymbol{r}_2)}{|\boldsymbol{r}_1 - \boldsymbol{r}_2|} \\ &= T + V_{ne} + V_{ee}. \end{aligned} \tag{2.54}$$

We focus on the last term V_{ee} of the ground-state energy. This term gives the electron-electron repulsion energy and depends directly on the spin-independent pair density ρ_2 . The classical part of ρ_2 generates the self-repulsion energy,

$$J[\rho] = \frac{1}{2} \int d\boldsymbol{r}_1 d\boldsymbol{r}_2 \frac{\rho_1(\boldsymbol{r}_1)\rho_1(\boldsymbol{r}_2)}{|\boldsymbol{r}_1 - \boldsymbol{r}_2|}. \tag{2.55}$$

Conveniently, to have the non-classical part written explicitly in V_{ee} we can rewrite ρ_2 as

$$\rho_2(\boldsymbol{r}_1, \boldsymbol{r}_2) = \rho(\boldsymbol{r}_1)\rho(\boldsymbol{r}_2)[1 + h(\boldsymbol{r}_1, \boldsymbol{r}_2)], \tag{2.56}$$

where this same equation *defines* the function $h(\boldsymbol{r}_1, \boldsymbol{r}_2)$ called the pair-correlation function. Rearranging the terms of the latter equation yields: *the exchange-correlation hole density* ρ_{xc}[18],

$$\begin{aligned} \frac{\rho_2(\boldsymbol{r}_1, \boldsymbol{r}_2)}{\rho(\boldsymbol{r}_1)} - \rho(\boldsymbol{r}_2) &= \rho(\boldsymbol{r}_2) h(\boldsymbol{r}_1, \boldsymbol{r}_2) \\ \rho_{xc}(\boldsymbol{r}_1, \boldsymbol{r}_2) &= \rho(\boldsymbol{r}_2) h(\boldsymbol{r}_1, \boldsymbol{r}_2). \end{aligned} \tag{2.57}$$

This density function is central in the design of functional approximations where it describes the exchange and correlation effects by creating a hole around every electron in a system while keeping other electrons from getting close to it. It is possible to analyse its action on the system from the point of view of probability density only, where ρ_{xc} gives the probability of finding one electron at $\boldsymbol{r}_1$ given another electron at $\boldsymbol{r}_2$. More information about ρ_{xc} will be given in this section and the ones that follows.

Hence, it is possible to recast the electron-electron repulsion energy as,

$$\begin{aligned} V_{ee}[\rho] &= \frac{1}{2}\int d\boldsymbol{r}_1 d\boldsymbol{r}_2 \frac{\rho_1(\boldsymbol{r}_1)\rho_1(\boldsymbol{r}_2)}{|\boldsymbol{r}_1-\boldsymbol{r}_2|} + \frac{1}{2}\int d\boldsymbol{r}_1 d\boldsymbol{r}_2 \frac{\rho_1(\boldsymbol{r}_1)\rho_1(\boldsymbol{r}_2)h(\boldsymbol{r}_1,\boldsymbol{r}_2)}{|\boldsymbol{r}_1-\boldsymbol{r}_2|} \\ &= \frac{1}{2}\int d\boldsymbol{r}_1 d\boldsymbol{r}_2 \frac{\rho_1(\boldsymbol{r}_1)\rho_1(\boldsymbol{r}_2)}{|\boldsymbol{r}_1-\boldsymbol{r}_2|} + \frac{1}{2}\int d\boldsymbol{r}_1 d\boldsymbol{r}_2 \frac{\rho_1(\boldsymbol{r}_1)\rho_{xc}(\boldsymbol{r}_1,\boldsymbol{r}_2)}{|\boldsymbol{r}_1-\boldsymbol{r}_2|} \end{aligned} \tag{2.58}$$

It is important to note that the normalization condition for the two-particle density matrix in equation 2.50 has to be present in ρ_{xc} according to the natural definition of the first[8, 10]. Thus, we have after integrating over the volume element $d\boldsymbol{r}_2$ the sum rule for the exchange-correlation hole,

$$\int d\boldsymbol{r}_2 \rho_{xc}(\boldsymbol{r}_1,\boldsymbol{r}_2) = -1. \tag{2.59}$$

This accounts for the reduction in the probability due to the presence of an electron at $\boldsymbol{r}_1$. From the positivity of 2.52 and from equations 2.56 and 2.57 we find that,

$$\rho_{xc}(\boldsymbol{r}_1,\boldsymbol{r}_2) \geqslant -\rho(\boldsymbol{r}_2). \tag{2.60}$$

The objective now is to find a single consistent expression for E_{xc} that at the end can be more tractable to construct density functional approximations. To solve this problem, we use a powerful technique called the *adiabatic connection*.

2.3.2 Adiabatic Connection

The adiabatic connection[18–21] is very useful for the design of functionals since it provides a deep understanding of the physics that governs the exchange and correlation energies thus pointing the path to the construction of their density functionals.

First we add a parameter λ to the universal functional defined in equation 2.18 ,

$$F_\lambda[\rho] = \min_{\Psi\to\rho} \langle\Psi|\hat{T} + \lambda\hat{V}_{ee}|\Psi\rangle = \langle\Psi_\rho^\lambda|\hat{T} + \lambda\hat{V}_{ee}|\Psi_\rho^\lambda\rangle. \tag{2.61}$$

With this new functional when $\lambda = 0$ we obtain, after the minimization under the constrained-

search, the universal functional of the reference system,

$$F_0[\rho] = T_s[\rho]. \tag{2.62}$$

For $\lambda = 1$ we have $F_1[\rho] = F[\rho]$ of the real system,

$$F[\rho] = T[\rho] + V_{ee}[\rho]. \tag{2.63}$$

Clearly, the parameter λ describes how much electron-electron interaction is present in $F[\rho]$. At this point we write the exchange-correlation energy as,

$$\begin{aligned} E_{xc}[\rho] &= V_{ee}[\rho] - J[\rho] + T[\rho] - T_s[\rho] \\ &= T[\rho] + V_{ee}[\rho] - T_s[\rho] - J[\rho] \\ &= F_1[\rho] - F_0[\rho] - J[\rho] \\ &= \int_0^1 d\lambda \frac{\partial F_\lambda[\rho]}{\partial \lambda} - J[\rho]. \end{aligned} \tag{2.64}$$

The integrand in E_{xc} can be simplified using the Hellmann-Feynmann theorem[7] yielding

$$\frac{\partial F_\lambda[\rho]}{\partial \lambda} = \langle \Psi_\rho^\lambda | \lambda \hat{V}_{ee} | \Psi_\rho^\lambda \rangle, \tag{2.65}$$

which is the final piece needed to rewrite $E_{xc}[\rho]$ as,

$$\begin{aligned} E_{xc}[\rho] &= \int_0^1 d\lambda \langle \Psi_\rho^\lambda | \lambda \hat{V}_{ee} | \Psi_\rho^\lambda \rangle - J[\rho] \\ &= \frac{1}{2} \int d\boldsymbol{r}_1 d\boldsymbol{r}_2 \int_0^1 d\lambda \frac{\rho_2^\lambda(\boldsymbol{r}_1, \boldsymbol{r}_2)}{|\boldsymbol{r}_1 - \boldsymbol{r}_2|} - J[\rho]. \end{aligned} \tag{2.66}$$

The average of the pair-density over the parameter λ leads to

$$\int_0^1 d\lambda \rho_2^\lambda(\boldsymbol{r}_1, \boldsymbol{r}_2) = \rho(\boldsymbol{r}_1)\rho(\boldsymbol{r}_2)[1 + \bar{h}(\boldsymbol{r}_1, \boldsymbol{r}_2)], \tag{2.67}$$

where $\bar{h}(\boldsymbol{r}_1, \boldsymbol{r}_2)$ is the average pair correlation function over the coordinate λ. This can

be extended to the exchange-correlation hole

$$\bar{\rho}_{xc}(\boldsymbol{r}_1,\boldsymbol{r}_2) = \int_0^1 d\lambda \rho_{xc}^{\lambda}(\boldsymbol{r}_1,\boldsymbol{r}_2), \tag{2.68}$$

where we have that for $\lambda = 0$ yields the spin-compensated exchange-hole ρ_x . Ultimately, we rewrite the exchange-correlation energy as[18],

$$\begin{aligned} E_{xc}[\rho] &= \frac{1}{2}\int d\boldsymbol{r}_1 d\boldsymbol{r}_2 \frac{\rho(\boldsymbol{r}_1)\rho(\boldsymbol{r}_2)}{|\boldsymbol{r}_1-\boldsymbol{r}_2|} + \frac{1}{2}\int d\boldsymbol{r}_1 d\boldsymbol{r}_2 \rho(\boldsymbol{r}_1)\frac{\rho(\boldsymbol{r}_2)\bar{h}(\boldsymbol{r}_1,\boldsymbol{r}_2)}{|\boldsymbol{r}_1-\boldsymbol{r}_2|} - J[\rho] \\ &= \frac{1}{2}\int d\boldsymbol{r}_1 d\boldsymbol{r}_2 \rho(\boldsymbol{r}_1)\frac{\rho(\boldsymbol{r}_2)\bar{h}(\boldsymbol{r}_1,\boldsymbol{r}_2)}{|\boldsymbol{r}_1-\boldsymbol{r}_2|} \\ &= \frac{1}{2}\int d\boldsymbol{r}_1 d\boldsymbol{r}_2 \rho(\boldsymbol{r}_1)\frac{\bar{\rho}_{xc}(\boldsymbol{r}_1,\boldsymbol{r}_2)}{|\boldsymbol{r}_1-\boldsymbol{r}_2|}. \end{aligned} \tag{2.69}$$

It has been shown[18, 22] that the exchange-correlation energy depends only on the spherical average of the exchange-correlation hole about the reference point $\boldsymbol{r}_1$. To calculate the spherical average of $\bar{\rho}_{xc}(\boldsymbol{r}_1,\boldsymbol{r}_2)$ first we use a change of variable: $\boldsymbol{r}_2 = \boldsymbol{r}_1 + \boldsymbol{u}$ followed by an integration over the angular part of $\boldsymbol{u}$ as follows,

$$\bar{\rho}_{xc}(\boldsymbol{r}_1,u) = \frac{1}{4\pi}\int_0^{2\pi} d\phi_u \int_0^{\pi} d\theta_u \sin\theta_u \bar{\rho}_{xc}(\boldsymbol{r}_1,\boldsymbol{r}_1+\boldsymbol{u}). \tag{2.70}$$

This is the average of the exchange-correlation hole on a sphere of radius $u = |\boldsymbol{r}_1 - \boldsymbol{r}_2|$ which is the interelectronic distance. Substituting equation 2.70 into 2.69 yields,

$$E_{xc}[\rho] = \frac{1}{2}\int d\boldsymbol{r}_1 \rho(\boldsymbol{r}_1)\int_0^{\infty} du 4\pi u^2 \frac{\bar{\rho}_{xc}(\boldsymbol{r}_1,u)}{u}. \tag{2.71}$$

From equation 2.71 we can also define the exchange-correlation energy density

$$\varepsilon_{xc}(\boldsymbol{r}) = \int_0^{\infty} du 4\pi u^2 \frac{\bar{\rho}_{xc}(\boldsymbol{r}_1,u)}{u}, \tag{2.72}$$

that gives the energy per volume of the system and that allows one to write the exchange-

correlation energy in terms of ε_{xc} as,

$$E_{xc}[\rho] = \frac{1}{2}\int d\boldsymbol{r}\varepsilon_{xc}(\boldsymbol{r}). \tag{2.73}$$

The exchange-correlation hole can be further separated into its components

$$\bar{\rho}_{xc}(\boldsymbol{r}_1,\boldsymbol{r}_2) = \rho_x(\boldsymbol{r}_1,\boldsymbol{r}_2) + \bar{\rho}_c(\boldsymbol{r}_1,\boldsymbol{r}_2), \tag{2.74}$$

where $\rho_x(\boldsymbol{r}_1,\boldsymbol{r}_2)$ and $\bar{\rho}_c(\boldsymbol{r}_1,\boldsymbol{r}_2)$ are the exchange and correlation holes, respectively. Note, that the bar over a hole function indicates a dependence on λ. Naturally, the noninteracting reference system or the Kohn-Sham system ($\lambda = 0$), only accounts for Fermi correlation leading to a λ-independent exchange hole ρ_x. However, Coulomb correlation appears for any fiction intermediate value of λ as well as in the real or physical system ($\lambda = 1$) where we have a λ-dependent correlation hole $\bar{\rho}_c$.

Recently, it has been shown[23] that is possible to express the exchange-correlation hole as a product by

$$\rho_{xc}(\boldsymbol{r},u) = \rho_x(\boldsymbol{r},u) f_c(\boldsymbol{r},u), \tag{2.75}$$

where in this context ρ_x is the spherically-averaged exchange hole and f_c is the spherically-averaged correlation factor, respectively.

Up to this point our discussion was restricted to spin-compensated systems: $\rho_\alpha = \rho_\beta$. From now on we change our formulation to that of spin-polarized systems where the exchange-correlation energy can be separated into its parallel-spin and opposite-spin components,

$$E_{xc}[\rho] = E_{xc}[\rho_\alpha,\rho_\beta]. \tag{2.76}$$

The real advantage of spin-polarized over spin-compensated formalism is that the first provides much better information for approximate functionals of spin-polarized systems than the latter[24, 25]. This explains why Local Spin-Density Approximation (LSDA) is better than Local Density Approximation (LDA) where LDA is defined for spin-compensated systems. This kind of treatment is also applied to exchange and correlation energies, and hole densities.

In the 1-determinant approximation, one can write the one-particle density matrix γ_1 in terms of orbitals as

$$\gamma_1(\boldsymbol{r}_1\sigma_1,\boldsymbol{r}'_1\sigma'_1) = \sum_i^{occ} \psi_i(\boldsymbol{r}_1\sigma_1)\psi_i^*(\boldsymbol{r}'_1\sigma'_1), \tag{2.77}$$

and γ_2 assumes the following form in terms of γ_1,

$$\gamma_2(\boldsymbol{r}_1\sigma_1,\boldsymbol{r}_2\sigma_2;\boldsymbol{r}'_1\sigma'_1,\boldsymbol{r}'_2\sigma'_2) = \gamma_1(\boldsymbol{r}_1\sigma_1,\boldsymbol{r}'_1\sigma'_1)\gamma_1(\boldsymbol{r}_1\sigma_1,\boldsymbol{r}'_2\sigma'_2) - \gamma_1(\boldsymbol{r}_2\sigma_2;\boldsymbol{r}'_1\sigma'_1)\gamma_1(\boldsymbol{r}_1\sigma_1,\boldsymbol{r}'_2\sigma'_2). \tag{2.78}$$

To move on further we want to write the spinless one-particle density matrix ρ_1 defined in equation 2.51 (now in the 1-determinant approximation) explicitly with its two spin components as,

$$\begin{aligned} \rho_1(\boldsymbol{r}_1,\boldsymbol{r}'_1) &= \gamma_1(\boldsymbol{r}_1\alpha,\boldsymbol{r}'_1\alpha) + \gamma_1(\boldsymbol{r}_1\beta,\boldsymbol{r}'_1\beta) \\ &= \rho_{1\alpha}(\boldsymbol{r}_1,\boldsymbol{r}'_1) + \rho_{1\beta}(\boldsymbol{r}_1,\boldsymbol{r}'_1). \end{aligned} \tag{2.79}$$

This result represents the average of spin of the diagonal elements of γ_1. Moreover, when $\boldsymbol{r}_1 = \boldsymbol{r}'_1$ we have the electron spin density,

$$\rho_\alpha(\boldsymbol{r}_1) = \rho_{1\alpha}(\boldsymbol{r}_1,\boldsymbol{r}_1). \tag{2.80}$$

This can be expressed in terms of orbitals as

$$\rho_\alpha(\boldsymbol{r}_1) = \sum_i^{\alpha} \phi_i(\boldsymbol{r}_1)\phi_i^*(\boldsymbol{r}_1), \tag{2.81}$$

where we have used the spatial part of the spin orbital $\psi_i = \phi_i\alpha$. Similar equations exists for beta spin. Therefore, with equations 2.78 , 2.79 and 2.80 we find that the spinless pair density is

$$P_2(\boldsymbol{r}_1,\boldsymbol{r}_2) = P_{2\alpha\alpha}(\boldsymbol{r}_1,\boldsymbol{r}_2) + P_{2\beta\beta}(\boldsymbol{r}_1,\boldsymbol{r}_2) + P_{2\alpha\beta}(\boldsymbol{r}_1,\boldsymbol{r}_2) + P_{2\beta\alpha}(\boldsymbol{r}_1,\boldsymbol{r}_2), \tag{2.82}$$

where

$$\begin{aligned} P_{2\alpha\alpha}(\boldsymbol{r}_1,\boldsymbol{r}_2) &= \rho_\alpha(\boldsymbol{r}_1)\rho_\alpha(\boldsymbol{r}_2) - \rho_{1\alpha}(\boldsymbol{r}_1,\boldsymbol{r}_2)\rho_{1\alpha}(\boldsymbol{r}_2,\boldsymbol{r}_1) \\ P_{2\alpha\beta}(\boldsymbol{r}_1,\boldsymbol{r}_2) &= \rho_\alpha(\boldsymbol{r}_1)\rho_\beta(\boldsymbol{r}_2). \end{aligned} \tag{2.83}$$

Expressions for $P_{2\beta\beta}$ and $P_{2\beta\alpha}$ are naturally similar to the last two equations. Thus, the spinless pair-density function is written generally as,

$$P_{2\sigma\sigma'}(\boldsymbol{r}_1,\boldsymbol{r}_2) = \rho_\sigma(\boldsymbol{r}_1)\rho_{\sigma'}(\boldsymbol{r}_2) - \delta_{\sigma\sigma'}\rho_{1\sigma}(\boldsymbol{r}_2,\boldsymbol{r}_1)\rho_{1\sigma'}(\boldsymbol{r}_1,\boldsymbol{r}_2). \tag{2.84}$$

Clearly, in the 1-determinant approximation the Fermi correlation is the only correlation taken into consideration through the same-spin pair probability. Hence, we concentrate our attention on the same-spin pair-density function,

$$P_{2\sigma\sigma}(\boldsymbol{r}_1,\boldsymbol{r}_2) = \rho_\sigma(\boldsymbol{r}_1)\rho_\sigma(\boldsymbol{r}_2) - \rho_{1\sigma}(\boldsymbol{r}_2,\boldsymbol{r}_1)\rho_{1\sigma}(\boldsymbol{r}_1,\boldsymbol{r}_2). \tag{2.85}$$

Rearranging the terms of $P_{2\sigma\sigma}$, we define the exchange-hole density as,

$$\begin{aligned} \frac{P_{2\sigma\sigma}(\boldsymbol{r}_1,\boldsymbol{r}_2)}{\rho_\sigma(\boldsymbol{r}_1)} &= \rho_\sigma(\boldsymbol{r}_2) - \frac{\rho_{1\sigma}(\boldsymbol{r}_2,\boldsymbol{r}_1)\rho_{1\sigma}(\boldsymbol{r}_1,\boldsymbol{r}_2)}{\rho_\sigma(\boldsymbol{r}_1)} \\ \frac{P_{2\sigma\sigma}(\boldsymbol{r}_1,\boldsymbol{r}_2)}{\rho_\sigma(\boldsymbol{r}_1)} - \rho_\sigma(\boldsymbol{r}_2) &= -\frac{\rho_{1\sigma}(\boldsymbol{r}_2,\boldsymbol{r}_1)\rho_{1\sigma}(\boldsymbol{r}_1,\boldsymbol{r}_2)}{\rho_\sigma(\boldsymbol{r}_1)} \\ \rho_x(\boldsymbol{r}_1,\boldsymbol{r}_2) &= -\frac{\rho_{1\sigma}(\boldsymbol{r}_2,\boldsymbol{r}_1)\rho_{1\sigma}(\boldsymbol{r}_1,\boldsymbol{r}_2)}{\rho_\sigma(\boldsymbol{r}_1)}. \end{aligned} \tag{2.86}$$

The exchange-hole plays a very important role in the design of exchange-correlation energy functionals[26]. We would like to postpone the description of its role and properties where we will also present the exchange and correlation energy functionals.

The $\rho_x(\boldsymbol{r}_1,\boldsymbol{r}_2)$ accounts for the reduction in the electron density $\rho_\sigma(\boldsymbol{r}_2)$ because of the spreading out of electron density $\rho_\sigma(\boldsymbol{r}_1)$ where $\boldsymbol{r}_1$ is the position of the reference electron. From its definition we verify that ρ_x is always negative.

It follows that ρ_x satisfies the sum rule,

$$\int d\boldsymbol{r}_2 \rho_x(\boldsymbol{r}_1, \boldsymbol{r}_2) = -1. \tag{2.87}$$

This is a very important result since it shows that the probability of finding one electron with spin σ at $\boldsymbol{r}_2$ given an electron at $\boldsymbol{r}_1$ is reduced by 1. The sum rule is due to the orthonormality of the orbitals present in the 1-determinant approximation.

Another important analytical property of ρ_x in the 1-determinant approximation is called the on-top value[27]. When $\boldsymbol{r}_1 = \boldsymbol{r}_2$ we have from equations 2.77 and 2.84 that

$$\rho_x(\boldsymbol{r}_1, \boldsymbol{r}_1) = -\rho_\sigma(\boldsymbol{r}_1), \tag{2.88}$$

where ρ_x is determined only by the density of the reference electron at $\boldsymbol{r}_1$. These conditions are quite restrictive and can be used to approximate exchange energy functionals based on models of ρ_x.

Substituting equation 2.85 into V_{ee} and 2.44 respectively we obtain the exchange energy,

$$E_{x\sigma}[\rho_\sigma] = \frac{1}{2} \int d\boldsymbol{r}_1 d\boldsymbol{r}_2 \frac{\rho_\sigma(\boldsymbol{r}_1)\rho_x(\boldsymbol{r}_1, \boldsymbol{r}_2)}{|\boldsymbol{r}_1 - \boldsymbol{r}_2|}. \tag{2.89}$$

The functional defined in equation 2.88 is *exact* in the context of DFT[10, 24, 26]. The same expression appears in the Hartree-Fock (HF) theory[9]. Although they share the same form, they are obtained from different equations and calculated with different types orbitals resulting in different quantities.

It is also interesting to average the angular part of the exchange-hole since E_x depends only on the spherical average of ρ_x. This is achieved integrating ρ_x over all its angular coordinates,

$$\rho_x(\boldsymbol{r}_1, u) = \frac{1}{4\pi} \int_0^{2\pi} d\phi_u \int_0^{\pi} d\theta_u \sin\theta_u \rho_x(\boldsymbol{r}_1, \boldsymbol{r}_1 + \boldsymbol{u}). \tag{2.90}$$

Conveniently, this allows one to write the E_x as,

$$E_{x\sigma}[\rho_\sigma] = \frac{1}{2} \int d\boldsymbol{r}_1 \rho(\boldsymbol{r}_1) \int_0^{\infty} du 4\pi u^2 \frac{\rho_x(\boldsymbol{r}_1, u)}{u}. \tag{2.91}$$

From the definition of ρ_x we find that this result is always negative.

Now, we go back to the separation of the exchange-correlation hole presented in equations 2.74 to define the correlation hole by

$$\bar{\rho}_c(\boldsymbol{r}_1,\boldsymbol{r}_2) = \bar{\rho}_{xc}(\boldsymbol{r}_1,\boldsymbol{r}_2) - \rho_x(\boldsymbol{r}_1,\boldsymbol{r}_2). \tag{2.92}$$

From equations 2.67 and 2.68 we note that the exchange hole is independent of the parameter λ while the correlation hole is λ-dependent. This dependence of $\bar{\rho}_c$ on λ imposes additional difficult to the already very complicated task of calculating $\bar{\rho}_c$ by first-principle methods[28].

Also, the correlation hole satisfies the sum rule by

$$\int d\boldsymbol{r}_2 \bar{\rho}_c(\boldsymbol{r}_1,\boldsymbol{r}_2) = 0, \tag{2.93}$$

where the latter is a consequence of the sum rules of the exchange-correlation and exchange holes. Equation 2.93 indicates that ρ_c must have negative and positive contributions. At the position of the reference electron $\boldsymbol{r}_1$ the correlation hole is nonpositive,

$$\bar{\rho}_c(\boldsymbol{r}_1,\boldsymbol{r}_1) \leqslant 0. \tag{2.94}$$

The correlation energy is then given by,

$$E_{c\sigma}[\rho_\sigma] = \frac{1}{2}\int d\boldsymbol{r}_1 d\boldsymbol{r}_2 \frac{\rho_\sigma(\boldsymbol{r}_1)\bar{\rho}_c(\boldsymbol{r}_1,\boldsymbol{r}_2)}{|\boldsymbol{r}_1-\boldsymbol{r}_2|}. \tag{2.95}$$

As mentioned before, integrals involving $\bar{\rho}_c$ are very complicated to calculate from first-principle methods and need to be approximated.

By applying on $\bar{\rho}_c$ the same procedure used to calculate the spherical average of ρ_{xc} and ρ_x we find that the correlation energy in terms of $\rho_c(\boldsymbol{r}_1,u)$ is,

$$E_{c\sigma}[\rho_\sigma] = \frac{1}{2}\int d\boldsymbol{r}_1 \rho(\boldsymbol{r}_1) \int_0^\infty du 4\pi u^2 \frac{\bar{\rho}_c(\boldsymbol{r}_1,u)}{u}. \tag{2.96}$$

In this section we developed the KS method and presented techniques that made possible the study of important physical properties of E_{xc}. The next section comes to show why we need to construct approximations to this functional. Also, what can be used and some techniques developed in the last years for this task.

2.4 Exchange-Correlation Functional Approximation

Approximations for the exchange-correlation functional are fundamental for the development of DFT. From its conventional decomposition into its exchange and correlation components we shown that the true form of the former,defined in equation 2.89, is exact through the exchange hole. However, the exact form of the correlation hole is unknown. Hence, one would be tempted to construct an exchange-correlation functional using the exact exchange functional and approximating the correlation part only. Unfortunately, this is not as straightfoward as it seems[29].

First, in DFT we seek functionals that depend on the density directly which is not the case for E_x. This is a big issue since we need to evaluate the derivatives of E_x with respect to $\rho(\boldsymbol{r})$ to obtain the exchange potential.

Secondly, when E_x is added to E_c to form the E_{xc}, part of the error cancelation that occurs in the sum is lost resulting in poor accuracy. The error cancelation will be explained using the concept of non-locality of hole densities in the next part of this section.

Hence, both the exchange and correlation functionals need to be approximated. We are going to introduce one important concept for the construction of density functionals and then we will present what one might use to construct reliable density functionals and the trends of these approximations.

2.4.1 Non-locality of hole densities

An important concept in DFT is the locality of functionals. A local functional has in its form an integrand that needs to be evaluated at the integration variable only. The exchange-correlation functional is an example of a local functional. It depends on $\varepsilon_{xc}(\boldsymbol{r}_1)$ which needs to be integrated over $\boldsymbol{r}$ only. Functionals whose integrands need to be

evaluated at two integration variables are said to be nonlocal[10]. This is the case of the exchange functional where its integrand involves the exchange hole $\rho_x(\boldsymbol{r}_1,\boldsymbol{r}_2)$.

We now analyse how the kernel of the exchange functional, the exchange hole, reacts on different environments. From equation 2.85 and its definition in equation 2.86, the exchange hole in one electron systems is the negative of the density at $\boldsymbol{r}_2$. This says that the probability density to find an electron at $\boldsymbol{r}_2$ is independent of reference point $\boldsymbol{r}_1$. Hence, the exchange hole does not follow the reference point $\boldsymbol{r}_1$ [29]. In general, when more than one orbital is occupied the exchange hole depend on both positions $\boldsymbol{r}_1$ and $\boldsymbol{r}_2$. When two electrons with the same spin configuration occupy different orbitals, the exchange hole changes to,

$$\rho_x(\boldsymbol{r}_1,\boldsymbol{r}_2) = -\frac{\psi_1^2(\boldsymbol{r}_1\sigma)\psi_1^2(\boldsymbol{r}_2\sigma)+\psi_2^2(\boldsymbol{r}_1\sigma)\psi_2^2(\boldsymbol{r}_2\sigma)+2\psi_1(\boldsymbol{r}_1\sigma)\psi_2(\boldsymbol{r}_1\sigma)\psi_1(\boldsymbol{r}_2\sigma)\psi_2(\boldsymbol{r}_2\sigma)}{\rho_\sigma(\boldsymbol{r}_1)}. \tag{2.97}$$

The first term in the right hand side of equation 2.97 is the product of the orbital densities at point $\boldsymbol{r}_1$ and $\boldsymbol{r}_2$, respectively. The second term in the right hand side we also have the product of the orbital densities but with switched positions. The last term accounts for those regions where there is overlap between the orbitals ψ_1 and ψ_2. We say that the exchange hole is delocalized in those regions. In an atom, the last term has a significant importance in the intershell and outer valence regions. In molecular systems the exchange hole may be delocalized over several centers.

For instance take the special case of stretched $H_2{}^+$ [2]. Rather simple, this molecule illustrates the problem of delocalization of $\rho_{x\sigma}$ in molecules. In this case, $\rho_{x\sigma}$ is half the value of the molecular orbital σ_g equally divided between the two cores. When the reference point $\boldsymbol{r}_1$ is close to one of the cores, the value of $\rho_{x\sigma}$ has only half an electron while the other half is in the other core.

Now, we want to explain with the aid of hole densities how the error cancelation occurs when we sum E_x and E_c to obtain E_{xc}. The exchange-correlation hole density is in great extent localized about the reference electron $\boldsymbol{r}_1$. As mentioned before, we know that the exact exchange hole may be strongly delocalized in molecular systems. Therefore, the correlation hole must be strongly delocalized so to cancel out the nonlocality of the

exchange hole.

Hence, to use the exact exchange functional together with an approximate correlation functional is not clever since one needs to construct approximate correlation functionals that would be able to cancel out the effects of the first which is not an easy task. If instead of the exact exchange functional we construct local approximations for both exchange and correlation functionals we can take advantage of the cancellation of errors and obtain an accurate functional.

In practice, when designing a functional we have a few ingredients and non-systematic procedures to rely upon.

2.4.2 Ingredients

The conception of new approximate functionals may look like an art since only a few procedures and ingredients are available to guide us. As we mentioned before, the central functional in KS DFT is E_{xc} which can, in this context, be written as

$$E_{xc\sigma}[\rho_\sigma] = \int d\boldsymbol{r}\varepsilon_{xc\sigma}(p_1, p_2, p_3, p_4, p_5, \ldots), \tag{2.98}$$

where $\varepsilon_{xc\sigma}$ is the exchange-correlation energy density and p_i are density-dependent parameters or ingredients. Notice that the requirement now is for a local E_{xc} which depends directly on ρ. Although we seek a local $E_{xc\sigma}$, when only local ingredients are used the accuracy is insatisfactory. Here, we present the most used ingredients. They are the modulus of the gradient of the density

$$p_1 = |\nabla\rho_\sigma(\boldsymbol{r})|, \tag{2.99}$$

the Laplacian of the density

$$p_2 = \nabla^2\rho_\sigma(\boldsymbol{r}), \tag{2.100}$$

the non-interacting kinetic energy density (with KS orbitals) $\tau_\sigma(\boldsymbol{r})$

$$p_3 = \sum_{k=1}^{\sigma} |\nabla \phi_k(\boldsymbol{r})|, \tag{2.101}$$

the closed-shell exact-exchange energy density $\varepsilon_{x\sigma}(\boldsymbol{r}_1)$

$$p_4 = -\sum_{k,l=1}^{N/2} \int d\boldsymbol{r}_2 \frac{\phi_k(\boldsymbol{r}_1)\phi_k^*(\boldsymbol{r}_2)\phi_l^*(\boldsymbol{r}_1)\phi_l(\boldsymbol{r}_2)}{|\boldsymbol{r}_1 - \boldsymbol{r}_2|}, \tag{2.102}$$

and the paramagnetic-current density $\boldsymbol{j}_\sigma(\boldsymbol{r})$,

$$p_5 = -\frac{i}{2} \sum_{k=1}^{occ} [\phi_k^*(\boldsymbol{r})\nabla\phi_k(\boldsymbol{r}) - \phi_k(\boldsymbol{r})\nabla\phi_k^*(\boldsymbol{r})]. \tag{2.103}$$

Derivatives of the density and any ingredient that does not depend directly on the density is seen as a semi-local ingredient which is the case for $\nabla\rho_\sigma$, $\nabla^2\rho_\sigma$, τ_σ and $\boldsymbol{j}_\sigma$ while $\varepsilon_{x\sigma}$ is completely nonlocal. Note that nonlocal ingredients need to be gauge-independent and invariant with respect to unitary transformation of the KS orbitals. Moreover, it is crucial to understand how exchange and correlation functionals change when the density is scaled by a uniform coordinate transformation.

2.4.3 Uniform Coordinate Scaling Transformation

Many properties of the exact exchange and correlation functionals were derived by Levy and Perdew[30–33]. These properties provide information on how E_x and E_c behave under a coordinate scaling transformation of the density and they are present in a set of conditions used to approximate functionals. What follows is a very short presentation of how the density, the exchange and correlation functionals behave under the uniform coordinate scaling transformation. A full description of this transformation is given in the appendix I of this work.

The uniform scaling of the density defined by

$$\rho_\gamma(\boldsymbol{r}) = \gamma^3 \rho(\gamma\boldsymbol{r}), \tag{2.104}$$

is the most important transformation. In equation 2.104, γ is a constant that when varied scales uniformly all components of $\boldsymbol{r}$. Hence, γ can contract or expand the density while leaving unaffected the integral involving ρ_γ in all space,

$$\int d\boldsymbol{r}\rho_\gamma(\boldsymbol{r}) = \gamma^3 \int d\boldsymbol{r}\rho(\gamma\boldsymbol{r}) = N. \tag{2.105}$$

The Hartree electrostatic self-repulsion term scales uniformly as,

$$J[\rho_\gamma] = \gamma J[\rho]. \tag{2.106}$$

Under a uniform coordinate scaling the non-interacting kinetic energy behaves as,

$$T_s[\rho_\gamma] = \gamma^2 T_s[\rho]. \tag{2.107}$$

The exchange functional has a simple coordinate scaling,

$$E_x[\rho_\gamma] = \gamma E_x[\rho]. \tag{2.108}$$

At the high-density limit $\gamma \to \infty$ it is easy to see that T_s will have the biggest contribution to the total energy defined in equation 2.37 . In an ionic system with a very large nuclear charge, the density would be distorted towards the nucleus with J and E_x contributing negligibly to the total energy. On the other hand, when $\gamma \to 0$, J and E_x give the biggest contributions to the total energy.

The correlation functional has a complex scaling relation,

$$\begin{aligned} E_c[\rho_\gamma] &< \gamma E_c[\rho] (\gamma < 1), \\ E_c[\rho_\gamma] &> \gamma E_c[\rho] (\gamma > 1). \end{aligned} \tag{2.109}$$

At the high limit of γ we have

$$\lim_{\gamma\to\infty} E_c[\rho_\gamma] > -\infty. \tag{2.110}$$

While at the low limit when $\gamma \to 0$, we obtain

$$E_c[\rho_\gamma] = \gamma D[\rho] + \ldots, \tag{2.111}$$

where $D[\rho]$ is an unknown functional.

The discrepancy between the scaling relations of E_x and E_c comes from the different definitions of the constrained-search for these functionals. In equation 2.44 the constrained-search for Φ_ρ^{min} *involves* $\hat{T}$ to find Φ_ρ^{min} but it only depends directly on V_{ee} which scales as,

$$V_{ee}[\rho_\gamma] = \gamma^{-1} V_{ee}[\rho]. \tag{2.112}$$

These two facts accounts for the simple scale relation of E_x. The correlation functional has the constrained-search for Ψ_ρ^{min} defined in equation 2.46 . In this case, the the constrained-search depends directly on two operators with different properties. The first, $\hat{T}$, is of homogeneous degree -2 while V_{ee} scales as shown in equation 2.112. This fact leads to the complicated scaling relation of E_c shown in equation 2.109. Consequently, approximations to E_c demand quite an effort in comparison to approximations to E_x.

2.5 Strategies for the Design of Functionals

The classification of density functional approximations by their level of sophistication was proposed by John Perdew and is called the "Jacob's Ladder"[34]. The idea is to have in each rung a number of conditions that have well defined levels of sophistication used to design functionals. It is important to clarify that climbing higher on the ladder does not necessarily gives a strictly more accurate functional.

At the bottom of the ladder we have the LSDA which is the first approximation proposed by Hohenberg and Kohn[12],

$$E_{xc}^{LSDA}[\rho_\sigma] = \int d\boldsymbol{r} \varepsilon_\sigma(\rho_\sigma). \tag{2.113}$$

The second step belongs to the Generalized Gradient Approximation (GGA). These

functionals depend on ρ_σ and $\nabla\rho_\sigma$,

$$E_{xc}^{GGA}[\rho_\sigma] = \int d\boldsymbol{r}\varepsilon_\sigma(\rho_\sigma, \nabla\rho_\sigma). \tag{2.114}$$

The meta-GGA (MGGA) appear in the third step because they use τ_σ and may also use $\nabla^2\rho_\sigma$,

$$E_{xc}^{MGGA}[\rho_\sigma] = \int d\boldsymbol{r}\varepsilon_\sigma(\rho_\sigma, \nabla\rho_\sigma, \tau_\sigma, \nabla^2\rho_\sigma). \tag{2.115}$$

In the fourth rung we found the hyper-GGA (HGGA) that use the exact exchange energy density $\varepsilon_{x\sigma}^{exact}$ in addition to the previous properties,

$$E_{xc}^{HGGA}[\rho_\sigma] = \int d\boldsymbol{r}\varepsilon_\sigma(\rho_\sigma, \nabla\rho_\sigma, \tau_\sigma, \nabla^2\rho_\sigma, \varepsilon_{x\sigma}^{exact}). \tag{2.116}$$

Higher rungs involve properties that depend on non-occupied KS orbitals[26]. The price to climb the ladder is the computational cost needed to calculate elaborated quantities such as $\varepsilon_{x\sigma}^{exact}$.

For a large extent, DFT has gained its fame with GGA. Many approximate density functionals, including the BLYP [35, 36] and PBE [37], are able to give reliable results for many properties such as geometries, vibrational frequencies, charge distributions, binding energies, etc[38–40].

2.5.1 The Generalized Gradient Approximation approach

Functionals based on GGA and MGGA by constriction are constrained to satisfacty known conditions of the exchange-correlation functional such as the asymptotic behavior of v_x [41, 42], lower and upper limits of E_{xc}[43], scaling relations of the density[30–33].

Here we focus on the GGA for exchange energy only. The starting point of this approach is the spin-unpolarized exchange energy functional written in terms of the exchange energy density

$$E_x[\rho] = \int d\boldsymbol{r}_1\rho(\boldsymbol{r}_1)\varepsilon_x(\boldsymbol{r}_1), \tag{2.117}$$

where the exchange energy density is,

$$\varepsilon_x(\boldsymbol{r}_1) = \frac{1}{2}\int d\boldsymbol{r}_2 \frac{\rho_x(\boldsymbol{r}_1,\boldsymbol{r}_2)}{|\boldsymbol{r}_1-\boldsymbol{r}_2|}. \tag{2.118}$$

Note that ρ_x is the exchange hole of a spin-unpolarized system defined as

$$\rho_x = -\frac{|\rho_1(\boldsymbol{r}_1,\boldsymbol{r}_2)|^2}{2\rho(\boldsymbol{r}_1)}, \tag{2.119}$$

where

$$\rho_1(\boldsymbol{r}_1,\boldsymbol{r}_2) = 2\sum_{i=1}^{occ} \psi_i^*(\boldsymbol{r}_1)\psi_i(\boldsymbol{r}_2) \tag{2.120}$$

is the Kohn-Sham one-particle density matrix. The use of the spin-unpolarized version of E_x is justifiable by the spin-scaling relation which shows that,

$$E_x[\rho_\alpha,\rho_\beta] = \frac{1}{2}E_x[2\rho_\alpha] + \frac{1}{2}E_x[2\rho_\beta]. \tag{2.121}$$

Generally, GGA are conceived in their spin-unpolarized forms because their formulations are easy to handle. Once the GGA is built, it is straightfoward to obtain their spin-polarized[24, 25, 44, 45] form through equation 2.121.

When the exchange hole of the GGA functional satisfies the uniform coordinate scaling property of equation 2.104, we can write it in terms of a dimensionless function J_x[45],

$$\rho_x(\rho,y,s) = \rho J_x(y,s) \tag{2.122}$$

where we have used the interelectronic distance

$$y = k_F u, \tag{2.123}$$

and the reduced density gradient

$$s = \frac{|\nabla\rho|}{2k_F\rho}. \tag{2.124}$$

Notice that both y and s are dimensionless quantities while the latter use the Fermi wave-

vector defined by,

$$k_F = (3\pi\rho)^{1/3}. \tag{2.125}$$

The reduced density gradient goes from 0 in regions where the density is strongly uniform to ∞ in regions where the density is weakly uniform thus providing an index of inhomogeneity of the density.

The construction of GGA[46] is written as

$$E_x^{GGA}[\rho] = \int d\boldsymbol{r}_1 \rho(\boldsymbol{r}_1) \varepsilon_x^{GGA}[\rho, s], \tag{2.126}$$

where

$$\varepsilon_x^{GGA}[\rho, s] = \varepsilon_x^{LDA}[\rho] F_x[s]. \tag{2.127}$$

$F_x[s]$ is called the enhancement factor and is a functional of s. It must reduce to unity when $s = 0$, so it can recover the LDA exchange energy. Its explicit form is given by,

$$\frac{8}{9} \int_0^\infty dy\, y J_x[s, y] = -F_x[s]. \tag{2.128}$$

Another important quantity present in the construction of GGA is the system-averaged exchange hole,

$$\langle \rho_x(u) \rangle = \frac{1}{N} \int d\boldsymbol{r}_1 \rho^2(\boldsymbol{r}_1) J_x[s, y]. \tag{2.129}$$

There are three main approaches to construct enhancement factors F_x. The first imposes a number of known exact conditions on the system- and spherically-averaged exchange hole. The second approach uses exact conditions of the exchange energy E_x while the last one uses exact conditions of the exchange energy density ε_x. We want to emphasize that there is no strict route that leads to an accurate functional, instead one should try to satisfy a number of conditions in a manner that leads to accurate functionals. For instance, both F_x^{PW86} and F_x^{91} of PW86[46] and PW91[47] functionals, were based on the first approach. The enhancement factor of the PBE [37], F_x^{PBE} is constructed using the second approach while using the first one as a guide. Becke's F_x^{88}[35] is based on both second and third approaches. The same steps and approaches employed

in constructing GGA are shared with MGGA[48] while the latter have in addition to the GGA ingredients the kinetic energy density τ.

One may also choose to fit the functional approximations to experimental results. This would cause unsatisfactory results when the functional is used outside its training set. By contrast, non-empirical functional approximations can be design to satisfy a set of constraints that yields a transferable functional that is uniformly accurate for different systems.

In the next rung passing over GGA and MGGA respectively we find functionals that mix exact properties to those used in lower rungs.

2.5.2 The Hybrid Approach

In this type of strategy, a quota of the exact exchange energy ε_x^{exact} is used in the construction process. Functionals based on this approach are called hybrids and some of the most important hybrids are the B3[49], PBE0[50, 51] and TPSSh[52]. These functionals have proven to be very accurate with respect to the estimation of several properties such as geometries, vibrational frequencies, charge distributions, binding energies, etc[38–40].

The addition of ε_x^{exact} leads to very accurate approximate functionals since here the non-local behavior of the exchange hole is captured naturally by the exact exchange kernel.

The first class of these functionals are called global hybrids and they have the following form (here we use E_{xc} in its spin-compensated form)

$$E_{xc}[\rho] = \int d\boldsymbol{r}\alpha\varepsilon_x^{exact}(\boldsymbol{r}) + (1-\alpha)\varepsilon_x(\boldsymbol{r}) + \varepsilon_c(\boldsymbol{r}), \tag{2.130}$$

where α is the mixing fraction a parameter which determines a quota of the exact exchange-energy density to be used. Note that α is a system-independent parameter.

A more interesting form for E_{xc} known as local hybrid has a system-dependent pa-

rameter $\alpha(\boldsymbol{r})$,

$$E_{xc}[\rho] = \int d\boldsymbol{r}\alpha(\boldsymbol{r})\varepsilon_x^{exact}(\boldsymbol{r}) + (1-\alpha(\boldsymbol{r}))\varepsilon_x(\boldsymbol{r}) + \varepsilon_c(\boldsymbol{r}). \tag{2.131}$$

Conveniently, the mixing fraction must vary between 0 and 1 where the first global hybrids had quotas up to a maximum of 25% of the ε^{exact}. In general, the mixing fractions are based on indexes that can indicate how much the hole is delocalized over a region in real space. This information can be obtained from quantities such as the kinetic energy densities and those involving derivatives of the density.

2.5.3 Exchange Hole Modelling

Another strategy for designing exchange density functionals is the modeling of the exchange hole function[26]. In this approach one proposes analytical exchange-hole models that can satisfy all known conditions of the exact exchange hole which are: the negativity of the hole, the normalization and its short-range behavior about the interelectronic distance.

Here, we adopt a different way to introduce the concept of exchange hole modeling. We are going to present two successful models that are related to crucial paradigms in condensed matter physics and quantum chemistry. In condensed matter physics one has the slowly varying density limit. The two others are the one- and two-electron densities limit that belong to quantum chemistry. By crucial we mean that functionals which cover both limits might attein a good level of accuracy in both fields.

The LSDA exchange hole[53] is known in condensed matter physics where it has been used as a starting point for many exchange functional approximations. It was also used in functionals conceived in quantum chemistry, such as PBE[37], PW91[47], TPSS[48] and many others. The BR model hole[3], based on quantum chemistry field, is also special since it can recover the one-electron density limit exactly.

Before we proceed to the exchange hole models we would like to introduce a very useful feature for design new hole models: the second-order Taylor expansion of the exact spherically-averaged exchange hole.

2.5.3.1 The Second-Order Expansion of the Exchange Hole

Becke[54] was the first to expand the spherically-averaged exchange hole in powers of u, the interelectronic distance. This expansion in the range[55] of $0 < u < |\boldsymbol{r}_1|$, where $\boldsymbol{r}_1$ is the position of the reference electron, has the form of a Taylor series. Here, we present the mathematical development of the expansion and the form of the second-order expansion.

Generally, the Taylor expansion of a function of two coordinates $f(\boldsymbol{r}_1, \boldsymbol{r}_2)$ is written as

$$f(\boldsymbol{r}_1, \boldsymbol{r}_1 + \boldsymbol{u}) = \sum_{j=0}^{\infty} \frac{1}{j!} (\boldsymbol{u} \cdot \nabla_{\boldsymbol{r}_2})^j f(\boldsymbol{r}_1, \boldsymbol{r}_2)|_{\boldsymbol{r}_2 = \boldsymbol{r}_1}, \tag{2.132}$$

where we have used $\boldsymbol{r}_2 = \boldsymbol{r}_1 + \boldsymbol{u}$.

In the last equation, one can easily identify the Taylor series of the exponential function which is,

$$\sum_{j=0}^{\infty} \frac{1}{j!} (\boldsymbol{u} \cdot \nabla_{\boldsymbol{r}_2})^j = e^{\boldsymbol{u} \cdot \nabla_{\boldsymbol{r}_2}}. \tag{2.133}$$

This last quantity can be seen as an operator. Before we apply it to $f(\boldsymbol{r}_1, \boldsymbol{r}_2)$ we need to calculate its spherical averaged to obtain,

$$\begin{aligned}
\langle e^{\boldsymbol{u} \cdot \nabla_{\boldsymbol{r}_2}} \rangle &= \frac{1}{4\pi} \int_0^{2\pi} \int_0^{\pi} d\phi d\theta \sin(\theta) e^{\boldsymbol{u} \cdot \nabla_{\boldsymbol{r}_2}} \\
&= \frac{1}{4\pi} \int_0^{2\pi} \int_0^{\pi} d\phi d\theta \sin(\theta) e^{u \nabla_{\boldsymbol{r}_2} \cos(\theta)} \\
&= \frac{\sinh(u \nabla_{\boldsymbol{r}_2})}{u \nabla_{\boldsymbol{r}_2}} \\
&= \frac{1}{u \nabla_{\boldsymbol{r}_2}} \sum_{n=0}^{\infty} \frac{(u \nabla_{\boldsymbol{r}_2})^{2n+1}}{(2n+1)!} \\
&= 1 + \frac{u^2 \nabla_{\boldsymbol{r}_2}^2}{3!} + \frac{u^4 \nabla_{\boldsymbol{r}_2}^4}{5!} + \frac{u^6 \nabla_{\boldsymbol{r}_2}^6}{7!} + \frac{u^8 \nabla_{\boldsymbol{r}_2}^8}{9!} + \ldots,
\end{aligned} \tag{2.134}$$

where $t = u \nabla_{\boldsymbol{r}_2} \cos(\theta)$ has been used in the evaluation of the integral. With the spherically-

averaged operator defined in equation 2.134, we can apply it to $f(\boldsymbol{r}_1,\boldsymbol{r}_2)$ to get,

$$\begin{aligned}\langle f(u)\rangle &= e^{\boldsymbol{u}\cdot\nabla_{r_2}} f(\boldsymbol{r}_1,\boldsymbol{r}_2)|_{\boldsymbol{r}_2=\boldsymbol{r}_1} \\ &= (1+\frac{1}{3!}u^2\nabla^2_{\boldsymbol{r}_2}+\frac{1}{5!}u^4\nabla^4_{\boldsymbol{r}_2}+...)f(\boldsymbol{r}_1,\boldsymbol{r}_2)|_{\boldsymbol{r}_2=\boldsymbol{r}_1}.\end{aligned} \tag{2.135}$$

We have a similar case for the exchange hole defined in equation 2.86 . When the operator $e^{\boldsymbol{u}\cdot\nabla_{r_2}}$ acts on $\rho_{x\sigma}(\boldsymbol{r}_1,\boldsymbol{r}_2)$ we get,

$$\begin{aligned}\langle \rho_{x\sigma}(u)\rangle &= e^{\boldsymbol{u}\cdot\nabla_{r_2}} \rho_{x\sigma}(\boldsymbol{r}_1,\boldsymbol{r}_2)|_{\boldsymbol{r}_2=\boldsymbol{r}_1} \\ &= (1+\frac{1}{3!}u^2\nabla^2_{\boldsymbol{r}_2}+\frac{1}{5!}u^4\nabla^4_{\boldsymbol{r}_2}+...)\rho_{x\sigma}(\boldsymbol{r}_1,\boldsymbol{r}_2)|_{\boldsymbol{r}_2=\boldsymbol{r}_1}.\end{aligned} \tag{2.136}$$

Applying each coefficient of the series on the exchange hole yelds the Taylor expansion of the exact spherically averaged exchage hole near the reference point

$$\langle \rho_{x\sigma}(u)\rangle = \rho_\sigma(\boldsymbol{r}_1)+\left[\nabla^2\rho_\sigma(\boldsymbol{r}_1)-\left(2\tau_\sigma+\frac{1}{4}\frac{|\nabla\rho_\sigma(\boldsymbol{r}_1)|^2}{\rho_\sigma(\boldsymbol{r}_1)}\right)\right]u^2+\ldots, \tag{2.137}$$

where the zeroth-term gives the density at the reference point and the second-order term gives the curvature of the exchange hole. All the steps involved to obtain equation 2.137 from equation 2.136 will be presented in the next chapter.

From the second-order expansion, we see that it involves non-local expressions for $E_{x\sigma}$ through the presence of electron density derivatives. This expansion was first explored by Becke to parameterize an exchange-hole model where some qualitative incorrect features of the exchange hole were fixed. Many other exchange functionals ranging from GGA to Hybrids also explores the second-order expansion.

Next, we introduce two important exchange-hole models, the LSDA[12] and the BR model[3].

2.5.3.2 The LSDA

The LSDA was the first approximation to E_{xc} and was proposed by Kohn and Sham[16]. The idea is to use the Uniform Electron Gas (UEG)[56] as a starting point to approxi-

mating E_{xc} for systems with a uniform or slow-varying density. In the UEG, the electrons occupy a infinite region of space, with a uniform positive external potential, which keeps the the neutrality of the system. Furthermore, the states of this system are doubly-occupied by the electrons in an ordered way from 0 to the Fermi level forming a surface of a sphere of radius $k_F = (3\pi\rho)^{1/3}$ where the Kohn-Sham orbitals are chosen to be plane waves. Hence, systems with uniform or slow-varying densities may be approximated by the UEG.

The spherically-averaged exchange hole in the unpolarized UEG is given by

$$\rho_x(\boldsymbol{r},u) = -2\frac{|\rho_1(\boldsymbol{r},\boldsymbol{r}+\boldsymbol{u})|^2}{\rho(\boldsymbol{r})}, \tag{2.138}$$

where

$$\rho_1(\boldsymbol{r},\boldsymbol{r}+\boldsymbol{u}) = \frac{k_F^3}{2\pi^2}\frac{\sin(k_F u) - k_F u\cos(k_F u)}{(k_F u)^3}. \tag{2.139}$$

Taking the exchange hole of the UEG and insterting it into the integral to calculate the exchange energy density we obtain

$$\begin{aligned}\varepsilon_x(\rho) &= \int_0^\infty du 2\pi u \rho_x(\boldsymbol{r},u) \\ &= \frac{3k_F}{4\pi},\end{aligned} \tag{2.140}$$

and the total exchange energy is given by

$$E_x[\rho] = -\frac{3}{4}\left(\frac{3}{\pi}\right)^{1/3}\int d\boldsymbol{r}\rho^{4/3}(\boldsymbol{r}). \tag{2.141}$$

To take into account the polarization of the system we introduce the local relative spin-polarization[24, 25]

$$\zeta(\boldsymbol{r}) = \frac{\rho_\alpha(\boldsymbol{r}) - \rho_\beta(\boldsymbol{r})}{\rho(\boldsymbol{r})}, \tag{2.142}$$

which is the ratio of the difference between spin densities and the total density. For the case of a polarized system ζ can assume the values of ± 1 and for the unpolarized case

$\zeta = 0$. Hence, the exchange energy density becomes

$$\varepsilon_{x\sigma}(\rho,\zeta) = \varepsilon_x(\rho)\frac{(1+\zeta(\boldsymbol{r}))^{4/3}+(1-\zeta(\boldsymbol{r}))^{4/3}}{2}, \tag{2.143}$$

and the total exchange energy is given by

$$E_{x\sigma}^{LSDA}[\rho_\alpha,\rho_\beta] = -\frac{3}{4}\left(\frac{3}{\pi}\right)^{1/3}\int d\boldsymbol{r}\rho^{4/3}(\boldsymbol{r})\frac{(1+\zeta(\boldsymbol{r}))^{4/3}+(1-\zeta(\boldsymbol{r}))^{4/3}}{2}. \tag{2.144}$$

Since the LSDA is classically the starting point for approximating E_{XC} , we must understand its features in order to profit from the good points and improve or avoid the bad points. We now present the good and bad aspects of the LSDA[57].

The good points:

- The LSDA for the exchange component is exact for the case of uniform densities and provides a good approximation for systems with a slowly-varying density.
- It satisfies the coordinate scaling inequality $E_x < 0$.
- LSDA is properly size-consistent[58].
- For the case of E_{xc} , LSDA satisfies the Lieb-Oxford bound[43].
- Its on-top exchange hole is exact while the KS wavefunction is a single Slater determinant.
- Its cusp condition is also realistic.
- As a consequence of the last points, the system-average of its hole "unweights" undesired regions of space where LSDA could incorrectly describe.

The bad points:

- LSDA does not describe systems with density inhomogeneity.
- The one-electron case is not treated exactly.

- LSDA misses the derivative discontinuity.
- Incorrect prediction of a hetero-nuclear molecule or solid dissociation.
- It does not satisfy the nonlocal constraint: $\rho_{xc}(\boldsymbol{r}_1,\boldsymbol{r}_2) \geq -\rho_x(\boldsymbol{r}_2)$

2.5.3.3 Becke-Roussel Exchange-Hole Model

As we discussed earlier, it is common to adopt the UEG[56] as a starting point to design exchange functionals. However, this choice is not unique. In this regard, BR[3] digress from the conventional path and proposed an interesting exchange-hole model based on the hydrogenic orbital,

$$\rho^H_{x\sigma}(\boldsymbol{r}) = \frac{\alpha^3}{8\pi}\exp^{-\alpha\boldsymbol{r}}. \tag{2.145}$$

One of the remarkable features of the model is that it satisfies all known conditions of the exact system up to date: the non-negativity of the hole, the normalization condition and the short-range behavior of the exchange-hole density. It is important to note that these conditions are present in all electronic systems and a systematic satisfaction of them would, in principle, lead to very reliable approximations of the exchange hole.

Another advantage of this model is the accurate total exchange energies for atomic systems. This could be attributed to the presumption that the exchange hole in different atomic systems are very similar in their forms to the hole of the hydrogen atom. In the case of molecular systems this is not always true because the hole can be delocalized over several centers of a molecule.

After evaluating the spherical average of ρ^H_x one obtains,

$$\begin{aligned}
\rho^H_{x\sigma}(\boldsymbol{r},u) &= -\frac{1}{4\pi}\int_0^{2\pi} d\phi_u \int_0^{\pi} d\theta_u \sin_{\theta_u}\rho^H_x(\boldsymbol{r}+\boldsymbol{u}) \\
&= -\frac{1}{4\pi}\int_0^{2\pi} d\phi_u \int_0^{\pi} d\theta_u \sin_{\theta_u}\frac{\alpha^3}{8\pi}\exp^{-\alpha\sqrt{r^2+u^2-2ru\cos\theta_u}} \\
&= -\frac{\alpha}{16\pi ru}\left[(\alpha|r-u|+1)e^{-\alpha|r-u|} - (\alpha|r+u|+1)e^{-\alpha|r+u|}\right].
\end{aligned} \tag{2.146}$$

Considering the analytical form of the spherically-averaged model as a mathematical object with two functions BR defined the following function

$$\rho_{x\sigma}^{BR}(a,b,u) = -\frac{a}{16\pi bu}\left[(a|b-u|+1)e^{-a|b-u|} - (a|b+u|+1)e^{-a|b+u|}\right]. \quad (2.147)$$

where the values of $a \equiv a(\boldsymbol{r})$ and $b \equiv b(\boldsymbol{r})$ for a given reference point $\boldsymbol{r}$ are determined by imposing the condition that Taylor expansion of equation 2.147

$$\rho_{x\sigma}^{BR}(a,b,u) = \frac{a^3 e^{-ab}}{8\pi} + \frac{a^4(-2+ab)e^{-ab}}{48b\pi}u^2, \quad (2.148)$$

reproduces the second-order expansion of the exact exchange hole,

$$\rho_{x\sigma}^{exact}(\boldsymbol{r}) = \rho_\sigma(\boldsymbol{r}) + \frac{1}{3!}\left[\nabla^2\rho_\sigma(\boldsymbol{r}) - \gamma\left(2\tau_\sigma(\boldsymbol{r}) + \frac{1}{4}\frac{|\nabla\rho_\sigma(\boldsymbol{r})|^2}{\rho_\sigma(\boldsymbol{r})}\right)\right]u^2. \quad (2.149)$$

Equating the coefficients yields, after some algebraic manipulations, two non-linear equations,

$$\begin{aligned} a^2 e^{-ab} &= 8\pi\rho_\sigma(\boldsymbol{r}) \\ a^2 b - 2a &= \frac{6bQ_\sigma(\boldsymbol{r})}{\rho_\sigma(\boldsymbol{r})}, \end{aligned} \quad (2.150)$$

where

$$Q_\sigma(\boldsymbol{r}) = \nabla^2\rho_\sigma(\boldsymbol{r}) - \gamma\left(2\tau_\sigma(\boldsymbol{r}) + \frac{1}{4}\frac{|\nabla\rho_\sigma(\boldsymbol{r})|^2}{\rho_\sigma(\boldsymbol{r})}\right), \quad (2.151)$$

and the parameter γ is set to unity for now.

Through a variable substitution $x = ab$, it is possible to simplify the system of equations into a single equation,

$$\frac{xe^{-2x/3}}{(x-2)} = \frac{2}{3}\pi^{2/3}\frac{\rho_\sigma(\boldsymbol{r})^{5/3}}{Q_\sigma(\boldsymbol{r})}. \quad (2.152)$$

This non-linear equation is solved by the Newton-Raphson method at each point of the

reference electron $\boldsymbol{r}$. The total exchange energy is obtained by

$$E_{x\sigma}[\rho] = \frac{1}{2}\int d\boldsymbol{r}\rho(\boldsymbol{r})\varepsilon_{x\sigma}^{BR}(\boldsymbol{r}), \tag{2.153}$$

where the exchange energy density is calculated by,

$$\varepsilon_{x\sigma}^{BR}(\boldsymbol{r}) = -\left[1-\exp^{-ab}\left(1+\frac{1}{2}ab\right)\right]\Big/2b. \tag{2.154}$$

The parameter γ when set to the empirical value of 0.8 allows one to recover, in part, the uniform gas limit. Note that this is does not change the result for the hydrogen atom where we have that the second term in Q_σ vanishes when in one electron orbital.

The BR model has important features that must be highlighted. The exchange hole ρ_x^{BR} satisfies important constraints such as the non-positivity, normalization and short-range behavior of the exact exchange hole. Moreover, its exchange energy density gives the correct asymptotic behavior,

$$\lim_{\boldsymbol{r}\to\infty}\varepsilon_{x\sigma}^{BR}(\boldsymbol{r}) = -\frac{1}{\boldsymbol{r}}. \tag{2.155}$$

Furthermore, the model provides the exact one-electron limit by definition, a deficiency frequently present in many exchange functional approximations. The relative success of the BR model for atoms may be attributed to the general form of the exact exchange hole in atomic systems where they resemble that of the hydrogenic exchange hole. Nevertheless, we have seen that in molecular systems the exact exchange hole can be quite delocalized. For this reason, we understand that, in molecular systems the BR model gives a limited description of the exchange effect. Therefore, the design of new exchange hole models that correctly describe atomic and molecular environments is necessary.

2.6 Conclusion

In this chapter, we have introduced, in a simplistic form, the theorems of Hohenberg and Kohn that are the pilars of DFT. We also exposed the development and improvement

of the theory during the last years that lead to the sophisticated method widely used nowadays.

Although DFT has attained a large popularity due to its ability to provide good accuracy for several properties due to successful functionals, it still has quite a few problems to be solved such as reaction barriers, s-d transfer energies, etc. In view of this, we present a new analytical property of the exact exchange hole. This new condition could be employed in the construction of new exchange hole models therefore extending the the short-range quadratic behavior of the exact exchange hole up to the fourth-order term. In view of this, we also propose three analytical exchange-hole models which employ all currently known conditions and our new one. Thus, we seek to construct accurate exchange functional approximations to calculate properties such as atomization energies, ionization energies, geometries, etc.

CHAPTER 3

THE FOURTH-ORDER EXPANSION OF THE EXCHANGE HOLE

The importance and popularity earned by modern DFT can be attributed to a number of density functional approximations for the, yet unknown, exact exchange-correlation functional. These approximations were devised not from a formal guideline, but from the application of human creative skill and imagination. In this respect, the analytic properties of the exchange-correlation functional play a fundamental role in the development of density functional approximations.

In regard of the above considerations, we present here a new condition of the exact exchange hole, thus, expanding, the current number of analytic properties of this function. This new condition is obtained from the fourth-order expansion of the spherically averaged exact exchange hole which gives the short-range quartic behavior of the exchange-hole function.

Hence, we expect that our new condition, used in conjunction with other ones, can better describe the exact exchange hole for atoms and molecules therefore leading to exchange functional approximations that are able to predict accurately atomization energies, ionization energies, etc.

In the last chapter, we have introduced the second-order expansion of the exact spherically averaged exchange hole and shown how BR[3] used it to construct a completely nonempirical exchange-hole model that sucessfully reproduces the short-range quadratic behavior of $\rho_x(\boldsymbol{r}, u)$.

What follows is the mathematical development to obtain the fourth-order term of the Taylor series of the exact spherically averaged exchange hole. The organization of this chapter is as follows. In the Theory section we present the full derivation of the second-order and fourth-order expansions. The details involved in the implementation of all quantities of the fourth-order term are given in the Implementation section. Next, in the Results and Discussion we describe how the fourth-order expansion improves over the second-order expansion and how it could be applied to functional designing. Finally, in

Conclusion we give our last remarks of the fourth-order expansion and future works.

3.1 Theory

The general form of the expansion presented in equation 2.136[54] is,

$$\langle \rho_{x\sigma}(u) \rangle = (1 + \frac{1}{3!}u^2\nabla^2_{\boldsymbol{r}_2} + \frac{1}{5!}u^4\nabla^4_{\boldsymbol{r}_2} + ...)\rho_x(\boldsymbol{r}_1, \boldsymbol{r}_2)|_{\boldsymbol{r}_2=\boldsymbol{r}_1}. \tag{3.1}$$

The derivation of the fourth-order term in u involves the first two terms of the expansion. From equations 2.80, 2.81 and 2.86 we can express the exchange hole in terms of real orbitals (KS orbitals[16]) as,

$$\rho_{x\sigma}(\boldsymbol{r}_1, \boldsymbol{r}_2) = \frac{1}{\rho_\sigma(\boldsymbol{r}_1)} \sum_{k,l}^{\sigma} \psi_k(\boldsymbol{r}_1)\psi_k(\boldsymbol{r}_2)\psi_l(\boldsymbol{r}_1)\psi_l(\boldsymbol{r}_2). \tag{3.2}$$

First, the second-order term of equation 3.1 is derived by applying Laplacian operator $\nabla^2_{\boldsymbol{r}_2}$ on $\rho_{x\sigma}$ which leads to,

$$\begin{aligned} K_2 &= \nabla^2_{\boldsymbol{r}_2}\rho_{x\sigma}(\boldsymbol{r}_1, \boldsymbol{r}_2) \\ &= \frac{1}{\rho_\sigma(\boldsymbol{r}_1)} \sum_{k,l}^{\sigma} \psi_k(\boldsymbol{r}_1)\psi_l(\boldsymbol{r}_1)\nabla^2_{\boldsymbol{r}_2}\psi_k(\boldsymbol{r}_2)\psi_l(\boldsymbol{r}_2). \end{aligned} \tag{3.3}$$

Note that the operator acts only on coordinate $\boldsymbol{r}_2$ of $\rho_{x\sigma}(\boldsymbol{r}_1, \boldsymbol{r}_2)$ yielding,

$$\nabla^2_{\boldsymbol{r}_2}\psi_k(\boldsymbol{r}_2)\psi_l(\boldsymbol{r}_2) = \psi_k(\boldsymbol{r}_2)\nabla^2_{\boldsymbol{r}_2}\psi_l(\boldsymbol{r}_2) + \psi_l(\boldsymbol{r}_2)\nabla^2_{\boldsymbol{r}_2}\psi_k(\boldsymbol{r}_2) + 2\nabla_{\boldsymbol{r}_2}\psi_l(\boldsymbol{r}_2)\cdot\nabla_{\boldsymbol{r}_2}\psi_k(\boldsymbol{r}_2) \tag{3.4}$$

Substituting this into 3.3, it follows that at the coalescense point (when $\boldsymbol{r}_2 = \boldsymbol{r}_1$) K_2 is,

$$K_2|_{\boldsymbol{r}_2=\boldsymbol{r}_1} = \frac{1}{\rho_\sigma(\boldsymbol{r}_1)} \sum_{k,l}^{\sigma} \psi_k(\boldsymbol{r}_1)\psi_l(\boldsymbol{r}_1) \left[\psi_k(\boldsymbol{r}_1)\nabla^2_{\boldsymbol{r}_1}\psi_l(\boldsymbol{r}_1) + \psi_l(\boldsymbol{r}_1)\nabla^2_{\boldsymbol{r}_1}\psi_k(\boldsymbol{r}_1) + 2\nabla_{\boldsymbol{r}_1}\psi_l(\boldsymbol{r}_1)\nabla_{\boldsymbol{r}_1}\psi_k(\boldsymbol{r}_1)\right]. \tag{3.5}$$

Rearranging, it leads to,

$$
\begin{aligned}
K_2|_{\boldsymbol{r}_2=\boldsymbol{r}_1} &= \frac{1}{\rho_\sigma(\boldsymbol{r}_1)} \sum_{k,l}^{\sigma} \left[\psi_k(\boldsymbol{r}_1)\psi_k(\boldsymbol{r}_1)\psi_l(\boldsymbol{r}_1)\nabla^2_{\boldsymbol{r}_1}\psi_l(\boldsymbol{r}_1) + \psi_l(\boldsymbol{r}_1)\psi_l(\boldsymbol{r}_1)\psi_k(\boldsymbol{r}_1)\nabla^2_{\boldsymbol{r}_1}\psi_k(\boldsymbol{r}_1) \right. \\
&\quad \left. + 2\psi_l(\boldsymbol{r}_1)\nabla_{\boldsymbol{r}_1}\psi_l(\boldsymbol{r}_1)\psi_k(\boldsymbol{r}_1)\cdot\nabla_{\boldsymbol{r}_1}\psi_k(\boldsymbol{r}_1) \right] \\
&= \frac{1}{\rho_\sigma(\boldsymbol{r}_1)} \left[\sum_{k}^{\sigma} \psi_k(\boldsymbol{r}_1)\psi_k(\boldsymbol{r}_1) \sum_{l}^{\sigma} \psi_l(\boldsymbol{r}_1)\nabla^2_{\boldsymbol{r}_1}\psi_l(\boldsymbol{r}_1) + \sum_{l}^{\sigma} \psi_l(\boldsymbol{r}_1)\psi_l(\boldsymbol{r}_1) \sum_{k}^{\sigma} \psi_k(\boldsymbol{r}_1)\nabla^2_{\boldsymbol{r}_1}\psi_k(\boldsymbol{r}_1) \right. \\
&\quad \left. + 2\sum_{l}^{\sigma} \psi_l(\boldsymbol{r}_1)\nabla_{\boldsymbol{r}_1}\psi_l(\boldsymbol{r}_1) \cdot \sum_{k}^{\sigma} \psi_k(\boldsymbol{r}_1)\nabla_{\boldsymbol{r}_1}\psi_k(\boldsymbol{r}_1) \right] \\
&= \sum_{l}^{\sigma} \psi_l(\boldsymbol{r}_1)\nabla^2_{\boldsymbol{r}_1}\psi_l(\boldsymbol{r}_1) + \sum_{k}^{\sigma} \psi_k(\boldsymbol{r}_1)\nabla^2_{\boldsymbol{r}_1}\psi_k(\boldsymbol{r}_1) \\
&\quad + \frac{1}{\rho_\sigma(\boldsymbol{r}_1)} \left[2\sum_{l}^{\sigma} \psi_l(\boldsymbol{r}_1)\nabla_{\boldsymbol{r}_1}\psi_l(\boldsymbol{r}_1) \sum_{k}^{\sigma} \psi_k(\boldsymbol{r}_1)\nabla_{\boldsymbol{r}_1}\psi_k(\boldsymbol{r}_1) \right] \\
&= 2\sum_{k}^{\sigma} \psi_k(\boldsymbol{r}_1)\nabla^2_{\boldsymbol{r}_1}\psi_k(\boldsymbol{r}_1) + \frac{1}{\rho_\sigma(\boldsymbol{r}_1)} \left[2\sum_{l}^{\sigma} \psi_l(\boldsymbol{r}_1)\nabla_{\boldsymbol{r}_1}\psi_l(\boldsymbol{r}_1) \cdot \sum_{k}^{\sigma} \psi_k(\boldsymbol{r}_1)\nabla_{\boldsymbol{r}_1}\psi_k(\boldsymbol{r}_1) \right]
\end{aligned}
\tag{3.6}
$$

This gives the curvature of the exchange hole in terms of orbitals at the position $\boldsymbol{r}$ of a reference electron. It is interesting to have equation 3.6 in terms of known quantities. This is achieved using the fact that the gradient of the spin-density is

$$
\nabla\rho_\sigma(\boldsymbol{r}_1) = \nabla\sum_{i}^{\sigma} [\psi_i(\boldsymbol{r}_1)]^2 = \sum_{i}^{\sigma} 2\psi_i(\boldsymbol{r}_1)\nabla\psi_i(\boldsymbol{r}_1) \tag{3.7}
$$

and the Laplacian of the spin-density is,

$$
\nabla^2\rho_\sigma(\boldsymbol{r}_1) = \nabla^2\sum_{i}^{\sigma} [\psi_i(\boldsymbol{r}_1)]^2 = \sum_{i}^{\sigma} 2\left[\psi_i(\boldsymbol{r}_1)\nabla^2\psi_i(\boldsymbol{r}_1) + \nabla\psi_i(\boldsymbol{r}_1)\cdot\nabla\psi_i(\boldsymbol{r}_1)\right]. \tag{3.8}
$$

Using equations 3.7, 3.8 we can rewrite equation 3.6 as,

$$\begin{aligned} K_2|_{\boldsymbol{r}_2=\boldsymbol{r}_1} &= \nabla^2\rho_\sigma(\boldsymbol{r}_1) - 2\sum_l^\sigma \nabla\psi_l(\boldsymbol{r}_1)\cdot\nabla\psi_l(\boldsymbol{r}_1) + \frac{1}{2}\frac{[\nabla\rho_\sigma(\boldsymbol{r}_1)]^2}{\rho_\sigma(\boldsymbol{r}_1)} \\ &= \nabla^2\rho_\sigma(\boldsymbol{r}_1) - 2\tau_\sigma(\boldsymbol{r}_1) + \frac{1}{2}\frac{[\nabla\rho_\sigma(\boldsymbol{r}_1)]^2}{\rho_\sigma(\boldsymbol{r}_1)}. \end{aligned} \tag{3.9}$$

Now we focus on the fourth-order term of equation 3.1 which is written as,

$$\begin{aligned} K_4|_{\boldsymbol{r}_2=\boldsymbol{r}_1} &= \nabla^4_{\boldsymbol{r}_2}\rho_{x\sigma}(\boldsymbol{r}_1,\boldsymbol{r}_2) \\ &= \frac{1}{\rho_\sigma(\boldsymbol{r}_1)}\sum_{k,l}^\sigma \psi_k(\boldsymbol{r}_1)\psi_l(\boldsymbol{r}_1)\nabla^4_{\boldsymbol{r}_2}\psi_k(\boldsymbol{r}_2)\psi_l(\boldsymbol{r}_2). \end{aligned} \tag{3.10}$$

Consider first, the part of equation 3.10 possessing the coordinate $\boldsymbol{r}_2$,

$$\nabla^4_{\boldsymbol{r}_2}\sum_{k,l}^\sigma \psi_k(\boldsymbol{r}_2)\psi_l(\boldsymbol{r}_2) = \nabla^2_{\boldsymbol{r}_2}\sum_{k,l}^\sigma \left[\psi_k(\boldsymbol{r}_2)\nabla^2_{\boldsymbol{r}_2}\psi_l(\boldsymbol{r}_2) + \psi_l(\boldsymbol{r}_2)\nabla^2_{\boldsymbol{r}_2}\psi_k(\boldsymbol{r}_2) + 2\nabla_{\boldsymbol{r}_2}\psi_l(\boldsymbol{r}_2)\cdot\nabla_{\boldsymbol{r}_2}\psi_k(\boldsymbol{r}_2)\right] \tag{3.11}$$

The first term of equation 3.11 is

$$\nabla^2_{\boldsymbol{r}_2}\sum_{k,l}^\sigma \psi_k(\boldsymbol{r}_2)\nabla^2_{\boldsymbol{r}_2}\psi_l(\boldsymbol{r}_2) = \sum_{k,l}^\sigma \psi_k(\boldsymbol{r}_1)\nabla^4\psi_l(\boldsymbol{r}_1) + 2\nabla\psi_k(\boldsymbol{r}_1)\cdot\nabla^3\psi_l(\boldsymbol{r}_1) + \nabla^2\psi_l(\boldsymbol{r}_1)\nabla^2\psi_k(\boldsymbol{r}_1), \tag{3.12}$$

where we have an equivalent result for the second term. In order to calculate the third term we make use of Green's second vector derivative identity,

$$\nabla^2(\boldsymbol{A}\cdot\boldsymbol{B}) = \boldsymbol{A}\cdot\nabla^2\boldsymbol{B} - \boldsymbol{B}\nabla^2\boldsymbol{A} + 2\nabla\cdot\left[(\boldsymbol{B}\cdot\nabla)\boldsymbol{A} + B\times\nabla\times\boldsymbol{A}\right]. \tag{3.13}$$

Hence, the third term [1] is written as

$$\begin{aligned}\nabla^2\sum_{k,l}^{\sigma}2\nabla\psi_k\cdot\nabla\psi_l &= \sum_{k,l}^{\sigma}2\big\{\nabla\psi_k\cdot\nabla^2\nabla\psi_l-\nabla\psi_l\cdot\nabla^2\nabla\psi_k+2\nabla\cdot\left[(\nabla\psi_l\cdot\nabla)\nabla\psi_k+\nabla\psi_l\times\nabla\times\nabla\psi_k\right]\big\}\\ &= \sum_{k,l}^{\sigma}2\big\{\nabla\psi_k\cdot\nabla^2\nabla\psi_l-\nabla\psi_l\cdot\nabla^2\nabla\psi_k+2\nabla\cdot\left[(\nabla\psi_l\cdot\nabla)\nabla\psi_k\right]\big\},\end{aligned} \tag{3.14}$$

where we have used the fact that $\nabla\times\nabla\psi_k=0$. Substituting equations 3.12 and 3.14 into equation 3.11 at the coalescense point leads to,

$$\begin{aligned}K_4|_{\boldsymbol{r}_2=\boldsymbol{r}_1} &= \frac{1}{\rho_\sigma(\boldsymbol{r}_1)}\sum_{k,l}^{\sigma}\psi_k(\boldsymbol{r}_1)\psi_l(\boldsymbol{r}_1)\Big\{\psi_k(\boldsymbol{r}_1)\nabla^4\psi_l(\boldsymbol{r}_1)+2\nabla\psi_k(\boldsymbol{r}_1)\cdot\nabla^3\psi_l(\boldsymbol{r}_1)+\nabla^2\psi_l(\boldsymbol{r}_1)\nabla^2\psi_k(\boldsymbol{r}_1)\\ &\quad+2\left[\nabla\psi_k(\boldsymbol{r}_1)\cdot\nabla^2\nabla\psi_l(\boldsymbol{r}_1)-\nabla\psi_l(\boldsymbol{r}_1)\cdot\nabla^2\nabla\psi_k(\boldsymbol{r}_1)+2\nabla\cdot\left((\nabla\psi_l(\boldsymbol{r}_1)\cdot\nabla)\nabla\psi_k(\boldsymbol{r}_1)\right)\right]\\ &\quad+\psi_l(\boldsymbol{r}_1)\nabla^4\psi_k(\boldsymbol{r}_1)+2\nabla\psi_l(\boldsymbol{r}_1)\cdot\nabla^3\psi_k(\boldsymbol{r}_1)+\nabla^2\psi_k(\boldsymbol{r}_1)\nabla^2\psi_l(\boldsymbol{r}_1)\Big\}\\ &= \frac{1}{\rho_\sigma(\boldsymbol{r}_1)}\sum_{k,l}^{\sigma}\psi_k(\boldsymbol{r}_1)\psi_l(\boldsymbol{r}_1)\Big\{\psi_k(\boldsymbol{r}_1)\nabla^4\psi_l(\boldsymbol{r}_1)+4\nabla\psi_k(\boldsymbol{r}_1)\cdot\nabla^3\psi_l(\boldsymbol{r}_1)+2\nabla^2\psi_l(\boldsymbol{r}_1)\nabla^2\psi_k(\boldsymbol{r}_1)\\ &\quad+\psi_l(\boldsymbol{r}_1)\nabla^4\psi_k(\boldsymbol{r}_1)+4\nabla\cdot\left((\nabla\psi_l(\boldsymbol{r}_1)\cdot\nabla)\nabla\psi_k(\boldsymbol{r}_1)\right)\Big\}.\end{aligned} \tag{3.15}$$

The last term of equation 3.15 is an unconventional expression that has never been seen before in the literature of DFT. In order to get more information from this term we proceed by writing it in terms of function derivatives. Consider first the following quantities which are presented in their basic mathematical forms,

$$\nabla g\cdot\nabla = g_x\frac{\partial}{\partial x}+g_y\frac{\partial}{\partial y}+g_z\frac{\partial}{\partial z} \tag{3.16}$$

[1] Ommiting the target coordinate $\boldsymbol{r}_2$.

$$
\begin{aligned}
(\nabla g \cdot \nabla)\nabla f = &(g_x f_{xx} + g_y f_{xy} + g_z f_{xz})\,\hat{x} \\
&+ (g_x f_{xy} + g_y f_{yy} + g_z f_{yz})\,\hat{y} \\
&+ (g_x f_{xz} + g_y f_{yz} + g_z f_{zz})\,\hat{z}
\end{aligned}
\tag{3.17}
$$

Using 3.16 and 3.17 we can write the last term of K_4 as,

$$
\begin{aligned}
\nabla \cdot (\nabla g \cdot \nabla)\nabla f = &(g_{xx} f_{xx} + g_x f_{xxx} + g_{xy} f_{xy} + g_y f_{xxy} + g_{xz} f_{xz} + g_z f_{xxz}) \\
&+ (g_{xy} f_{xy} + g_x f_{xyy} + g_{yy} f_{yy} + g_y f_{yyy} + g_{yz} f_{yz} + g_z f_{yyz}) \\
&+ (g_{xz} f_{xz} + g_x f_{xzz} + g_{yz} f_{yz} + g_y f_{yzz} + g_{zz} f_{zz} + g_z f_{zzz})\,.
\end{aligned}
\tag{3.18}
$$

Rearranging the terms we have

$$
\begin{aligned}
\nabla \cdot (\nabla g \cdot \nabla)\nabla f = &\nabla g \cdot \nabla^3 f \\
&+ (g_{xx} f_{xx} + g_{yy} f_{yy} + g_{zz} f_{zz} \\
&+ 2g_{xy} f_{xy} + 2g_{xz} f_{xz} + 2g_{yz} f_{yz})\,,
\end{aligned}
\tag{3.19}
$$

where we used,

$$
\begin{aligned}
\nabla^3 f &= \nabla\left(\nabla^2 f\right) \\
&= \nabla^2 (\nabla f) \\
&= (f_{xxx} + f_{xyy} + f_{xzz})\,\hat{x} \\
&+ (f_{xxy} + f_{yyy} + f_{yzz})\,\hat{y} \\
&+ (f_{xxz} + f_{yyz} + f_{zzz})\,\hat{z}.
\end{aligned}
\tag{3.20}
$$

In equation equation 3.19 , the term inside the parenthesis can be recast by defining a vetor with of 6 components,

$$
\boldsymbol{f}^{6v} = \left(f_{xx}, f_{yy}, f_{zz}, \sqrt{2} f_{xy}, \sqrt{2} f_{xz}, \sqrt{2} f_{yz}\right). \tag{3.21}
$$

Conveniently, it leads to a short form of equation 3.19 ,

$$\nabla\cdot(\nabla g\cdot\nabla)\nabla f=\nabla g\cdot\nabla^3 f+\boldsymbol{f}^{6v}\cdot\boldsymbol{g}^{6v}. \tag{3.22}$$

Hence, K_4 is written as,

$$\begin{aligned}
K_4|_{\boldsymbol{r}_2=\boldsymbol{r}_1} &= \frac{1}{\rho_\sigma(\boldsymbol{r}_1)}\sum_{k,l}^{\sigma}\psi_k(\boldsymbol{r}_1)\psi_l(\boldsymbol{r}_1)\Big\{\psi_k(\boldsymbol{r}_1)\nabla^4\psi_l(\boldsymbol{r}_1)+4\nabla\psi_k(\boldsymbol{r}_1)\cdot\nabla^3\psi_l(\boldsymbol{r}_1)+2\nabla^2\psi_l(\boldsymbol{r}_1)\nabla^2\psi_k(\boldsymbol{r}_1)\\
&\quad+\psi_l(\boldsymbol{r}_1)\nabla^4\psi_k(\boldsymbol{r}_1)+4\nabla\psi_l(\boldsymbol{r}_1)\cdot\nabla^3\psi_k(\boldsymbol{r}_1)+4\psi_l^{6v}(\boldsymbol{r}_1)\cdot\psi_k^{6v}(\boldsymbol{r}_1)\Big\}\\
&= \frac{1}{\rho_\sigma(\boldsymbol{r}_1)}\Big\{2\sum_{k}^{\sigma}\psi_k(\boldsymbol{r}_1)\psi_k(\boldsymbol{r}_1)\sum_{l}^{\sigma}\psi_l(\boldsymbol{r}_1)\nabla^4\psi_l(\boldsymbol{r}_1)+8\sum_{k}^{\sigma}\psi_k(\boldsymbol{r}_1)\nabla\psi_k(\boldsymbol{r}_1)\cdot\sum_{l}^{\sigma}\psi_l(\boldsymbol{r}_1)\nabla^3\psi_l(\boldsymbol{r}_1)\\
&\quad+2\sum_{k}^{\sigma}\psi_k(\boldsymbol{r}_1)\nabla^2\psi_k(\boldsymbol{r}_1)\sum_{l}^{\sigma}\psi_l(\boldsymbol{r}_1)\nabla^2\psi_l(\boldsymbol{r}_1)+4\sum_{k}^{\sigma}\psi_k(\boldsymbol{r}_1)\psi_k^{6v}(\boldsymbol{r}_1)\cdot\sum_{l}^{\sigma}\psi_l(\boldsymbol{r}_1)\psi_l^{6v}(\boldsymbol{r}_1)\Big\}.
\end{aligned} \tag{3.23}$$

Note that in rearranging the terms we used the fact that,

$$\sum_{k}^{\sigma}\psi_k\psi_k\sum_{l}^{\sigma}\psi_l\nabla^4\psi_l=\sum_{l}^{\sigma}\psi_l\psi_l\sum_{k}^{\sigma}\psi_k\nabla^4\psi_k. \tag{3.24}$$

We now seek to express K_4 in terms of the density and other known quantities. The procedure that follows is analogous to what we have done with K_2 from equation 3.7 to 3.9. The biharmonic of the density is defined by,

$$\begin{aligned}
\nabla^4\rho_\sigma &= 2\sum_{i}^{\sigma}\nabla^2\left[\psi_i(\boldsymbol{r}_1)\nabla^2\psi_i(\boldsymbol{r}_1)+\nabla\psi_i(\boldsymbol{r}_1)\cdot\nabla\psi_i(\boldsymbol{r}_1)\right]\\
&= 2\sum_{i}^{\sigma}\left[\psi_i(\boldsymbol{r}_1)\nabla^4\psi_i(\boldsymbol{r}_1)+2\nabla\psi_i(\boldsymbol{r}_1)\cdot\nabla^3\psi_i(\boldsymbol{r}_1)+\nabla^2\psi_i(\boldsymbol{r}_1)\nabla^2\psi_i(\boldsymbol{r}_1)\right]\\
&\quad+4\sum_{i}^{\sigma}\nabla\cdot\left[(\nabla\psi_i(\boldsymbol{r}_1)\cdot\nabla)\nabla\psi_i(\boldsymbol{r}_1)\right]
\end{aligned} \tag{3.25}$$

Solving equation 3.25 for the third term in the first squared braket we obtain,

$$\begin{aligned}
2\psi_i(\boldsymbol{r}_1)\nabla^4\psi_i(\boldsymbol{r}_1) &= \nabla^4\rho_\sigma - 4\sum_i^\sigma \nabla\psi_i(\boldsymbol{r}_1)\cdot\nabla^3\psi_i(\boldsymbol{r}_1) - 2\sum_i^\sigma \nabla^2\psi_i(\boldsymbol{r}_1)\nabla^2\psi_i(\boldsymbol{r}_1) \\
&\quad - 4\sum_i^\sigma \nabla\cdot\left[\left(\nabla\psi_i(\boldsymbol{r}_1)\cdot\nabla\right)\nabla\psi_i(\boldsymbol{r}_1)\right] \\
&= \nabla^4\rho_\sigma - 8\sum_i^\sigma \nabla\psi_i(\boldsymbol{r}_1)\cdot\nabla^3\psi_i(\boldsymbol{r}_1) - 2\sum_i^\sigma \nabla^2\psi_i(\boldsymbol{r}_1)\nabla^2\psi_i(\boldsymbol{r}_1) \\
&\quad - 4\sum_i^\sigma \psi_i^{6v}(\boldsymbol{r}_1)\cdot\psi_i^{6v}(\boldsymbol{r}_1)
\end{aligned} \tag{3.26}$$

Substituting it into equation 3.23 leads to the final form of K_4,

$$\begin{aligned}
K_4|_{\boldsymbol{r}_2=\boldsymbol{r}_1} &= \frac{1}{\rho_\sigma(\boldsymbol{r}_1)}\Bigg\{\sum_k^\sigma \psi_k(\boldsymbol{r}_1)\psi_k(\boldsymbol{r}_1) \\
&\quad\times\left[\nabla^4\rho_\sigma - 8\sum_i^\sigma \nabla\psi_l(\boldsymbol{r}_1)\cdot\nabla^3\psi_l(\boldsymbol{r}_1) - 2\sum_i^\sigma \nabla^2\psi_l(\boldsymbol{r}_1)\nabla^2\psi_l(\boldsymbol{r}_1) - 4\sum_i^\sigma \psi_l^{6v}(\boldsymbol{r}_1)\cdot\psi_l^{6v}(\boldsymbol{r}_1)\right] \\
&\quad + 8\sum_k^\sigma \psi_k(\boldsymbol{r}_1)\nabla\psi_k(\boldsymbol{r}_1)\cdot\sum_l^\sigma \psi_l(\boldsymbol{r}_1)\nabla^3\psi_l(\boldsymbol{r}_1) + 2\sum_k^\sigma \psi_k(\boldsymbol{r}_1)\nabla^2\psi_k(\boldsymbol{r}_1)\sum_l^\sigma \psi_l(\boldsymbol{r}_1)\nabla^2\psi_l(\boldsymbol{r}_1) \\
&\quad + 4\sum_k^\sigma \psi_k(\boldsymbol{r}_1)\psi_k^{6v}(\boldsymbol{r}_1)\cdot\sum_l^\sigma \psi_l(\boldsymbol{r}_1)\psi_l^{6v}(\boldsymbol{r}_1)\Bigg\} \\
&= \nabla^4\rho_\sigma - 8\sum_i^\sigma \nabla\psi_l(\boldsymbol{r}_1)\cdot\nabla^3\psi_l(\boldsymbol{r}_1) - 2\sum_i^\sigma \nabla^2\psi_l(\boldsymbol{r}_1)\nabla^2\psi_l(\boldsymbol{r}_1) - 4\sum_i^\sigma \psi_l^{6v}(\boldsymbol{r}_1)\cdot\psi_l^{6v}(\boldsymbol{r}_1) \\
&\quad + \frac{1}{\rho_\sigma(\boldsymbol{r}_1)}\Bigg\{8\sum_k^\sigma \psi_k(\boldsymbol{r}_1)\nabla\psi_k(\boldsymbol{r}_1)\cdot\sum_l^\sigma \psi_l(\boldsymbol{r}_1)\nabla^3\psi_l(\boldsymbol{r}_1) + 2\sum_k^\sigma \psi_k(\boldsymbol{r}_1)\nabla^2\psi_k(\boldsymbol{r}_1)\sum_l^\sigma \psi_l(\boldsymbol{r}_1)\nabla^2\psi_l(\boldsymbol{r}_1) \\
&\quad + 4\sum_k^\sigma \psi_k(\boldsymbol{r}_1)\psi_k^{6v}(\boldsymbol{r}_1)\cdot\sum_l^\sigma \psi_l(\boldsymbol{r}_1)\psi_l^{6v}(\boldsymbol{r}_1)\Bigg\}.
\end{aligned} \tag{3.27}$$

With the fourth-order term K_4 fully determined, we need to validate its results in order to use it as a new constraint for exchange hole models. The procedure employed in the validation of K_4 depends on the recent work of Antaya, Zhou and Ernzerhof [59]. In this work they constructed the exact analytical form of the non-local exchange hole

in terms of Gaussian functions. Thus, by comparing the values of K_4 with the values of the fourth-order term of the non-local exchange hole for the same points in space it is possible to assure K_4. The details involving the implementation of K_4 follows in the next section while its validation and results will be presented in the section Results.

3.2 Implementation

The fourth-order term was implemented using the computer language fortran 77 into GAUSSIAN code[60]. Initially the GAUSSIAN code had to be modified to support the complete computation of the quantities needed to construct the fourth-order term. This involves derivatives up to the fourth order of orbitals with respect to the electron coordinates. Although much of the orbital derivatives were already implemented in the GAUSSIAN code, there were not any currently method using these quantities. Hence, a modification of the code had to be performed to allow these computations.

First, we modified the GAUSSIAN code to increase the number of its memory allocated to calculate the fourth-order term. Note that the fourth-order term does not need an additional large amount of memory. This patch of the code is related to the limitation of the code since none of its methods used it before. Therefore, the code could not account for the size needed to store the values of these orbital derivatives of fourth degree.

Secondly, we implemented all quantities of equation 3.27 which includes the biharmonic of the density defined in equation 3.25.

3.3 Results and Discussion

The calculations involving the expansions of the exact spherically averaged exchange hole and the densities of atoms and molecules were done using the 6-311G+(2d,p) basis set in the Gaussian program system. This basis set represents the orbitals of each atom where it has 6 gaussian functions for the inner shell, 3 gaussian functions for the valence orbitals and two gaussian functions with different sizes for extended valence orbitals. The specification (2d,p) indicates that one p-type function is added to the hydrogen atom and two more d-type functions to atoms with $Z > 2$. Moreover, cartesian functions were

used for d-type orbitals. The grid employed in our calculations has 75 radial shells and 302 angular points per shell, giving approximately 7000 points per atom. Experimental geometries were used as inputs throughout all our calculations.

3.3.1 Study of the Expansions of $\rho_x(\boldsymbol{r}_1, u)$

In this section, the exact analytic spherically averaged exchange hole results were obtained from the program developed in the GAUSSIAN code by Antaya, Zhou and Ernzerhof[59]. The calculations involving this program were done with the same basis set and grid as used in the calculations of the expansions of the exact spherically averaged exchange hole. From now on we use the term exact exchange hole in reference to the exact spherically averaged exchange hole for the sake of brevity where the latter is used when necessary.

As mentioned before in 2.5.3.1, the second- and fourth-order expansions are obtained through the Taylor series expansion of the exact spherically averaged hole[54] when the interelectronic distance u is equal to 0. In this regard, these expansions are not expected to represent the exact hole in the whole space but in its definition range $(0 < u < r_1)$, where r_1 is the distance from the reference electron to the nearest nucleus.

In figure 3.1, the second- and fourth-order expansions are compared with the exact analytic exchange hole at different reference points in the Be and N atoms.

In figure 3.1 (a), when the reference point is inside the 1s shell the exact exchange hole assumes the form of a Gaussian-like function. This is attributed to the fact that the 1s orbital gives the biggest contribution to the density, causing the exact hole to adopt the form of this orbital. In Figure 3.1 (b), the reference point has been placed in the region between core and valence shells. In this region, there is a significant overlap between different orbitals contributing to the density. Hence, the exact analytic exchange hole exhibits a strong dependence on both positions $\boldsymbol{r}_1$ and $\boldsymbol{r}_2$ resulting in a nonlocal maximum. Within the valence-shell region the exact exchange hole has a remarkable structure near the position of the nucleus at $u = 2.0$ a.u. as shown in figure 3.1 (c). This indicates that even when the reference point is placed far from the nucleus the exact hole remains trapped into the system. Moreover, the valence-shell region is known to be

slightly more homogeneous than the other parts of an atom thus reflecting the smooth behavior of the exact analytic hole.

We observed from the inset of figure 3.1 (a) that both expansions agree qualitatively to the exact exchange hole, reflecting that when the exact exchange hole is localized both expansions are able to correctly represent it. On the contrary, when the exact exchange hole is delocalized over a region of space the expansions differ quite considerably in how they represent the former, as shown in the insets of figures 3.1 $(b) - (c)$. The fourth-order expansion reproduces the form of the exact curve longer,within their definition range $(0 < u < r_1)$, whereas the second-order expansion diverges much sooner. Outside its definition range, we cannot expect that the Taylor series expansions of the exact spherically averaged exchange hole recover the exact exchange hole[55].

Therefore, the fourth-order expansion can, in general, better represent the exact exchange hole in the core, core-valence and valence regions of the Be atom.

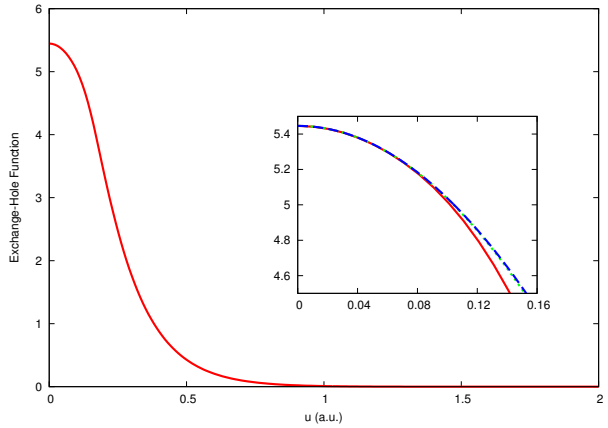

(a) r_1 is 0.15 a.u.

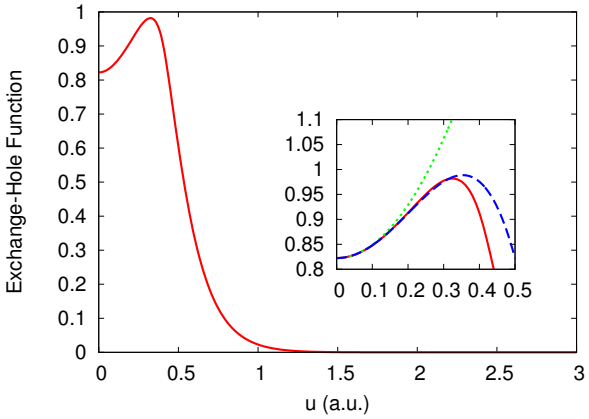

(b) r_1 is 0.40 a.u.

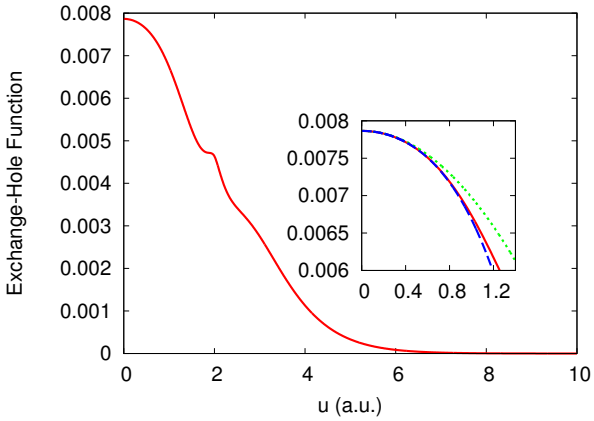

(c) r_1 is 2.00 a.u.

Figure 3.1: Comparison of the expansions, in their definition ranges $(0 < u < r_1)$, with the exact hole. Exact exchange hole (solid red lines), second-order expansion (dotted green lines) and fourth-order expansion (dashed blue lines) of the exact exchange hole of the Be atom.

Figures 3.2 (a)-(c) show the same graphical comparison of the expansions with the exact exchange hole at the core, core-valence and valence regions of the N atom. Here, the exact holes of the N atom have a similar form to those observed in the Be atom. However, when the reference point is in the valence region the exact exchange hole does not show any structure.

From the insets of figures 3.2 (a)-(c), significant improvement is observed with re-

spect to the representation of the exact exchange hole by the fourth-order expansion in the core and valence regions. In the intershell region, shown in inset of figure 3.2 (b), the second- and fourth-order expansions are indistinguishable. Hence, we observed a qualitative improvement of the fourth-order expansion on the second-order expansion,within their definition range $(0 < u < r_1)$, in the description of the exact exchange hole when the reference point is in three distinct regions of the N atom.

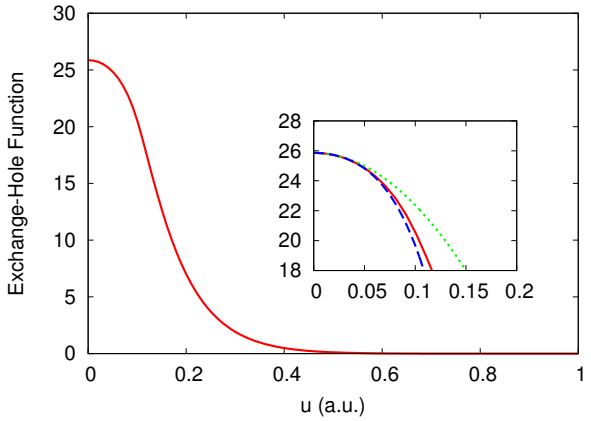

(a) r_1 is 0.10 a.u.

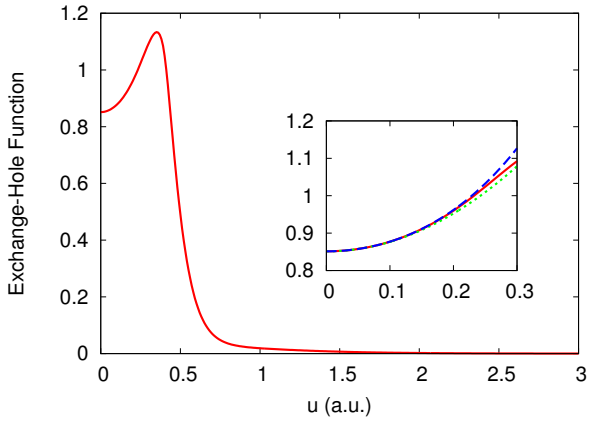

(b) r_1 is 0.40 a.u.

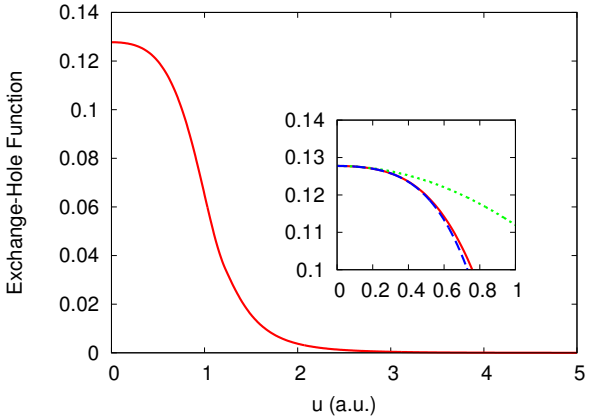

(c) r_1 is 1.25 a.u.

Figure 3.2: Comparison of the expansions, in their definition ranges $(0 < u < r_1)$, with the exact hole. Exact exchange hole (solid red lines), second-order expansion (dotted green lines) and fourth-order expansion (dashed blue lines) of the exact exchange hole of the N atom.

The results of the fourth-order expansion presented above shown a remarkable improvement upon the second-order expansion to describe the exact exchange hole in atomic systems. However, the focus of this work is the calculation of molecular properties that depend on the energy exchange e.g. atomization energies. In view of this, we studied the performance of the fourth-order expansion against the second-order expansion of the exchange hole for two molecular systems the H_2 and N_2. This has been done by comparing the two expansions with the exact analytic exchange hole at four distinct regions: the inner- and outer-valence regions, the midpoint of the σ bond and for a reference point placed perpendicular to the axis of σ bond. The results for the H_2 and N_2 are presented in figures 3.3 and 3.4, respectively.

Because the H_2 has only one electron of each spin, its exchange hole is given by half of the density $\rho_x(\boldsymbol{r}_1,\boldsymbol{r}_2) = \rho(\boldsymbol{r}_2)/2$ and it is independent of $\boldsymbol{r}_1$, the reference electron. This effect is characteristic of any two-electron system and it is known by the name of self-interaction correction. Figures 3.3 $(a)-(d)$ show the plots of the second-, fourth-order expansions and the exact analytic exchange hole. As mentioned before, the expansions must be compared in their definition range $(0 < u < r_1)$ where for values of $u > r_1$ the Taylor series expansions of the exact spherically exchange hole will diverge.

In figure 3.3 (a) and (b), the reference point is placed in the inner and outer valence, respectively. At these points, the exact exchange holes show a smooth behavior which can be attributed to the σ bond. A similar form is seen when the reference point is at the midpoint of the σ bond. For a reference point placed perpendicular to the axis of the σ bond from 1.30874 a.u. from the midpoint, the exchange hole shows a nonlocal maximum.

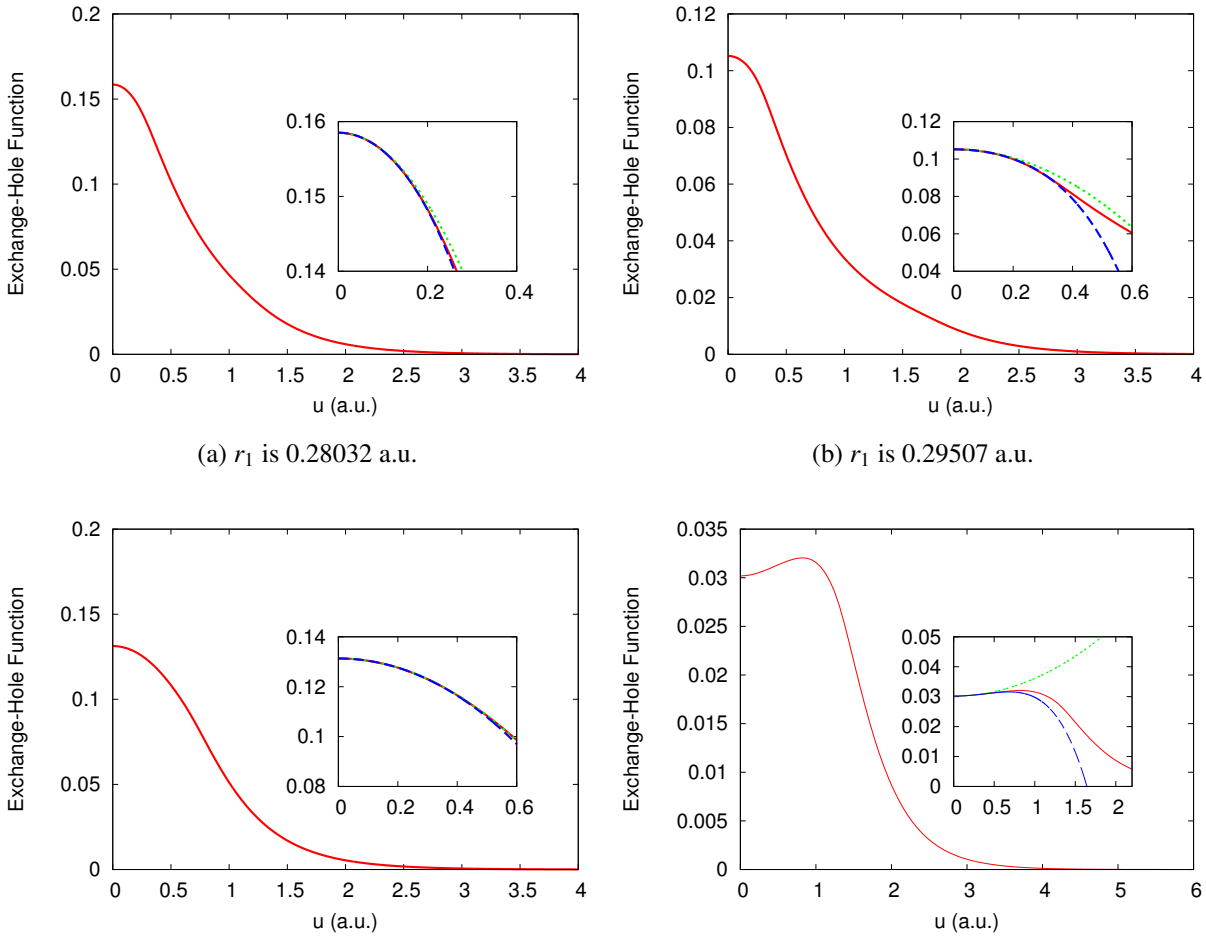

(a) r_1 is 0.28032 a.u.

(b) r_1 is 0.29507 a.u.

(c) r_1 is 0.72293 a.u.

(d) r_1 is 1.30874 a.u.

Figure 3.3: Comparison of the expansions, in their definition ranges $(0 < u < r_1)$, with the exact hole. Exact exchange hole (solid red lines), second-order expansion (dotted green lines) and fourth-order expansion (dashed blue lines) of the exact exchange hole of the H_2 molecule.

In the insets of figures 3.3 $(a) - (c)$, the fourth-order expansion does not show a remarkable improvement. This can be explained by the fact that the exchange hole is well localized in these regions. However, in the inset of figure 3.3 (d), the fourth-order expansion can correctly describe the form of the exact exchange hole longer indicating that it is better suited to handle nonlocal regions of molecules than the second-order expansion.

In figure 3.4 (a), the reference point is placed in the inner valence of the N_2 the exact analytic exchange hole shows significant structure due to the nucleus which is near $u = 0.54$. At the outer valence, the curve of the exact hole is well-behaved and symmetric resembling a σ-like orbital. This is due to the 2s orbitals which give the biggest contribution to the σ bond. When the reference point is at the midpoint of the σ-bond the exact hole has a form very close to the outer valence, a σ-like orbital. We also placed the reference point perpendicular to the axis of the σ bond at a distance of 1.92896 a.u. from the midpoint. At this reference point the exact analytic exchange hole describes a nonlocal maximum. This is due to the overlap of different orbitals in this region.

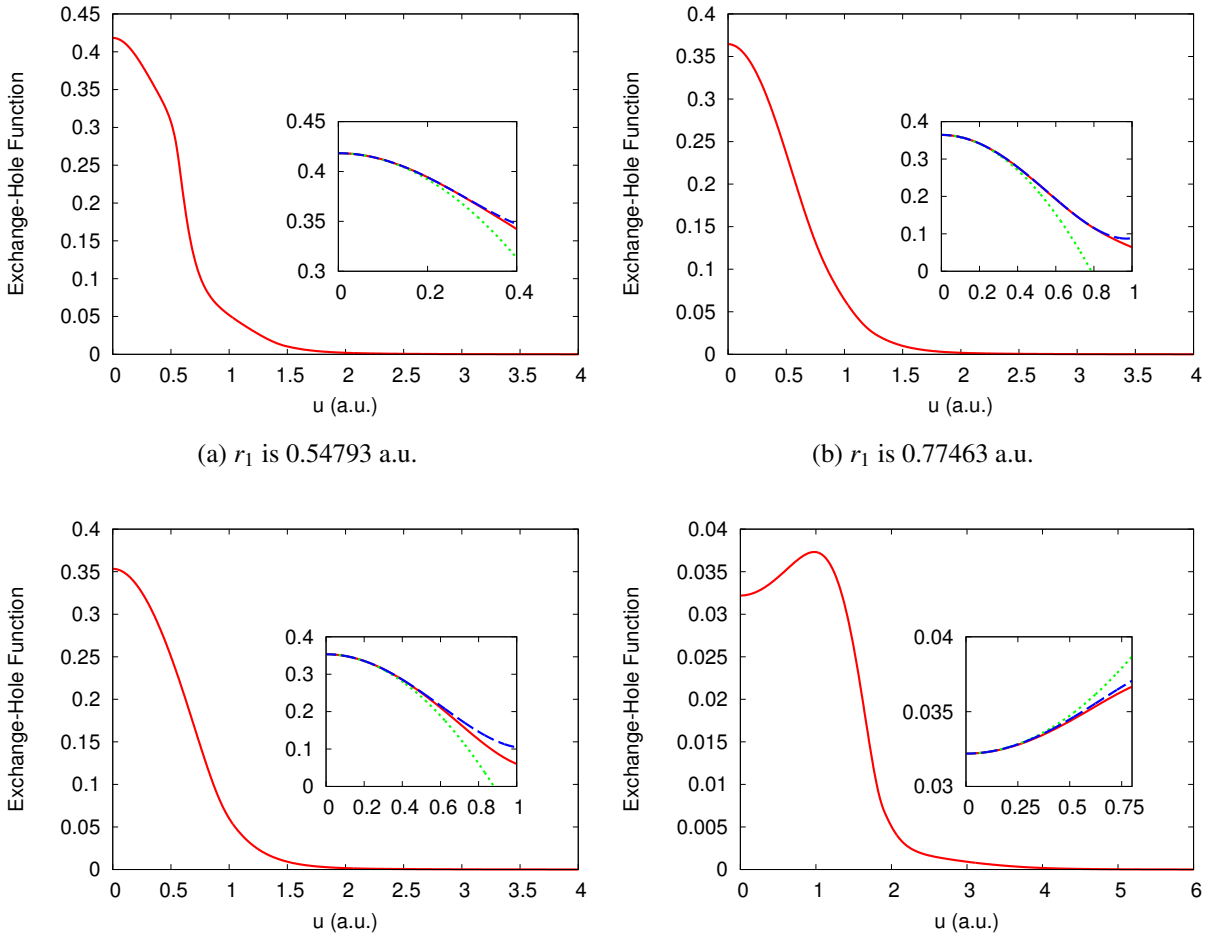

(a) r_1 is 0.54793 a.u.

(b) r_1 is 0.77463 a.u.

(c) r_1 is 0.99952 a.u.

(d) r_1 is 1.92896 a.u.

Figure 3.4: Comparison of the expansions, in their definition ranges $(0 < u < r_1)$, with the exact hole. Exact exchange hole (solid red lines), second-order expansion (dotted green lines) and fourth-order expansion (dashed blue lines) of the exact exchange hole of the N_2 molecule.

From the results presented in figure 3.4 (a)-(d) we observed that the fourth-order expansion, within their definition range $(0 < u < r_1)$, improves the description of the exact exchange hole upon the second-order expansion. Particularly in the region where the exact hole does delocalized, as in the inner valence and in the bond region off the axis of the σ-bond, the fourth-order expansion shows better qualitative agreement to the exact curve.

3.3.2 Basis Set Influence on the Expansions of $\rho_x(\boldsymbol{r}_1, u)$

Up to this point, we have validated and assessed the fourth-order expansion in describing the exact exchange holes in several reference points of atoms and molecules. In order to employ the fourth-order expansion in the construction of exchange functional approximations, we study how Gaussian-type basis sets influence its applications.

Gaussian-type basis set artifacts are not new in quantum chemistry. For instance, oscillations and divergences are an unpleasant reality in the development of KS effective potentials[61]. These artifacts can be amplified when derivatives of orbitals and densities are necessary during calculations. Since the fourth-order expansion contains derivatives of orbitals and densities and we intend to employ it in the construction of exchange functional approximations, we studied how Gaussian-type basis sets influence the application of the biharmonic condition.

From the biharmonic condition defined in 3.27, it is straightfoward to verify that the highest order derivative with respect to the orbitals is in the leading term, the biharmonic of the density. Therefore, it is sufficient to study the influence of Gaussian-type basis sets on this term alone. We also studied the influence on the laplacian of the density, the leading term of the curvature condition defined in equation 3.9.

The biharmonic of the density of the 1s orbital of H atom has been analytically calculated with three basis sets. These basis sets are linear combinations of primitive Gaussian functions and are known in the quantum chemistry community as STO-nG where n stand for the number of primitive functions employed. In figure 3.5, we compared the biharmonic of the densities obtained with STO-1G, STO-2G and STO-3G with the exact curve given by the biharmonic of the density of the 1s Slater-type orbital of the Hydrogen atom. These curves are denoted as BHDGn where the they indicate the Biharmonic of the Density calculated by the STO-nG basis set, i.e. BHDG1 denotes the biharmonic of the density obtained with the STO-1G basis set. The notation BHDS indicates the curve of the Biharmonic of the Density obtained with the Slater-type orbital of the Hydrogen atom.

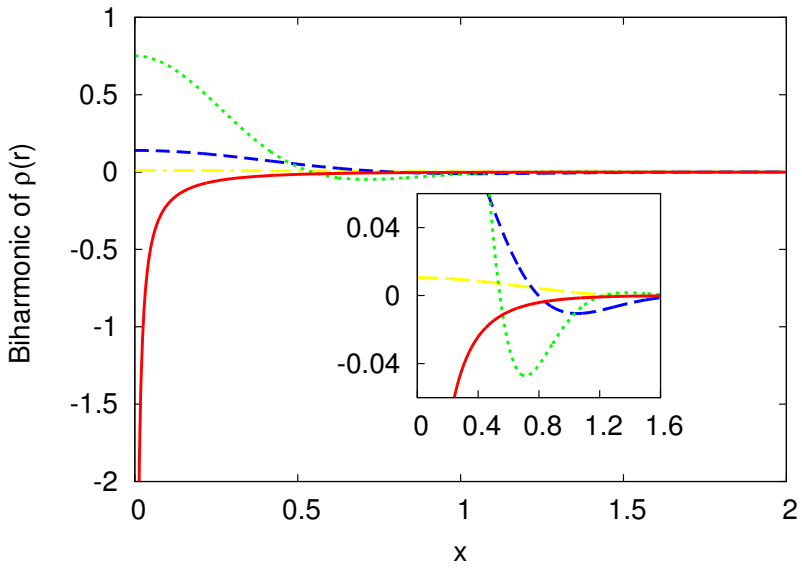

Figure 3.5: BHDG1 (yellow dashed-dotted line), BHDG2 (blue dashed line) and BHDG3 (greed dotted line) correspond to the biharmonic of the density of the 1s orbital obtained with a STO-1G, STO-2G and STO-3G basis set, respectively. BHDS (red solid line) is the biharmonic of the density of the density of the 1s Slater-type orbital of the Hydrogen atom.

We observe in figure 3.5 that BHDG1, BHDG2 and BHDG3 do not describe correctly the exact curve. However, the curve generated by BHDG3 seems to better describe the asymptotic behavior of the exact curve BHDS.

Also, we analytically calculated and plotted in figure 3.6 the laplacian of the density of the 1s orbital of H atom. The densities were calculated with the STO-1G, STO-2G,STO-3G basis set and a Slater-type orbital. These curves are denoted as LPDGn where the they indicate the Laplacian of the Density calculated with the STO-nG basis set, i.e. LPDG1 denotes the biharmonic of the density obtained with the STO-1G basis set. The notation LPDS indicates the curve of the Laplacian of the Density obtained with the Slater-type orbital of the Hydrogen atom.

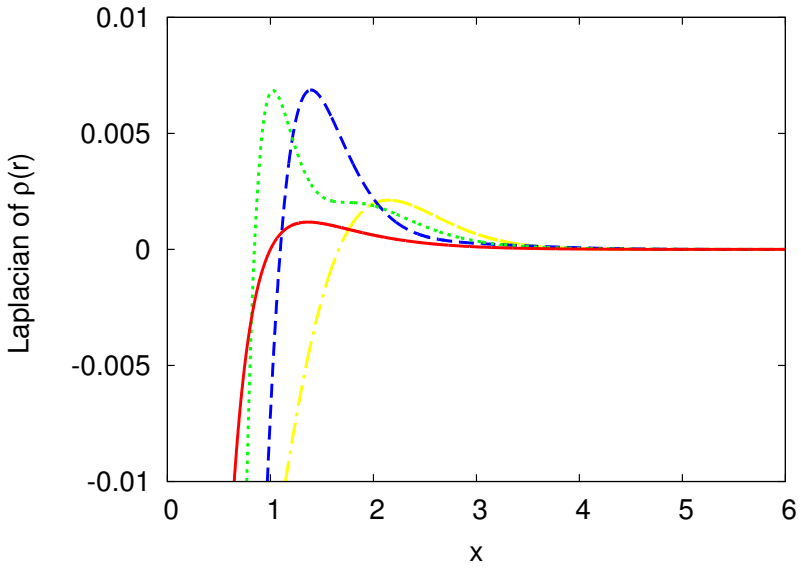

Figure 3.6: LPGD1 (yellow dashed-dotted line), LPGD2 (blue dashed line) and LPGD3 (greed dotted line) correspond to the laplacian of the density of the 1s orbital obtained with a STO-1G, STO-2G and STO-3G basis set, respectively. LPDS (red solid line) is the laplacian of the density of the 1s Slater-type orbital of the Hydrogen atom.

We observe in figure 3.6 that LPGD3 shows a qualitative improvement on LPGD1 and LPGD2 but it still not able to recover the exact curve LPDS. Many functionals were constructed employing the curvature condition which contains the laplacian of the density. Furthermore, the curvature condition and the laplacian of the density alone are extensively used in bonding analysis where functions based on these quantities are able to localized electrons in regions of space. Clearly, a small Gaussian-type basis set such as the STO-3G, cannot be used in these applications when chemical accuracy is taken into consideration.

The influence of the basis set oscillations on exchange hole models can be explained by comparing the plots of exchange energy densities, $\varepsilon_\sigma(\boldsymbol{r})$, of the H atom. This is done by obtaining, in a post-HF calculation[2], the exchange energy densities of the original BR model (BR2) and the BR model parameterized with the biharmonic condition (BR4) in place of the curvature condition [3]. The plot of exact exchange energy density of the H

[2]Details of calculations are given in section 4.4 of chapter 4.

[3]For further details of the BR4 model see section 4.4 of chapter 4.

atom was obtained with the following formula,

$$\varepsilon_{x\sigma}(r) = -\left[1-\exp^{-\alpha r}\left(1+\frac{1}{2}\alpha r\right)\right]\Big/ 2r. \tag{3.28}$$

Note that equation 3.28 is basis set independent and has the same form as the exchange energy density of the BR model defined in equation 2.154. However, according to the hydrogenic orbital we set $\alpha = 2$ in equation 3.28 in our calculations while varying r along the x-axis.

Since BR2 and BR4 models are based on the hydrogenic orbital and both models are parameterized with the Taylor series expansion of the exact spherically averaged exchange hole, we expect that their exchange energy density curves recover the exact one. In figure 3.7, we compare the exchange energy densities of BR2 and BR4 models with the exact one for the H atom.

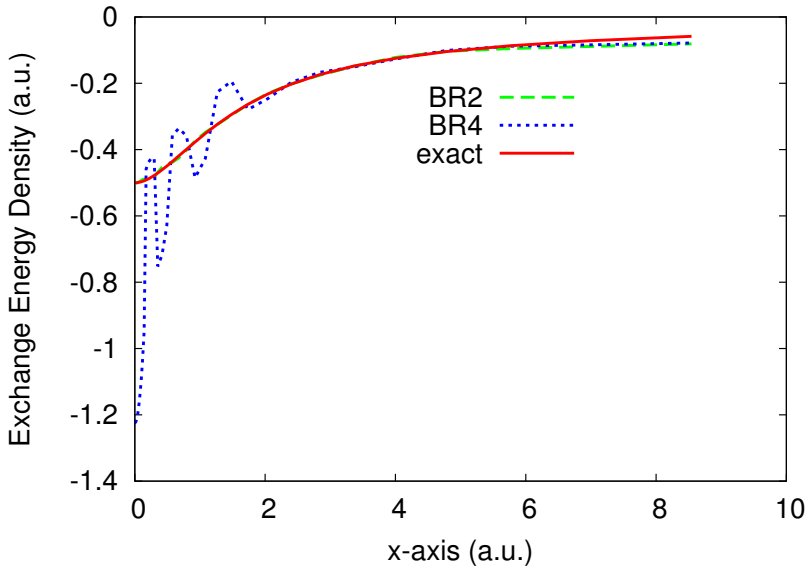

Figure 3.7: Comparison of Exchange Energy Densities (a.u.) of BR2 and BR4 with the exact for the H atom along the x-axis (a.u.)

The exact exchange energy density obtained by equation 3.28 is smooth in all its extention, whereas the exchange energy density obtained by BR4 oscillates with amplitude increasing toward the nucleus. It recovers the exact one in the interval of $(3 \leq x \leq 5)$

and reproduce BR2 exchange energy density for $(x > 5)$. The curve obtained by BR2 recovers the exact exchange energy density for $(x \leq 5)$. We do not expect any of the two models to recover the exact exchange energy density when $(x > 5)$. In this range, the contribution of the exchange energy density to the total exchange energy is very small due to the low-density limit. The oscillations observed in figure 3.7 arise from small undulations in Kohn-Sham orbitals[62] that are amplified by any derivative of the orbitals or the density. In this regard the biharmonic condition, which contains the biharmonic of the density and other high derivatives of orbitals, transfers these oscillations into the BR4 model during the its parameterization causing oscillations in the exchange energy density. It is important to mention that models constructed to satisfy the short-range quartic behavior (the on-top, the curvature and the biharmonic conditions) along with the normalization condition could present unexpected behaviors related to these oscillations. By "unexpected", we mean for instance the impossibility to satisfy all constraints imposed on the model therefore leading to unphysical total exchange energies.

3.4 Conclusion

We have focused here on the assessment of the fourth-order expansion for the description of the exact exchange hole. The second-order and fourth-order expansions were compared with the exact analytic exchange holes of several reference points in the Be, N, H_2 and N_2 systems. Here, we found that, in its definition range $(0 < u < r_1)$[55], the fourth-order expansion remarkably improves the representation of the exact exchange hole compared to the second-order expansion.

We observed that the fourth-order expansion, in general, represent quite accurately the short-range quartic behavior of the exact exchange hole compared to the second-order expansion. In regions where the exact exchange hole is delocalized (Figures 3.1 (c), 3.2 (c)), 3.3 (d) and 3.4 (d)), we observed that the fourth-order expansion is able to remarkably mimic the exact exchange hole.

Also, we verified the influence of Gaussian-type basis sets oscillations on the expansions of the exact exchange hole by studying the behavior of the leading terms of the

curvature and biharmonic conditions with different Gaussian-type basis sets. It has been found that these basis sets artifacts indeed cause instabilities in the leading terms of the two conditions.

Moreover, in figure 3.7, we observed by comparing the exchange energy densities of BR2 and BR4 with the exact one for the H atom that these oscillations originated in the basis set have a strong influence in the BR4 model. Consequently, we believe that any other exchange hole model parameterized with the biharmonic condition would be critically affected by this effect.

One way around this problem would be to implement and perform our computations based on plane waves where this oscillations would not be present. Another possibility is to calculate the weighted averaged of the exchange energy densities of the BR2 and BR4 as

$$\varepsilon_{x\sigma}(\boldsymbol{r}) = \omega(\boldsymbol{r})\varepsilon_{x\sigma}^{BR2}(\boldsymbol{r}) + [1-\omega(\boldsymbol{r})]\varepsilon_{x\sigma}^{BR4}(\boldsymbol{r}), \tag{3.29}$$

where the function $\omega(\boldsymbol{r})$ can determine how much contributions from BR2 and BR4 will be used to generate $\varepsilon_{x\sigma}(\boldsymbol{r})$ with aim of supressing parts of the oscillations in the exchange energy density observed in figure 3.7. Development of $\omega(\boldsymbol{r})$ is under development by the author.

CHAPTER 4

EXCHANGE-HOLE MODELS

It is known that many exchange functional approximations are based on the LDA exchange hole[53]. However, this first approximation suffers from many problems, pointed out by us in chapter 2, that lead to poor results when applied to molecular systems. For instance, LDA exchange hole is always localized to some extent around the reference point. In contrast, the exact exchange hole in a molecular system may be delocalized over several centers. Even when the reference point is far from the molecule, the exchange hole is still trapped at the molecule. This fact leads to an asymptotic behavior of the form $1/\boldsymbol{r}$ of the exchange energy density and the exchange potential. Furthermore, the LDA exchange hole does not account for the short-range behavior given by the expansion of the exact spherically averaged exchange hole.

In the last chapter we also presented the BR exchange-hole model[3] which is based on a physical system but differently from LDA[16], the BR model is based on an inhomogeneous system. By parameterizing their model to the second-order expansion of the exact exchange hole, the BR model can describe exactly the short-range behavior of the exchange hole up to the second-order. The result of this new approach is an striking improvement over LDA in terms of atomic exchange energies.

Altough the LDA exchange hole can deliver good results for homogeneous systems and the BR exchange hole is accurate in the description of atomic systems, the main concern of chemists is the breaking and formation of chemical bonds. In this regard, we believe that there still room for improvement at the level of exchange hole modeling. In this second part of this work we propose three exchange hole models. We adopted the framework used in the construction of the BR model where a systematic constraint satisfaction is employed. In general, we apply all current known conditions of the exact exchange hole as well as the new condition derived by us in the last chapter.

The organization of this chapter is as follows. For every model we first give an introduction followed by the Development section where all mathematical details are

present. Next, in Implementation, we describe how the models were used in realistic calculations. In the Results and Discussion we assess the exchange hole models and describe their particularities and finally, in Conclusion, we give our final remarks.

4.1 The Four-Parameter Model

The Four-Parameter (FP) model is an analytic form aimed to approximate the exchange hole. Its construction, based on a polynomial tamed by an exponential function, clearly is not based on any physical system differing in this aspect from the LSDA[53] and BR exchange holes[3]. However, this is not a new approach. Becke[54] and Ernzerhof and Perdew[53] have also proposed exchange hole functions with similar forms. The FP model is tought to be flexibe enough to be parameterized by the fourth-order expansion of the exact exchange hole. We also apply the normalization and non-negativity conditions.

4.1.1 Development

The FP model is built from the positive series expansion about the variable u

$$v(a,b,c,u) = \left(a + bu + cu^2\right)^2, \tag{4.1}$$

where the coefficients are parameters to be determined from analytical properties of the exact exchange hole. Note that, alone, these parameters carry no physical meaning.

Since we seek to construct a density function from an ordinary function we need to symmetrize equation 4.1 with respect to the y-axis which gives,

$$\begin{aligned} v(a,b,c,u) + v(a,b,c,-u) &= -2\left(a^2 + b^2u^2 + 2acu^2 + c^2u^4\right) \\ f(a,b,c,u) &= 2\left(a^2 + b^2u^2 + 2acu^2 + c^2u^4\right). \end{aligned} \tag{4.2}$$

Normalization of the model is enforced by a damping factor which has the form of a

Gaussian-like function which multiplies $f(a,b,c,u)$,

$$\rho_{x\sigma}^{FP}(a,b,c,d,u) = 2\left(a^2 + b^2u^2 + 2acu^2 + c^2u^4\right)e^{-du^2}. \tag{4.3}$$

The exponential works by taming the core of the density function. When $u \to \infty$ the polynomial part goes to infinity very fast while the gaussian-like function goes to zero thus smoothing the function.

At this point we expand the FP model in a Taylor series and equate its coefficients

$$\begin{aligned}
\rho_{x\sigma}^{FP,(0)} &= -2a^2 \\
\rho_{x\sigma}^{FP,(2)} &= \left(-2b^2 - 4ac + 2a^2d\right) \\
\rho_{x\sigma}^{FP,(4)} &= \left(-2c^2 + 2b^2d + 4acd - a^2d^2\right),
\end{aligned} \tag{4.4}$$

to those of the exact hole denoted K_0, K_2 and K_4.Note that the numbers between parenthesis in superscripts indicate the order of each coefficient in the expansion. With this procedure, the parameter a is determined by the zeroth-order term K_0 which gives the density at the reference point,

$$a = \frac{\sqrt{K_0}}{\sqrt{2}}. \tag{4.5}$$

Once the form of a is determined we have that b gives,

$$b = \frac{\sqrt{2c\sqrt{2}\sqrt{K_0} + dK_0 + K_2}}{\sqrt{2}}. \tag{4.6}$$

From a and b we get c,

$$c = \frac{\sqrt{\frac{d^2K_0}{2} + dK_2 + K_4}}{\sqrt{2}}. \tag{4.7}$$

Note that the terms K_2 and K_4 are the second-order and fourth-order terms of the fourth-order expansion of the exact exchange hole, respectively. Hence, the FP model can represent the short-range quaternary behavior of the exact spherically averaged exchange hole.

Imposing the normalization condition we obtain,

$$\begin{aligned} \int du^2 4\pi\rho_{x\sigma}^{FP}(a,b,c,u) &= 1 \\ \frac{(7d(5dK_0+6K_2)+30K_4)\pi^{3/2}}{8d^{7/2}} &= 1. \end{aligned} \tag{4.8}$$

Equation 4.8 does not have a simple linear expression and it is not possible to solve it in terms of d. A numerical approach needs to be employed to determine the value of d. There are a number of mathematical methods to determine the solutions of a nonlinear equation. The Newton-Raphson method is one of the most reliable root-finding methods used in many areas in science. It also happens to have a very simple implementation which is definitely an advantage. Note that equation 4.8 can have multiple solutions however, this version of the algorithm only employes the first one found by the Newton-Raphson scheme.

In order to apply the Newton-Raphson scheme, we define the following function

$$N(d) = \frac{(7d(5dK_0+6K_2)+30K_4)\pi^{3/2}}{8d^{7/2}} - 1. \tag{4.9}$$

When equation 4.9 vanish, then the parameter d should be determined by the Newton-Raphson method.

Once we have solved equation 4.8 , the exchange energy density at the reference point $\boldsymbol{r}$ is given by,

$$\varepsilon_{x\sigma}^{FP}(\boldsymbol{r}) = \int_0^\infty du 4\pi\rho_{x\sigma}^{FP}(a,b,c,d,u) = -\frac{2(3d(dK_0+K_2)+2K_4)\pi}{d^3}. \tag{4.10}$$

From equation 4.10, it is clear that all parameters, a, b, c and d must have been determined previously.

4.1.2 Implementation

The FP model was implemented into the GAUSSIAN code[60] with the computer language fortran 77. The implementation of the Newton-Raphson method was obtained

from the Numerical Recipes in Fortran 77.

In summary, the algorithm build for the FP model works as this:

1. First, the GAUSSIAN program calculates densities and all quantities needed by the fourth-order expansion of the exact spherically averaged exchange hole.

2. Second, the Newton-Raphson method is employed, in every point of the grid, to find a solution to equation 4.9. Once the parameter d is determined, the code calculates the values of the other parameters a, b and c, thus solving the model.

3. Third, the exchange energy density is calculated by equation 4.10 and then passed to the GAUSSIAN program where it will be used to obtain the total exchange energy of the target system.

4.1.3 Results and Discussion

Calculations of the total exchange energies with the FP model were done using the 6-311G+(2d,p) basis set in the GAUSSIAN program. This basis set represent the orbitals of each atom where it has 6 gaussian functions for the inner shell, 3 gaussian functions for the valence orbitals and two gaussian functions with different sizes for extended valence orbitals. The specification (2d,p) indicates that one p-type function is added to the hydrogen atom and two more d-type functions to atoms with $Z > 2$.Moreover, cartesian functions were used for d-type orbitals. The grid employed in our calculations has 75 radial shells and 302 angular points per shell, giving approximately 7000 points per atom. Experimental geometries were used as inputs through out all our calculations.

We begin to assess the FP model with small systems such as the atoms of the first and second row of the periodic table. We verified, however, that it is not possible to find solutions of equation 4.9, which would determine the parameter d, in all points of space. Note that the parameters b and c are coupled to the parameter d through equations 4.6 and 4.7, respectively. Thus, for the points where equation 4.6 does not have a solution the model cannot satisfy all conditions. This problem leads, in general, to unphysical results, therefore compromising the calculation of total exchange energies. Any exchange-hole

model that does not satisfy the normalization condition could, for instance, remove more than one electron from the system.

4.1.4 Conclusion

Unfortunately, equation 4.9 cannot be solved for every point in the space. Consequently, the FP model does not satisfy the normalization condition in all space. Since the normalization is one of the most restrictive analytical properties of the exact exchange hole this poses a serious problem for the application for this model.

Since the FP model is built to reproduce the short-range quaternary behavior of the exact spherically averaged exchange hole, the oscillations verified in derivatives of orbitals and densities is clearly transfered to the model through its parameterization. Hence, these oscillations corroborate to generate instabilities in the solution of the FP model.

The advantage of the FP model lies in its simple mathematical form and flexibility to represent the fourth-order expansion of the exchange hole. Therefore, we believe that the FP model could be a good exchange hole approximation once the instabilities produced by the basis set are solved.

4.2 Extension of Becke-Roussel Model

It is known that the BR model[3] reproduce the short-range quadratic behavior of the exact spherically averaged exchage hole. However, we shown in the last chapter that the fourth-order expansion of the exact exchange hole improves the representability of the short-range behavior over the second-order expansion for atomic and molecular systems. This lead us to propose a correction or an extension to the BR model. A modification to the BR model is supported by its simple analytic form and good results in terms of atomic exchange energies.

4.2.1 Development

We begin with the unnormalized form of the spherically averaged BR model defined by

$$\rho_{x\sigma}^{BR}(a,b,u) = \frac{1}{2a^2bu}\left[(a|b-u|+1)e^{-a|b-u|} - (a|b+u|+1)e^{-a|b+u|}\right], \tag{4.11}$$

where u is the interelectronic distance and a and b are parameters to be determined. With the unnormalized BR model we construct a new exchange hole model (EBR model)

$$\rho_{x\sigma}^{EBR}(a,b,c,u) = (1+cu^4)\rho_{x\sigma}^{BR}(a,b,u), \tag{4.12}$$

where c is a new parameter to be determined. Note here that when $c = 0$ we obtain the original unnormalized BR model.

The normalization condition is satisfied through the normalization factor calculated by,

$$\begin{aligned}\int du^2 4\pi\rho_{x\sigma}^{EBR}(a,b,c,u) &= \frac{8\left(360c^2+40a^2b^2c^2+a^4\left(1+b^4c^2\right)\right)\pi}{a^7} \\ &= N(a,b,c)\end{aligned} \tag{4.13}$$

where $N(a,b,c)$ is the normalization factor. Notice that $N(a,b,c)$ depends on all parameters of the EBR model. Hence, the normalized form of the EBR model is,

$$\rho_{x\sigma}^{EBR}(a,b,c,u) = \frac{1}{N(a,b,c)}\left[(1+cu^4)\rho_{x\sigma}^{BR}(a,b,u)\right]. \tag{4.14}$$

The normalization factor does not affect the ability of the EBR model to obtain the original BR model. In fact, with the normalization factor when $c = 0$ we obtain the normalized BR model in its original form.

Expansion of equation 4.14 in a Taylor series about u up to the fourth-order provides

three coefficients,

$$\begin{aligned}
\rho_{x\sigma}^{EBR,(0)}(a,b,c) &= \frac{a^7 e^{-ab}}{8\left(\left(360c^2+40a^2b^2c^2+a^4\left(1+b^4c^2\right)\right)\pi\right)} \\
\rho_{x\sigma}^{EBR,(2)}(a,b,c) &= \frac{a^8(-2+ab)e^{-ab}}{48b\left(360c^2+40a^2b^2c^2+a^4\left(1+b^4c^2\right)\right)\pi} \\
\rho_{x\sigma}^{EBR,(4)}(a,b,c) &= \frac{a^7\left(\frac{a^4}{120}-\frac{a^3}{30b}+c^2\right)e^{-ab}}{8\left(360c^2+40a^2b^2c^2+a^4\left(1+b^4c^2\right)\right)\pi}.
\end{aligned} \tag{4.15}$$

Note that the numbers between parenthesis in superscripts indicate the order of each coefficient in the expansion. Equating these coefficients to those of the expansion of the exact hole in a Taylor series produces three non-linear equations,

$$\begin{aligned}
F(a,b,c) &= \rho_{x\sigma}^{EBR,(0)}(a,b,c) - K_0 \\
G(a,b,c) &= \rho_{x\sigma}^{EBR,(2)}(a,b,c) - K_2 \\
H(a,b,c) &= \rho_{x\sigma}^{EBR,(4)}(a,b,c) - K_4
\end{aligned} \tag{4.16}$$

Clearly, to determine all parameters a system of three nonlinear equations needs to be solved numerically. For this purpose, the Broyden's method is employed and all parameters are determined when all three functions F, G and H vanish simultaneously. It is known that a system of nonlinear equations can have multiple solutions for a single point $\boldsymbol{r}$ therefore, in this version we only use the first solution found by the Broyden's method.

The exchange energy density at the reference point is given by,

$$\begin{aligned}
\varepsilon_{x\sigma}^{EBR} &= \int_0^\infty du 4\pi\rho_{x\sigma}^{EBR}(a,b,c,u) \\
&= \frac{-2a^4-144c^2-48a^2b^2c^2-2a^4b^4c^2+2a^4e^{-ab}+a^5be^{-ab}+144c^2e^{-ab}+24abc^2e^{-ab}}{2b\left(360c^2+40a^2b^2c^2+a^4\left(1+b^4c^2\right)\right)}.
\end{aligned} \tag{4.17}$$

4.2.2 Implementation

In order to calculate the total exchange energy of a system, first a Hartree-Fock computation is performed to obtain the target system wavefunction. Then, this wavefunction

is used as an initial guess in our calculations which consists of a single SCF iteration, in a post-HF calculation. In this single iteration the GAUSSIAN program[60] generates the densities and all other quantities necessary to build the fourth-order expansion of the exact exchange hole which are then passed into the function code where the EBR model is implemented.

The EBR model was implemented in the GAUSSIAN code using the computer language Fortran 77. In order to determine the parameters of the model we need to solve the system of nonlinear equations defined in 4.15. The Broyden's method which is a root-finding algorithm for multidimensional problems was implemented. This algorithm is a quasi-Newton method that does not need to calculate the Jacobian matrix of the functions F, G and H defined in equation 4.16.

The code of the EBR model was made to be called for each point of the grid produced by the GAUSSIAN program. Hence, at each of these points we seek to determine the parameters of the EBR model to finally calculate the total exchange energy.

In summary, the algorithm build for the EBR model works as this:

1. First, the GAUSSIAN program calculates densities and all quantities needed by the fourth-order expansion of the exact spherically averaged exchange hole.

2. Second, the Broyden's method is employed, in every point of the grid, to find a solution to the model. Once a solution is found all parameters are determined.

3. Third, with the parameters determined the exchange energy density is calculated by equation 4.17 and then passed to the GAUSSIAN program where it will be used to calculate the total exchange energy of the target system.

4.2.3 Results and Discussion

The actual calculations were done using the 6-311G+(2d,p) basis set in the GAUSSIAN program. This basis set represent the orbitals of each atom where it has 6 gaussian functions for the inner shell, 3 gaussian functions for the valence orbitals and two gaussian functions with different sizes for extended valence orbitals. The specification (2d,p)

indicates that one p-type function is added to the hydrogen atom and two more d-type functions to atoms with $Z > 2$. Moreover, cartesian functions were used for d-type orbitals.The grid employed in our calculations has 75 radial shells and 302 angular points per shell, giving approximately 7000 points per atom. Experimental geometries were used as inputs through out all calculations.

In our calculations we have tested all solutions of the system of nonlinear equations 4.16 where Broyden's method found multiple solutions. Unfortunately, none of them lead to better results. The addition of the fourth-order term correction to the EBR model, in most cases, did not improve the results for exchange energies of atoms and molecules over the BR model. The MAE of the atomic and molecular subsets show a very small reduction compared with original BR.

From the results of table 4.*I*, it is possible to conclude that the correction proposed to the original BR model does not produce any improvement to the exchange energies.

System	E_x^{Exact}	E_x^{BR}	E_x^{EBR}
H	-0.313	-0.313	-0.313
He	-1.026	-1.039	-1.039
Li	-1.781	-1.793	-1.793
Be	-2.666	-2.680	-2.680
B	-3.768	-3.783	-3.774
C	-5.074	-5.093	-5.092
N	-6.603	-6.629	-6.629
O	-8.210	-8.252	-8.251
F	-10.035	-10.093	-10.086
Ne	-12.097	-12.176	-12.176
Na	-14.015	-14.072	-14.072
Cl	-27.539	-27.474	-27.473
P	-22.641	-22.626	-22.626
MAEs	0.000	0.032	0.030
H2	-0.658	-0.658	-0.658
HF	-10.420	-10.509	-10.509
LiH	-2.146	-2.165	-2.165
LiF	-11.994	-12.112	-12.107
Li2	-3.564	-3.591	-3.591
Na2	-28.021	-28.144	-28.137
F2	-19.949	-20.157	-20.157
Cl2	-55.092	-54.982	-54.973
NH3	-7.665	-7.717	-7.702
P2	-45.201	-45.205	-45.205
N2	-13.092	-13.235	-13.234
NO	-14.725	-14.875	-14.875
NO2	-22.897	-23.166	-23.166
O2	-16.259	-16.452	-16.452
MAEs	0.000	0.107	0.106
MAE	0.000	0.071	0.070

Table 4.I: Exchange energies of atoms and molecules (in Hartree). MAE, mean absolute error. MAEs of a set of atoms and molecules and Total MAE are shown.

Since the main concern of chemists lies with the breaking and formation of chemical bonds the calculation of energy changes upon chemical transformation is fundamental. In regard of this, we calculate the exchange-energy contribution to the atomization energy (Table 4.*II*), $\Delta E_x = E_x^{molecules} - E_x^{atoms}$.

Molecules	E_x^{Exact}	E_x^{BR}	E_x^{EBR}
H2	-0.033	-0.033	-0.033
HF	-0.073	-0.103	-0.110
LiH	-0.053	-0.060	-0.060
LiF	-0.179	-0.226	-0.228
Li2	-0.003	-0.006	-0.006
Na2	0.009	0.000	0.007
F2	0.121	0.029	0.015
Cl2	-0.013	-0.034	-0.027
NH3	-0.125	-0.151	-0.135
P2	0.082	0.048	0.048
MAEs	0.000	0.027	0.027
N2	0.114	0.023	0.024
NO	0.089	0.006	0.006
NO2	0.126	-0.033	-0.034
O2	0.162	0.052	0.051
MAEs	0.000	0.111	0.111
MAE	0.000	0.051	0.051

Table 4.II: Exchange-energy contributions to the atomization energies (in Hartree). MAE, mean absolute error. MAEs of a set of single- and multi-bonded molecules and Total MAE are shown.

Again, the EBR model does not show any improvement to the exchange-energy contribution to the atomization energies over the BR model. The failure of the EBR model to improve the results of exchange energies and their contributions to the atomization energies can be directly related to oscillations present in the fourth-order term which

causes instabilities in the solution of the model. By solution of the model we mean that the system of nonlinear equations defined in equation 4.16 does not have a solution in a large number of points of the space. When this is the case, the EBR model recover the BR model by taking the parameter $c = 0$ in the equation 4.14. Hence, the major contribution to the results presented here belong to the BR model.

4.2.4 Conclusion

The fourth-order expansion of the exact spherically averaged exchange hole provides a systematic improvement over its second-order version. In this part of the work, we applied the former expansion as a correction to the BR model resulting in the EBR model. We tested its ability to describe exchange energies and chemical transformations such as atomization energies. We found that oscillations due to the basis set hinder the solution of the EBR model leading to unsatisfactory results in terms of an improvement over the original BR model.

4.3 H_2 Model

The H_2 model is based on the density of the bonding orbital of the molecule H_2. The idea is to construct an exchange hole model that has the characteristics of a two-electron system hole and that could be used to correctly describe the exact exchange hole during its dissociation process. Moreover, the H_2 model is designed to represent exactly the short-range quatic behavior of the exact spherically averaged exchange hole. Furthermore, two other conditions are imposed on this model: the non-positivity and normalization of the exchange hole.

4.3.1 Development

The molecular orbital σ_g of H_2 can be constructed with two gaussian functions by

$$\rho^{H_2}(\boldsymbol{r},\boldsymbol{R}_1,\boldsymbol{R}_2,\alpha,\lambda) = \left[\lambda e^{-\alpha^2(\boldsymbol{r}-\boldsymbol{R}_1)^2} + (1-\lambda)e^{-\alpha^2(\boldsymbol{r}-\boldsymbol{R}_2)^2}\right]^2, \tag{4.18}$$

where $\boldsymbol{R}_1$ and $\boldsymbol{R}_2$ are vectors representing the positions of two nuclei while $\boldsymbol{r}$ is the reference vector, α corresponds to an exponential factor and λ is a parameter which assumes values between 0 and 1. When λ is equal to 0, the function $\rho^{H_2}(\boldsymbol{r},\boldsymbol{R}_1,\boldsymbol{R}_2,\alpha,\lambda)$ reduces to a single nucleus system expressed by a single gaussian-like function centered at $\boldsymbol{R}_2$, while when λ equals to 1 it is also reduced to the same case of a single nucleus centered $\boldsymbol{R}_1$ as shown below

$$\rho^{H}(\boldsymbol{r},\boldsymbol{R}_1,\boldsymbol{R}_2,\alpha,\lambda=0)=\left[e^{-\alpha^2(\boldsymbol{r}-\boldsymbol{R}_2)^2}\right]^2, \tag{4.19}$$

where the superscript H in this particular case indicates that it represents the orbital density of a hydrogen atom. Yet, when $\boldsymbol{R}_2=\boldsymbol{R}_1$ the equation 4.16 reduces to 4.17. In regard of this, equation 4.16 is named the general case of the H_2 model and 4.17 is named the particular case. The parameter λ acts as a switching factor by balancing charge density between the nuclei, which could be very useful in the description of ionic and covalent bonds. Taking the average over all angular parts we obtain

$$\begin{aligned}\rho_{x\sigma}^{H_2}(r,R_1,R_2,\alpha,\lambda,u) = &-\lambda^2\frac{e^{-2\alpha^2((r-R_1)-u)^2}-e^{-2\alpha^2((r-R_1)+u)^2}}{8\alpha^2u(r-R_1)}\\ &+(1-\lambda)^2\frac{e^{-2\alpha^2((r-R_2)-u)^2}-e^{-2\alpha^2((r-R_2)+u)^2}}{8\alpha^2u(r-R_2)}\\ &+(-\lambda^2+\lambda)\frac{e^{-\alpha^2\left[((r-R_1)-u)^2+((r-R_2)-u)^2\right]}-e^{-\alpha^2\left[((r-R_1)+u)^2+((r-R_2)+u)^2\right]}}{2\alpha^2u((r-R_1)+(r-R_2))},\end{aligned} \tag{4.20}$$

where u is the interelectronic distance.

Note that the model is not normalized. We impose the normalization condition through a normalization factor. This is obtained by,

$$\int du^2 4\pi\rho_{x\sigma}^{H_2}(r,R_1,R_2,\alpha,\lambda,u)=1. \tag{4.21}$$

Applying the normalization factor to equation 4.18 yelds the normalized exchange hole

model,

$$\rho_{x\sigma}^{H_2}(r,R_1,R_2,\alpha,\lambda,u) = \frac{2\sqrt{2}\alpha^3}{\pi^{3/2}\left[1+2\left(\lambda^2-\lambda\right)\left(1-e^{-\alpha^2(R_1-R_2)^2/2}\right)\right]} \times \left\{ \lambda^2 \frac{e^{-2\alpha^2((\boldsymbol{r}-\boldsymbol{R}_1)-u)^2} - e^{-2\alpha^2((\boldsymbol{r}-\boldsymbol{R}_1)+u)^2}}{8\alpha^2 u(\boldsymbol{r}-\boldsymbol{R}_1)} + (1-\lambda)^2 \frac{e^{-2\alpha^2((\boldsymbol{r}-\boldsymbol{R}_2)-u)^2} - e^{-2\alpha^2((\boldsymbol{r}-\boldsymbol{R}_2)+u)^2}}{8\alpha^2 u(\boldsymbol{r}-\boldsymbol{R}_2)} + (-\lambda^2+\lambda) \frac{e^{-\alpha^2\left[((\boldsymbol{r}-\boldsymbol{R}_1)-u)^2+((\boldsymbol{r}-\boldsymbol{R}_2)-u)^2\right]} - e^{-\alpha^2\left[((\boldsymbol{r}-\boldsymbol{R}_1)+u)^2+((\boldsymbol{r}-\boldsymbol{R}_2)+u)^2\right]}}{2\alpha^2 u((\boldsymbol{r}-\boldsymbol{R}_1)+(\boldsymbol{r}-\boldsymbol{R}_2))} \right\}. \tag{4.22}$$

At this point, we use the uniform coordinate scaling property of the density to generate a dimensionless exchange hole function. This is done to reduce the number of parameters. First, we define five quantities to help in the coordinate scaling transformation

$$\begin{aligned} a &= \frac{\alpha}{k_F} \\ b &= (\boldsymbol{r}-\boldsymbol{R}_1)k_F \\ c &= (\boldsymbol{r}-\boldsymbol{R}_2)k_F \\ d &= \lambda \\ y &= k_F u, \end{aligned} \tag{4.23}$$

where $k_F = (6\pi^2\rho)^{1/3}$ is the local Fermi wave vector for spin-polarized systems. Next,

we substitute these quantities into equation 4.20 to obtain,

$$J_x^{H_2}(a,b,c,d,y) = \frac{-2\sqrt{2}ak_F^3}{\left(\left(1+2(-1+d)d\left(1-e^{-\frac{1}{2}a^2(c-b)^2}\right)\right)\pi^{3/2}\right)} \times \left[\frac{d^2\left(e^{-2a^2(b-y)^2}-e^{-2a^2(b+y)^2}\right)}{8by} + \frac{(1-d)^2\left(e^{-2a^2(c-y)^2}-e^{-2a^2(c+y)^2}\right)}{8cy} + \frac{\left(d-d^2\right)\left(e^{-a^2\left((b-y)^2+(c-y)^2\right)}-e^{-a^2\left((b+y)^2+(c+y)^2\right)}\right)}{2y(b+c)}\right]. \quad (4.24)$$

The parameters a, b, c and d are related to the exponent of the gaussian function, the position of the first center, the position of the second center and the switching factor, respectively. The reference vector has been eliminated during the density scaling.Note also that the parameter y is related to the interelectronic distance u by $y = k_F u$. The fourth-order expansion of $J_x^{H_2}$ around y gives the zeroth-order term

$$J_x^{H_2,(0)}(a,b,c,d) = \frac{1}{\left(e^{\frac{1}{2}a^2(b-c)^2}-2d\left(-1+e^{\frac{1}{2}a^2(b-c)^2}\right)+2d^2\left(-1+e^{\frac{1}{2}a^2(b-c)^2}\right)\right)\pi^{3/2}} \times \left[2\sqrt{2}a^3e^{-\frac{1}{2}a^2\left(3b^2+2bc+3c^2\right)}\left((-1+d)e^{a^2b^2}-de^{a^2c^2}\right)^2k_F^3\right], \quad (4.25)$$

the second-order term

$$J_x^{H_2,(2)}(a,b,c,d) = \frac{1}{\left(3\left(e^{\frac{1}{2}a^2(b-c)^2}-2d\left(-1+e^{\frac{1}{2}a^2(b-c)^2}\right)+2d^2\left(-1+e^{\frac{1}{2}a^2(b-c)^2}\right)\right)\pi^{3/2}\right)} \times \left[4\sqrt{2}a^5e^{-\frac{1}{2}a^2\left(3b^2+2bc+3c^2\right)}\left(\left(-3+4a^2c^2\right)(-1+d)^2e^{2a^2b^2}+\left(-3+4a^2b^2\right)d^2e^{2a^2c^2}\right.\right.$$
$$\left.\left.-2\left(-3+a^2(b+c)^2\right)(-1+d)de^{a^2\left(b^2+c^2\right)}\right)k_F^3\right], \quad (4.26)$$

and the fourth-order term,

$$J_x^{H_2,(4)}(a,b,c,d) = \frac{1}{\left(15\left(e^{\frac{1}{2}a^2(b-c)^2} - 2d\left(-1+e^{\frac{1}{2}a^2(b-c)^2}\right) + 2d^2\left(-1+e^{\frac{1}{2}a^2(b-c)^2}\right)\right)\pi^{3/2}\right)}$$
$$\times \left[4\sqrt{2}k_F^3 a^7 e^{-\frac{1}{2}a^2\left(3b^2+2bc+3c^2\right)}\left(\left(15-40a^2c^2+16a^4c^4\right)(-1+d)^2 e^{2a^2b^2}\right.\right.$$
$$+\left(15-40a^2b^2+16a^4b^4\right)d^2e^{2a^2c^2}$$
$$\left.\left.-2\left(15-10a^2(b+c)^2+a^4(b+c)^4\right)(-1+d)de^{a^2\left(b^2+c^2\right)}\right)\right]. \quad (4.27)$$

Note that the numbers between parenthesis in superscripts indicate the order of each coefficient in the expansion. Hence, a system of nonlinear equations is formed by equating the coefficients $J_x^{H_2,(0)}$, $J_x^{H_2,(2)}$ and $J_x^{H_2,(4)}$ to those coefficients of the fourth-order expansion of the exact exchange hole. In order to search for solutions of the nonlinear system of equations first we define the three functions

$$\begin{aligned} F(a,b,c,d) &= J_x^{H_2,(0)}(a,b,c,d) - K_0/\rho \\ G(a,b,c,d) &= J_x^{H_2,(2)}(a,b,c,d) - K_2/\rho \\ H(a,b,c,d) &= J_x^{H_2,(4)}(a,b,c,d) - K_4/\rho \end{aligned} \quad (4.28)$$

where coefficients of the fourth-order expansion of the exact exchange hole are denoted K_0, K_2 and K_4. In the density scaling process, the density is scaled out of the analytic form of the exchange hole model. Consequently, when the model is expanded in a Taylor series the densities are present in each coefficient. For this reason, when we form the system of nonlinear equations the density appears dividing K_0, K_2 and K_4. When a solution of system of nonlinear equations is found all three equations defined in equation 4.26 simultaneously vanish, then all parameters of $J_{x\sigma}^{H_2}$ are be determined.

The exchange energy density at the reference point is given by

$$\begin{aligned}\varepsilon_{x\sigma}^{H2}(\boldsymbol{r}) &= \frac{2\pi\rho}{k_F^2}\int_0^\infty dy\, y J_{x\sigma}^{H_2}(a,b,c,d,y) \\ &= \frac{1}{-bc(b+c)\left(-2\left(d^2-d\right)+e^{\frac{a^2(c-b)^2}{2}}\left(2d^2-2d+1\right)\right)} \\ &\times\left[e^{\frac{a^2(c-b)^2}{2}}c(b+c)d^2\mathrm{Erf}\left(ab\sqrt{2}\right)+e^{\frac{a^2(c-b)^2}{2}}b(b+c)(d-1)^2\mathrm{Erf}\left(ac\sqrt{2}\right)\right. \\ &\left.-4bc\mathrm{Erf}\left(\frac{(b+c)a}{\sqrt{2}}\right)d(d-1)\right],\end{aligned} \tag{4.29}$$

where Erf is the error function.

Figure 1 shows the behavior of the weighted $J_{x\sigma}^{H_2}(a,b,c,d,y)$ for three distinct values of d. Note the shift in the density between centers while we vary d.

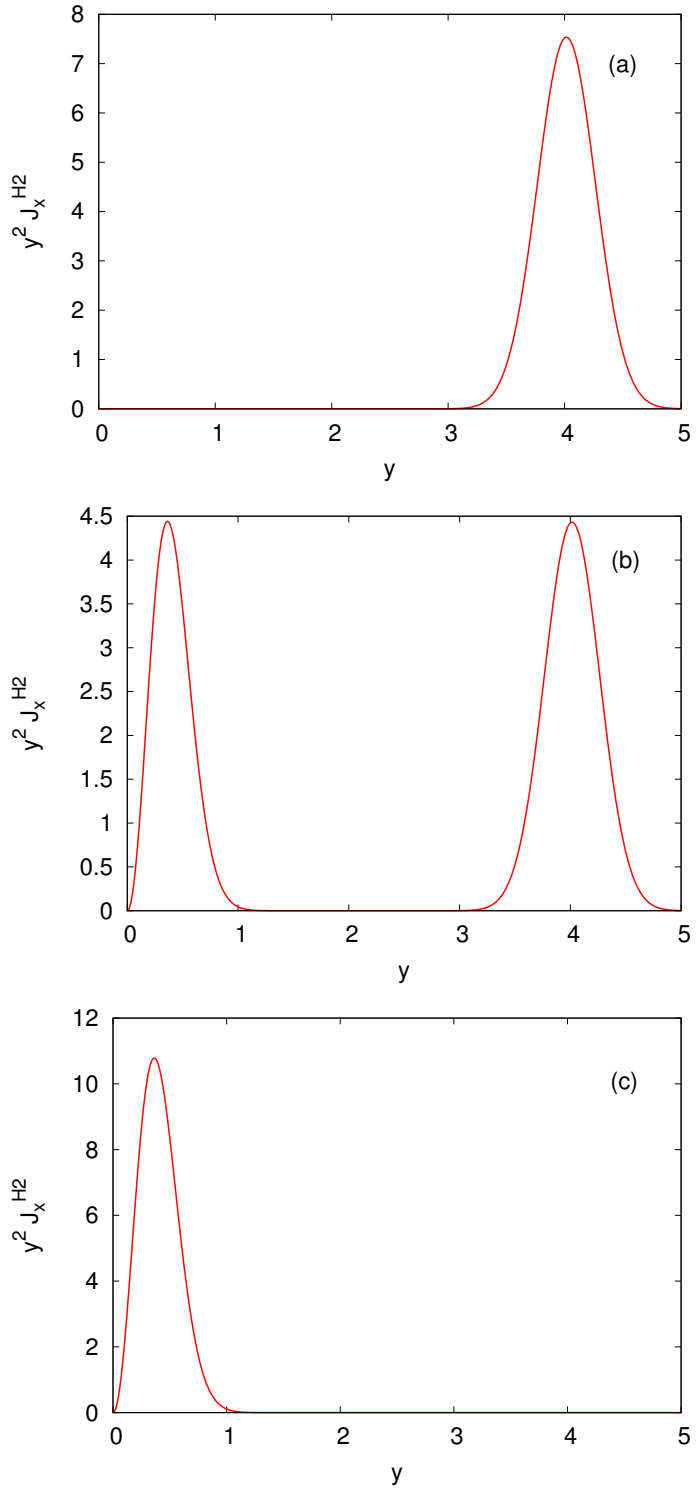

Figure 4.1: H_2 exchange holes weighted by y with arbitrary parameters $a = 2$, $b = 0.1$ and $c = 4$. In the panels (a), (b) and (c), the value of d has different values, $d = 0$, $d = 0.5$ and $d = 1$, respectively.

4.3.2 Implementation

In order to calculate the total exchange energy of a system, first a Hartree-Fock computation is performed to obtain the target system wavefunction. Then, this wavefunction is used as an initial guess in our calculations which consists of a single SCF iteration, in a post-HF calculation. In this single iteration the GAUSSIAN program[60] generates the densities and all other quantities necessary to build the fourth-order expansion of the exact exchange hole which are then passed into the function code where the H_2 model is implemented.

The H_2 model was implemented in the GAUSSIAN code using the computer language Fortran 77. In order to determine the parameters of the model we need to solve the system of nonlinear equations defined in 4.28. The Broyden's method which is a root-finding algorithm for multidimensional problems was implemented. This algorithm is a quasi-Newton method that does not need to calculate the Jacobian matrix of the functions F, G and H defined in equation 4.28.

The code of the H_2 model was made to be called for each point of the grid produced by the GAUSSIAN program. Hence, at each of these points we seek to determine the parameters of the H_2 model to finally calculate the total exchange energy.

In summary, building the algorithm for the H_2 model works as this:

1. First, the GAUSSIAN program calculates densities and all quantities needed by the fourth-order expansion of the exact spherically averaged exchange hole.

2. Second, the Broyden's method is employed, in every point of the grid, to find a solution to the model. Once a solution is found all parameters are determined.

3. Third, with the parameters determined the exchange energy density is calculated by equation 4.29 and then passed to the GAUSSIAN program where it will be used to calculate the total exchange energy of the target system.

4.3.3 Results and Discussion

The actual calculations were done using the 6-311G+(2d,p) basis set in the GAUSSIAN program. This basis set represent the orbitals of each atom where it has 6 gaussian functions for the inner shell, 3 gaussian functions for the valence orbitals and two gaussian functions with different sizes for extended valence orbitals. The specification (2d,p) indicates that one p-type function is added to the hydrogen atom and two more d-type functions to atoms with $Z > 2$. Moreover, cartesian functions were used for d-type orbitals. The grid employed in our calculations has 75 radial shells and 302 angular points per shell, giving approximately 7000 points per atom. Experimental geometries were used as inputs through out all calculations.

We begin to assess the H_2 model with small systems such as the atoms of the first and second row of the periodic table. In these calculations the switching factor was set to 0.5.

Unfortunately, we cannot find a solution to the system of nonlinear equations for any of these atoms. In other words, we could not find a solution for the model which leads to the determination of all parameters and consequently to the calculation of the total exchange energy.

When we have the particular case of the model, represented by a single gaussian-like density function in equation 4.17, the system of nonlinear equations is reduced to a single nonlinear equation. However, we also verified that, in all chemical systems assessed, the model cannot be solved in all points of the grid.

The failure to solve the model is not due to the choice of the root-finding algorithm but to the complexity of the problem itself. From the theory of numerical analysis, there is no guarantee to find a root for this type of system of nonlinear equations. Although the model posseses flexibility to accomodate all conditions of the exact exchange hole its solution is not possible. This issue could be attributed to oscillations caused by the basis set representation of orbitals. These basis set artifact is then transfered to densities. Moreover, any orbital and density derivatives would amplify such effects thus producing instabilities in the parameterization of the H_2 model.

However, the particular case of H_2 was designed to represent the short-range quadratic behavior of the exact spherically averaged exchange hole and yet we verified that it cannot be solved. Therefore, we believe that a Gaussian function cannot represent the short-range behavior in all space which is in contrast to the Slater function employed by the BR model.

4.3.4 Conclusion

Despite its flexibility to parameterize the fourth-order expansion of the exact exchange hole together with the normalization and non-negativity conditions, the model cannot be solved in all space. Hence, we believe that the lack of solutions is attributed to two factors, to the system of highly nonlinear equations and to instabilities produced by the basis set. We also verified that the particular case cannot represent the short-range quadratic behavior of the exact spherically averaged exchange hole in all space. Therefore, the H_2 model needs to be reformulated in order to be a good candidate for a exchange hole function.

4.4 Becke Roussel Model with the Fourth-Order Term

The BR Model[3] is known to represent the short-range quadratic behavior of the spherically averaged exact exchange hole. This implies that the first two terms of the expansion are used to parameterize the analytic form of the model. Here, we introduce a different parameterization to the BR model. The fourth-order term will be used in place of the second-order term to assess how the model reacts to this change. This model is called BR4 in reference to the fourth-order term.

4.4.1 Development

The development of the BR4 follows exactly the framework adopted in the construction of the original BR. We refer the reader to the first chapter of this work where we

give all the details of its construction. The spherically averaged BR model is defined by

$$\rho_{x\sigma}^{BR}(a,b,u) = -\frac{a}{16\pi bu}\left[(a|b-u|+1)e^{-a|b-u|} - (a|b+u|+1)e^{-a|b+u|}\right], \qquad (4.30)$$

where a and b are parameters to be determined from the short-range behavior of the exact exchange hole.

The expansion of the BR model in a Taylor series up to the fourth-order term gives three coefficients,

$$\begin{aligned}
\rho_{x\sigma}^{BR4,(0)}(a,b) &= \frac{a^3 e^{-ab}}{8\pi} \\
\rho_{x\sigma}^{BR4,(2)}(a,b) &= \frac{a^4(-2+ab)e^{-ab}}{48b\pi} \\
\rho_{x\sigma}^{BR4,(4)}(a,b) &= \frac{a^6(-ab-4)e^{-ab}}{960b\pi}.
\end{aligned} \qquad (4.31)$$

To determine the parameters a and b the zeroth- and fourth-order terms from the expansion of the analytic model and from the exact exchange holes are equated yelding the system of nonlinear equations,

$$\begin{aligned}
F(a,b) &= \rho_{x\sigma}^{BR4,(0)}(a,b) - K_0 \\
G(a,b) &= \rho_{x\sigma}^{BR4,(4)}(a,b) - K_4.
\end{aligned} \qquad (4.32)$$

The system of nonlinear equation defined in equation 4.32 can be simplified by using a variable substitution $x = ab$. Substituting x into the functions F and G we obtain,

$$\frac{xe^{-4x/3}}{(x-4)} = \frac{2\pi^4/3}{15}\frac{K_0^{7/3}}{K_4}. \qquad (4.33)$$

As in the original BR model[3], equation 4.33 has a unique and positive solution for all conditions. To find these solutions we rely on the Newton-Raphson method.

The exchange energy density at the reference point is given by,

$$\varepsilon_{x\sigma}^{BR4}(\boldsymbol{r}) = \left[1 - \exp^{-ab}\left(1 + \frac{1}{2}ab\right)\right]. \qquad (4.34)$$

Note that the exchange energy density of the BR4 model and BR model defined in equation 2.154 are identical. Clearly, the parameters necessary to calculate the exchange energy density are different.

4.4.2 Implementation

In order to calculate the total exchange energy of a system, first a Hartree-Fock computation is performed to obtain the target system wavefunction. Then, this wavefunction is used as an initial guess in our calculations which consists of a single SCF iteration, in a post-HF calculation. In this single iteration the GAUSSIAN program[60] generates the densities and all other quantities necessary to build the fourth-order expansion of the exact exchange hole which are then passed into the function code where the BR4 model is implemented.

The BR4 model was implemented in the GAUSSIAN code using the computer language Fortran 77. In order to determine the parameters of the model we need to solve a nonlinear one-dimensional The Newton-Raphson method which is a root-finding algorithm for unidimensional problems was implemented to search for solutions of equation 4.32.

The code of the BR4 model was made to be called for each point of the grid produced by the GAUSSIAN program. Hence, at each of these points we seek to determine the parameters of the BR4 model to finally calculate the total exchange energy.

In summary, the algorithm build for the BR4 model works as this:

1. First, the GAUSSIAN program calculates densities and all quantities needed by the fourth-order expansion of the exact spherically averaged exchange hole.

2. Second, the Newton-Raphson method is employed, in every point of the grid, to find a solution to the model. Once a solution is found all parameters are determined.

3. Third, with the parameters determined the exchange energy density is calculated by equation 4.33 and then passed to the GAUSSIAN program where it will be used to calculate the total exchange energy of the target system.

4.4.3 Results and Discussion

The actual calculations were done using the 6-311G+(2d,p) basis set in the GAUSSIAN program. This basis set represent the orbitals of each atom where it has 6 gaussian functions for the inner shell, 3 gaussian functions for the valence orbitals and two gaussian functions with different sizes for extended valence orbitals. The specification (2d,p) indicates that one p-type function is added to the hydrogen atom and two more d-type functions to atoms with $Z > 2$. Moreover, cartesian functions were used for d-type orbitals. The grid employed in our calculations has 75 radial shells and 302 angular points per shell, giving approximately 7000 points per atom. Experimental geometries were used as inputs through out all calculations.

The BR4 exchange-hole function does not improve the results of exchange energies of atoms and molecules (Table 4.III). Because the analytic form of BR4 model is based on a physical system and its construction follows the same steps used in the original BR, the failure of the model to deliver exchange energies close to those given by the BR model indicates an important issue with its parameterization.

System	E_x^{Exact}	E_x^{BR}	E_x^{BR4}
H	-0.313	-0.313	-0.315
He	-1.026	-1.039	-1.027
Li	-1.781	-1.793	-1.778
Be	-2.666	-2.680	-2.601
B	-3.768	-3.783	-3.852
C	-5.074	-5.093	-5.212
N	-6.603	-6.629	-7.024
O	-8.210	-8.252	-8.804
F	-10.035	-10.093	-11.031
Ne	-12.097	-12.176	-13.596
Na	-14.015	-14.072	-15.682
Cl	-27.539	-27.474	-31.719
P	-22.641	-22.626	-24.830
MAEs	0.000	0.032	0.911
H2	-0.658	-0.658	-0.637
HF	-10.420	-10.509	-11.577
LiH	-2.146	-2.165	-2.158
LiF	-11.994	-12.112	-13.137
Li2	-3.564	-3.591	-3.576
Na2	-28.021	-28.144	-31.389
F2	-19.949	-20.157	-22.030
Cl2	-55.092	-54.982	-63.620
NH3	-7.665	-7.717	-8.156
P2	-45.201	-45.205	-49.625
N2	-13.092	-13.235	-13.889
NO	-14.725	-14.875	-15.750
NO2	-22.897	-23.166	-24.680
O2	-16.259	-16.452	-17.485
MAEs	0.000	0.107	1.862
MAE	0.000	0.071	1.404

Table 4.III: Exchange energies of atoms and molecules (in Hartree). MAE, mean absolute error. MAEs of a set of atoms and molecules and Total MAE are shown.

We also studied the ability of the BR4 model to describe chemical transformations such as atomization energies, $\Delta E_x = E_x^{molecules} - E_x^{atoms}$. In Table 4.*IV*, the exchange-energy contribution to the atomization energies is presented.

Molecules	E_x^{Exact}	E_x^{BR}	E_x^{BR4}
H2	-0.033	-0.033	-0.006
HF	-0.073	-0.103	-0.231
LiH	-0.053	-0.060	-0.065
LiF	-0.179	-0.226	-0.328
Li2	-0.003	-0.006	-0.020
Na2	0.009	0.000	-0.024
F2	0.121	0.029	0.031
Cl2	-0.013	-0.034	-0.182
NH3	-0.125	-0.151	-0.186
P2	0.082	0.048	0.035
MAEs	0.000	0.030	0.082
N2	0.114	0.023	0.160
NO	0.089	0.006	0.078
NO2	0.126	-0.033	-0.048
O2	0.162	0.052	0.123
MAEs	0.000	0.111	0.068
MAEs	0.000	0.051	0.074

Table 4.IV: Exchange-energy contributions to the atomization energies (in Hartree). MAE, mean absolute error. MAEs of a set of single- and multi-bonded molecules and Total MAE are shown.

The ΔE_x of singly-bonded molecules show a worsening which is in contrast to the results of multi-bonded molecules where a significant improvement is observed. Yet, in the singly-bonded subset, the H_2 is an exception with a large improvement over the BR model. These multi-bonded molecules are formed by several electron pairs working as binding or as antibinding pairs. During the atomization process, the exchange holes

change forms very rapidly and may be highly delocalized over the nuclei. This chemical transformation is directly related to the valence region where the fourth-order term of the expansion of the exact exchange hole has less influence from basis set oscillations. In regard of these facts, and in view of the results of ΔE_x for multi-bonded molecules, we suggest that the fourth-order term is better suited for those regions where the exchange holes are not in the vicinity of the reference point but delocalized over several centers. Note here that our suggestion is based on a deficiency of the basis set and not on a problem with the fourth-order expansion of the exact exchange hole.

The model's ability to describe accurately delocalized systems encourages further studies. An interesting idea would be the interpolation of two models based on the original form of the BR exchange-hole function where each model would have different parameterization. One designed to handle regions where the exchange holes are localized while the other would deal with delocalized exchange holes.

The parameterization of the BR4 exchange hole with the zeroth- and fourth-order terms, in general, have worsened the results compared with the original parameterization used in the BR model. A possible justification for this might be that oscillations caused by the basis set are transfered to the BR4 model through the zeroth- and fourth-order terms. These terms are composed by orbitals, densities and their derivatives where the latter amplify these oscillations then, causing instabilities in the parameterization of the model. However, these oscillations do not appear to completely compromise the results of ΔE_x for multi-bonded molecules.

4.4.4 Conclusion

In this part of the work, we examined a new parameterization of the BR model with the zeroth- and fourth-order terms of the expansion of the exact spherically averaged exchange hole. We found that while, in general, the results are unsatisfactory from the viewpoint of chemical accuracy, the model gave interesting results for the exchange-energies contributions to the atomization energies of multi-bonded molecules. Also, basis set artifact appears to produce instabilities in the model thus compromising its results. Therefore, further improvement depends directly on the removal of oscillations

from our calculations.

CHAPTER 5

CONCLUSION

The development of exchange-correlation functionals under the KS theory is ongoing in quantum chemistry and solid state physics. Although the exchange-correlation functional and its hole function do not have closed forms, which would lead to systematic improvement, the systematically satisfaction of a number of conditions has proven to be fundamental to obtain successively improved approximations. DFT has evolved from LDA, which takes into consideration only the density at each point in space, to hybrids being able to give a better description of molecules and solids. Therefore, theoretical conditions have been and will be fundamental to further development of density functional approximations.

The goal of this work is twofold: to unveil a new condition of the exact exchange hole, thus expanding the actually limited number of known conditions, and to propose four exchange hole models, to which we enforce all these conditions to construct exchange functional approximations.

In the first part of this work, details of the biharmonic condition are presented. This new condition gives the short-range quartic behavior of the exact spherically averaged exchange hole. We have assessed the performance of this condition for atomic and molecular systems. We have graphically compared the second- and fourth-order expansions with the exact exchange hole in several reference points. It has been demonstrated that the fourth-order expansion can represent quite accurately the short-range behavior of the exact exchange hole. The new condition particularly gives better results when the exchange hole is delocalized. Also, we have examined the effects of Gaussian-type basis sets on the fourth-order expansion by studying how the leading term in biharmonic condition behaves when oscillations are inherited from densities and orbitals. We observed that these oscillations can potentially cause instabilities in applications of the new conditions.

In the second part of this work, we proposed four analytic completely nonempirical,

exchange hole models: FP, EBR, the H2 Model and BR4. Our approach to the construction of these models follows the same framework adopted by Becke and Roussel in the construction of the BR exchange hole model. It consists of systematic satisfaction of all currently known conditions of the exact exchange hole, namely the normalization, the non-negativity and the short-range behavior. Our models were designed to be sufficiently flexible to parameterize the short-range quartic behavior of the exact exchange hole in any system. The solution of a model begins by determining its parameters in all space, which yields its distribution with respect to the reference point. It has been found that the FP and H_2 models do not have solutions in all points of space.

The FP model is based on an analytic function designed to mimic the exact exchange hole in any system. In this model, a nonlinear one-dimension equation needs to be solved in every point of the grid to determine the parameter which is directly related to the normalization condition and, consequently, solve the hole model. However, we have found that the model cannot be realized for atoms.

The motivation to find an exchange hole model able to correctly describe chemical bonding has lead us to propose the H_2 model, which is based on the density of the bonding orbital of the H_2 molecule. We have shown that, in order to solve the H_2 model, a system of three nonlinear equations must be solved in all grid points. Also, we verified that this highly nonlinear problem cannot be solved for simple systems such as atoms.

Since the EBR and BR4 models do have solutions in space, we have assessed their performances by computing total exchange energies and contributions of the exchange energies to the atomization energies of small molecules.

In the EBR model, we have introduced a parameter to the original BR model in order to accomodate the biharmonic condition. The introduction of a new parameter consequently added a new nonlinear equation yielding a system of three nonlinear equations. It has been found that the EBR does not improve on the BR model with respect to exchange energies and exchange-energy contributions to the atomization energies. This can be explained by the difficulty in finding solutions to the model in all grid points.

Our last proposed model is based on the BR model the difference being that we have used the fourth-order term instead of the second-order term of the expansion of

the exact exchange hole. We have examined the accuracy of this model to calculate exchange energies and exchange-energy contributions to simple chemical systems. It has been demonstrated that the BR4 does not improve on the BR model with respect to exchange energies. In reality, in most cases the use of the fourth-order term worsens the results compared to the BR model as shown in table 4.*III*. The accuracy of the model to compute exchange-energy contributions to the atomization energies for single bonded molecules, shown in table 4.*IV*, is worse than the BR model. However, for multi-bonded molecules the BR4 significantly improves on the BR model.

Althought the results of the test calculations have shown unsatisfactory accuracies for EBR and BR4 models and failures to solve the FP and H_2 models in all space, they served the important purpose of understanding and pinpointing the common problem of all models. We strongly believe that these oscillations originated in the Gaussian-type basis sets are the root cause of the problems found in our exchange hole models. This idea is supported by our study on the influence that Gaussian-type basis sets have on the expansions of the exact exchange hole.

By inheriting oscillations from orbitals, densities and their derivatives during the parameterization process, where the fourth-order term of the expansion of the exact exchange hole is present, our models become greatly unstable. Thus, these instabilities added to the natural difficult to solve systems of nonlinear equations can completely compromise the realization of models(as seen in the FP and H_2) or undermine the performance of computations of exchange energies as well as its contributions to the atomization energies(in the case of EBR and BR4). In view of this one may ask: Why not use very large Gaussian-type basis sets in the test calculations ? Rather than use very large basis sets in our calculations and find a palliative solution, we prefer to work on a long-term solution. An interesting idea is to apply the biharmonic condition in regions where it is more effective than the second-order expansion. We have seen that the former significantly improves the description of the exact exchange hole for nonlocal regions of molecular systems. Therefore, interpolating two exchange holes parameterized for different regions of a system could be seen as a solution to the problem discussed.

We conclude that the biharmonic condition is a valuable constraint to be employed

in the parameterization of exchange hole models. However, oscillations originated in Gaussian-type basis sets can compromise the computations of exchange energies and its contributions to atomization energies, therefore they should be properly addressed. In future work we will describe the construction of a new exchange functional which explores the idea of interpolating two exchange hole models parameterized for distinct subregions, one exchange hole model enforcing the biharmonic condition for those regions where the exact exchange hole is delocalized while the other applies the curvature condition to regions where the exact exchange hole is localized.

BIBLIOGRAPHY

[1] G. N. Lewis. *Jour. Am. Chem. SOC.*, 38(762), 1916.

[2] Axel D. Becke. *The Journal of Chemical Physics*, 112(9):4020–4026, 2000.

[3] A. D. Becke and M. R. Roussel. *Phys. Rev. A*, 39:3761–3767, 1989.

[4] M. Born and R. Oppenheimer. *Annalen der Physik*, 389(20):457–484, 1927.

[5] M. Born and K. Huang. 389:406–407, 1954.

[6] G. E. Uhlenbeck and S. Goudsmit. *Die Naturwissenschaften*, 13(47):953–954, 1925.

[7] I. N. Levine. *Quantum Chemistry*. Allyn and Bacon, Boston, 1974.

[8] R. McWeeny and B.T. Sutcliffe. *Methods of Molecular Quantum Mechanics.* London: Academic Press., 1969.

[9] A. Szabo and N. S. Ostlund. *Modern Quantum Chemistry*. Macmillan Publishing, New York, 1982.

[10] R. G. Parr and W. Yang. *Density-Functional Theory of Atoms and Molecules Oxford University Press*. Oxford, 1989.

[11] Norman H. March. Oxford ; New York : Pergamon Press, 1st ed. edition, 1975.

[12] P. Hohenberg and W. Kohn. *Phys. Rev.*, 136:B864–B871, 1964.

[13] R. M. Dreizler and E. K. U. Gross. *Density Functional Theory*. Springer Verlag, Berlin, 1990.

[14] Mel Levy. *Proceedings of the National Academy of Sciences*, 76(12):6062–6065, 1979.

[15] P. A. M. Dirac. *Mathematical Proceedings of the Cambridge Philosophical Society*, 26:376–385, 1930.

[16] W. Kohn and L. J. Sham. *Phys. Rev.*, 140:A1133–A1138, 1965.

[17] J. P. Perdew and Alex Zunger. *Phys. Rev. B*, 23:5048–5079, 1981.

[18] O. Gunnarsson and B. I. Lundqvist. *Phys. Rev. B*, 13:4274–4298, 1976.

[19] J Harris and R O Jones. *Journal of Physics F: Metal Physics*, 4(8):1170, 1974.

[20] D.C. Langreth and J.P. Perdew. *Solid State Communications*, 17(11):1425 – 1429, 1975.

[21] David C. Langreth and John P. Perdew. *Phys. Rev. B*, 15:2884–2901, 1977.

[22] Kieron Burke and John P. Perdew. *International Journal of Quantum Chemistry*, 56(4):199–210, 1995.

[23] Hilke Bahmann and Matthias Ernzerhof. *The Journal of Chemical Physics*, 128(23), 2008.

[24] M. Ernzerhof, K. Burke, and J. P. Perdew. *in Recent Developments and Applications of Modern Density Functional Theory, Theoretical and Computational Chemistry, edited by J. M. Seminario*. Elsevier, Amsterdam, 1997.

[25] John P. Perdew, Kieron Burke, and Yue Wang. *Phys. Rev. B*, 54:16533–16539, Dec 1996.

[26] G. E. Scuseria and V. N. Staroverov. *Progress in the development of exchange-correlation functionals.* Elsevier, Amsterdam, 2005.

[27] Tom Ziegler, Arvi Rauk, and EvertJ. Baerends. *Theoretica chimica acta*, 43(3):261–271, 1977.

[28] D. M. Ceperley and B. J. Alder. *Phys. Rev. Lett.*, 45:566–569, Aug 1980.

[29] E. J. Baerends, , and O. V. Gritsenko. *The Journal of Physical Chemistry A*, 101(30):5383–5403, 1997.

[30] Mel Levy and John P. Perdew. *Phys. Rev. A*, 32:2010–2021, 1985.

[31] M. Levy. *in Single-Particle Density in Physics and Chemistry edited by N. H. March and B. M. Deb*. Academic, London, 1987.

[32] Mel Levy. *Phys. Rev. A*, 43:4637–4646, 1991.

[33] Mel Levy and John P. Perdew. *Phys. Rev. B*, 48:11638–11645, 1993.

[34] John P Perdew, Karla Schmidt, V Van Doren, et al. Density functional theory and its application to materials. *Van Doren, V*, pages 1–20, 2001.

[35] A. D. Becke. *Phys. Rev. A*, 38:3098–3100, 1988.

[36] Chengteh Lee, Weitao Yang, and Robert G. Parr. *Phys. Rev. B*, 37:785–789, 1988.

[37] John P. Perdew, Kieron Burke, and Matthias Ernzerhof. *Phys. Rev. Lett.*, 77:3865–3868, 1996.

[38] W. Koch and M. C. Holthausen. *A ChemistâĂŹs Guide to Density Functional Theory*. Wiley-VCH, Weinheim, 2001.

[39] Matthias Ernzerhof and Gustavo E. Scuseria. *The Journal of Chemical Physics*, 110(11):5029–5036, 1999.

[40] Larry A. Curtiss, Paul C. Redfern, and Krishnan Raghavachari. *The Journal of Chemical Physics*, 123(12), 2005.

[41] Mel Levy, John P. Perdew, and Viraht Sahni. *Phys. Rev. A*, 30:2745–2748, 1984.

[42] Fabio Della Sala and Andreas Görling. *Phys. Rev. Lett.*, 89:033003, 2002.

[43] Elliott H. Lieb and Stephen Oxford. *International Journal of Quantum Chemistry*, 19(3):427–439, 1981.

[44] G. L. Oliver and J. P. Perdew. *Phys. Rev. A*, 20:397–403, 1979.

[45] John P. Perdew and Yue Wang. *Phys. Rev. B*, 46:12947–12954, 1992.

[46] John P. Perdew and Wang Yue. *Phys. Rev. B*, 33:8800–8802, 1986.

[47] John P. Perdew, J. A. Chevary, S. H. Vosko, Koblar A. Jackson, Mark R. Pederson, D. J. Singh, and Carlos Fiolhais. *Phys. Rev. B*, 46:6671–6687, 1992.

[48] Jianmin Tao, John P. Perdew, Viktor N. Staroverov, and Gustavo E. Scuseria. *Phys. Rev. Lett.*, 91:146401, 2003.

[49] Axel D. Becke. *The Journal of Chemical Physics*, 98(7):5648–5652, 1993.

[50] John P. Perdew, Matthias Ernzerhof, and Kieron Burke. *The Journal of Chemical Physics*, 105(22):9982–9985, 1996.

[51] Carlo Adamo and Vincenzo Barone. *The Journal of Chemical Physics*, 110(13):6158–6170, 1999.

[52] Jianmin Tao, John P. Perdew, Viktor N. Staroverov, and Gustavo E. Scuseria. *Phys. Rev. Lett.*, 91:146401, 2003.

[53] Matthias Ernzerhof and John P. Perdew. *The Journal of Chemical Physics*, 109(9):3313–3320, 1998.

[54] A. D. Becke. *International Journal of Quantum Chemistry*, 23(6):1915–1922, 1983.

[55] Vincenzo Tschinke and Tom Ziegler. *Canadian Journal of Chemistry*, 67(3):460–472, 1989.

[56] P. Fulde. *Electron Correlations in Molecules and Solids 3rd ed.* Springer, Berlin, 2013.

[57] J. P. Perdew and S. Kurth. *in Density Functionals: Theory and Applications, Lecture Notes in Physics Vol. 500, edited by D. P. Joubert*. Springer Verlag, Berlin, 1998.

[58] John P. Perdew. Size-consistency, self-interaction correction, and derivative discontinuity in density functional theory. In Per-Olov Loewdin, editor, *Density Functional Theory of Many-Fermion Systems*, volume 21 of *Advances in Quantum Chemistry*, pages 113 – 134. Academic Press, 1990.

[59] Hélène Antaya, Yongxi Zhou, and Matthias Ernzerhof. *Phys. Rev. A*, 90:032513, 2014.

[60] M. J. Frisch, G. W. Trucks, H. B. Schlegel, G. E. Scuseria, M. A. Robb, J. R. Cheeseman, J. A. Montgomery, Jr., T. Vreven, K. N. Kudin, J. C. Burant, J. M. Millam, S. S. Iyengar, J. Tomasi, V. Barone, B. Mennucci, M. Cossi, G. Scalmani, N. Rega, G. A. Petersson, H. Nakatsuji, M. Hada, M. Ehara, K. Toyota, R. Fukuda, J. Hasegawa, M. Ishida, T. Nakajima, Y. Honda, O. Kitao, H. Nakai, M. Klene, X. Li, J. E. Knox, H. P. Hratchian, J. B. Cross, V. Bakken, C. Adamo, J. Jaramillo, R. Gomperts, R. E. Stratmann, O. Yazyev, A. J. Austin, R. Cammi, C. Pomelli, J. W. Ochterski, P. Y. Ayala, K. Morokuma, G. A. Voth, P. Salvador, J. J. Dannenberg, V. G. Zakrzewski, S. Dapprich, A. D. Daniels, M. C. Strain, O. Farkas, D. K. Malick, A. D. Rabuck, K. Raghavachari, J. B. Foresman, J. V. Ortiz, Q. Cui, A. G. Baboul, S. Clifford, J. Cioslowski, B. B. Stefanov, G. Liu, A. Liashenko, P. Piskorz, I. Komaromi, R. L. Martin, D. J. Fox, T. Keith, M. A. Al-Laham, C. Y. Peng, A. Nanayakkara, M. Challacombe, P. M. W. Gill, B. Johnson, W. Chen, M. W. Wong, C. Gonzalez, and J. A. Pople. Gaussian 03, Revision C.02. Gaussian, Inc., Wallingford, CT, 2004.

[61] Alex P. Gaiduk, Ilya G. Ryabinkin, and Viktor N. Staroverov. *Journal of Chemical Theory and Computation*, 9(9):3959–3964, 2013.

[62] P. R. T. Schipper, O. V. Gritsenko, and E. J. Baerends. *Theoretical Chemistry Accounts*, 98(1):16–24, 1997.

Appendix I

Uniform Coordinate Scaling

Let $\Psi(\boldsymbol{r}_1,...,\boldsymbol{r}_N)$ be a normalized function of N-electrons. We follow with the scaling of Ψ:

$$\Psi \equiv \Psi(\gamma\boldsymbol{r}_1,...,\gamma\boldsymbol{r}_N) \tag{I.1}$$

where γ is a scale factor which affects only the length of the N-particle coordinates $\boldsymbol{r}_i$ without change on their direction. The physical effect of scaling Ψ in a 3n-dimensional space is: for $\gamma < 1$, Ψ is more diffuse and for $\gamma > 1$, the function is contracted. We must verify that Ψ is normalized after we introduced the scale factor γ. It is known that

$$\begin{aligned} 1 &= \int d\upsilon \Psi^*(\boldsymbol{r}_1,...,\boldsymbol{r}_N)\Psi(\boldsymbol{r}_1,...,\boldsymbol{r}_N) \\ &= \int d(\gamma\upsilon)\Psi^*(\gamma\boldsymbol{r}_1,...,\gamma\boldsymbol{r}_N)\Psi(\gamma\boldsymbol{r}_1,...,\gamma\boldsymbol{r}_N), \end{aligned}$$

where the volume element is

$$\begin{aligned} d(\gamma\upsilon) &= (\gamma r_1)^2 \sin\theta_1 d(\gamma r_1)...\gamma r_N)^2 \sin\theta_N d(\gamma r_N) \\ &= \gamma^3 (r_1)^2 sin\theta_1 d(r_1)...\gamma^3 (r_N)^2 sin\theta_N d(r_N). \end{aligned}$$

Note that the scale factor γ^3 multiplies N particle coordinates, therefore

$$1 = \gamma^{3N} \int d\upsilon \Psi^* \Psi, \tag{I.2}$$

which gives the normalized scale function Ψ

$$\Psi_\gamma \equiv \gamma^{3N/2} \Psi(\gamma\boldsymbol{r}_1,...,\gamma\boldsymbol{r}_N). \tag{I.3}$$

We define now the kinetic $\hat{T}$

$$\hat{T} = \sum_{i=1}^{N} -\frac{1}{2}\nabla_i^2, \tag{I.4}$$

and the potential $\hat{V}$

$$\hat{V} = -\sum_{i=1}^{N} \frac{Z}{|\boldsymbol{R} - \boldsymbol{r}_i|} + \sum_{i \neq j} \frac{1}{|\boldsymbol{r}_i - \boldsymbol{r}_j|}, \tag{I.5}$$

operators for a N-electron atom. Therefore, the expectation values of the respective operators are

$$T = \int d\upsilon \Psi^*(\boldsymbol{r}_1, ..., \boldsymbol{r}_N) \sum_{i=1}^{N} -\frac{1}{2} \nabla_i^2 \Psi(\boldsymbol{r}_1, ..., \boldsymbol{r}_N). \tag{I.6}$$

and

$$V = \int d\upsilon \Psi^*(\boldsymbol{r}_1, ..., \boldsymbol{r}_N) - \sum_{i=1}^{N} \frac{Z}{|\boldsymbol{R} - \boldsymbol{r}_i|} + \sum_{i \neq j} \frac{1}{|\boldsymbol{r}_i - \boldsymbol{r}_j|} \Psi(\boldsymbol{r}_1, ..., \boldsymbol{r}_N), \tag{I.7}$$

The expectation value for the potential energy with the scaled functionis obtain by

$$V_\gamma = \gamma^{3N} \int d\upsilon \Psi^*(\gamma \boldsymbol{r}_1, ..., \gamma \boldsymbol{r}_N) \sum_{i=1}^{N} \left(\frac{Z}{|\boldsymbol{R} - \boldsymbol{r}_i|} \right) \Psi(\gamma \boldsymbol{r}_1, ..., \gamma \boldsymbol{r}_N). \tag{I.8}$$

In order to make the $\hat{V}_\gamma$ equal to $\hat{V}$ we have to scale all terms involving $\mathbf{r}$, including the operator. By definition, the potential operator has an r term as r^{-1} because in general (VR)

$$\frac{1}{|\boldsymbol{u} - \boldsymbol{v}|} = \frac{1}{r_{uv}} \tag{I.9}$$

In the case of the kinetic operator, the Laplacian operator may be written as

$$\nabla_i^2 = \frac{1}{r^2} \left[\frac{\partial}{\partial r} \left(\frac{r^2 \partial}{\partial r} \right) + \frac{1}{\sin\theta} \frac{\partial}{\partial \theta} \left(\frac{\sin\theta \partial}{\partial \theta} \right) + \frac{1}{\sin^2\theta} \frac{\partial^2}{\partial \phi^2} \right], \tag{I.10}$$

where the r term shows as r^{-2}. Therefore, to get the scale factor in the potential operator

we have to multiply the integral in eq.$(I.6)$ by $\gamma\gamma^{-1}$ to get

$$\begin{aligned} V_\gamma &= (\gamma\gamma^{-1})\,\gamma^{3N}\int d\upsilon\Psi^*(\gamma\boldsymbol{r}_1,...,\gamma\boldsymbol{r}_N)\sum_{i=1}^{N}\left(\frac{Z}{\gamma|\boldsymbol{R}-\boldsymbol{r}_i|}\right)\Psi(\gamma\boldsymbol{r}_1,...,\gamma\boldsymbol{r}_N) \\ &= \gamma\int d(\gamma\upsilon)\Psi^*(\gamma\boldsymbol{r}_1,...,\gamma\boldsymbol{r}_N)\sum_{i=1}^{N}\left(\frac{Z}{\gamma|\boldsymbol{R}-\boldsymbol{r}_i|}\right)\Psi(\gamma\boldsymbol{r}_1,...,\gamma\boldsymbol{r}_N) \\ &= \gamma V. \end{aligned}$$

We apply the same procedure to the kinetic operator to obtain

$$\begin{aligned} T_\gamma &= (\gamma^2\gamma^{-2})\gamma^{3N}\int d\upsilon\Psi^*(\gamma\boldsymbol{r}_1,...,\gamma\boldsymbol{r}_N)\sum_{i=1}^{N}\left(-\frac{1}{2}\nabla_i^2\right)\Psi(\gamma\boldsymbol{r}_1,...,\gamma\boldsymbol{r}_N) \\ &= \gamma^2\int d(\gamma^{3N}\upsilon)\Psi^*(\gamma\boldsymbol{r}_1,...,\gamma\boldsymbol{r}_N)\sum_{i=1}^{N}\left(-\frac{1}{2}\frac{1}{\gamma^{-2}}\nabla_i^2\right)\Psi(\gamma\boldsymbol{r}_1,...,\gamma\boldsymbol{r}_N) \\ &= \gamma^2 T. \end{aligned}$$